U. S. ARMY
TRANSPORTATION RESEARCH COMMAND
FORT EUSTIS, VIRGINIA

TREC TECHNICAL REPORT 61-61

EFFUSION PHENOMENA APPLIED TO A LIFTING SYSTEM

Project 9R99-20-001

Contract DA-44-177-TC-697

April 1961

prepared by :

THE HAYES CORPORATION
Birmingham, Alabama

DISCLAIMER NOTICE

When Government drawings, specifications, or other data are used for any purpose other than in connection with a definitely related Government procurement operation, the United States Government thereby incurs no responsibility nor any obligation whatsoever; and the fact that the Government may have formulated, furnished, or in any way supplied the said drawings, specifications, or other data is not to be regarded by implication or otherwise as in any manner licensing the holder or any other person or corporation, or conveying any rights or permission, to manufacture, use, or sell any patented invention that may in any way be related thereto.

ASTIA AVAILABILITY NOTICE

Qualified requesters may obtain copies of this report from

Armed Services Technical Information Agency
Arlington Hall Station
Arlington 12, Virginia

This report has been released to the Office of Technical Services, U. S. Department of Commerce, Washington 25, D. C., for sale to the general public.

The information containede herein will not be used for advertising purposes.

The findings and recommendations contained in this report are those of the contractor and do not necessarily reflect the views of the Chief of Transportation or the Department of the Army.

Project 9R99-20-001
Contract DA-44-177-TC-697
April 1961

EFFUSION PHENOMENA AS APPLIED TO A LIFTING DEVICE

Engineering Report Number 595

Prepared by
The Hayes Corporation
Birmingham, Alabama

for
U. S. ARMY TRANSPORTATION RESEARCH COMMAND
FORT EUSTIS, VIRGINIA

FOREWORD

This document contains the results of a theoretical study and laboratory evaluation program dealing with the phenomenon of gaseous effusion as applied to a lifting system.

The technical personnel associated with this research program were as follows:

Dr. Charles M. Askey, Technical and Administrative Director

Clarence D. Doyle, Mathematician

Norman A. W. MacQueen, Design Engineer

Lucas H. Moe, Jr., Instrument Design

Arthur R. Phillips, Physicist

Ural M. Robinson, Materials Engineer

Gratitude is hereby extended to Dr. G. D. Sands and James P. Waller of the U. S. Army Transportation Research Command for their co-operation during the performance of this contract.

CONTENTS

ILLUSTRATIONS

TABLES

SYMBOLS

A_B	area of effusion surface
A_p	porous area of effusion surface
A'	ratio of A_p to A_B
A_o	Avogadro's number, 6.0228×10^{23} molecules $\cdot$ mole^{-1}
$\overset{o}{A}$	Angstrom unit, $(1 \times 10^{-8}$ cm)
a	tube radius
H	heat energy per second per unit area
k	Boltzmann's constant, 1.3803×10^{-16} gram $\cdot$ cm^2 $\cdot$ deg^{-1} $\cdot$ sec^{-2}
L	tube length
$\dot{M}$	molecular flow rate
M_{air}	molecular weight of air, 28.96 gram $\cdot$ mole^{-1}
m_{air}	mass of one air molecule, 48.11×10^{-24} gram $\cdot$ molecule^{-1}
N	number of molecules
n	molecules per unit volume
P	pressure
R_M	universal gas constant, 83.15×10^6 gram $\cdot$ cm^2 $\cdot$ deg^{-1} $\cdot$ sec^{-1}
T	temperature in ^oK
V_M	mixing region volume
$\bar{v}$	average molecular speed
η	coefficient of viscosity
$\bar{\lambda}$	mean free path
ρ	density
σ	molecular diameter

SUBSCRIPTS

0	denotes conditions at the external effusion-surface
1	denotes conditions inside effusion chamber
2	denotes ambient conditions
STP	denotes standard temperature and pressure:

$N_{STP} = 2.686 \times 10^{6}$ molecule $\cdot$ cm^{-3}

$T_{STP} = 273.16\ ^{o}K$

$P_{STP} = 1.0132 \times 10^{6}$ dyne $\cdot$ cm^{-2}

SUMMARY

This document constitutes the final report on the Effusion Research Program (Contract DA-44-177-TC-697) conducted by the Research Section of The Hayes Corporation, Birmingham, Alabama, from September 26, 1960 through April 25, 1961, for the U. S. Army Transportation Research Command, Fort Eustis, Virginia.

An account of a theoretical study and an experimental evaluation of the phenomenon of gaseous effusion, as applied to a lift system, is given. The purpose of the theoretical study was to determine the magnitude of lift arising from the effusion process. The laboratory evaluation program involved two phases; namely, the selection of microporous media that would satisfy the effusion requirements and the design and fabrication of a test apparatus for testing the porous materials selected.

In the initial phases of the work, the experimental and theoretical investigations were carried on concurrently. An effusion chamber was constructed to test four different types of microporous media which were ordered early in the program. The test apparatus was essentially a rectangular air chamber, with the porous medium being tested constituting one face of the chamber. Auxiliary apparatus was used to control the air pressure inside the chamber. A means of measuring chamber air temperature was also provided.

The four types of porous material, each having an effective area of one square foot, were evaluated by maintaining the chamber air pressure higher than ambient pressure. Air was allowed to effuse through the porous media. According to the preliminary calculations in the contract proposal, the effusion process should increase the density of molecules in the region adjacent to the external surface of the porous media, thus producing an increased pressure, or lift. No lift was detected during any of the tests. The experimental phase was discontinued January 25, 1961.

The theoretical work consisted in part in re-evaluating the ideas involved in the original proposal. Weaknesses in that treatment are discussed. Calculations, based upon a physical model in which a tube is placed over the effusion surface, indicate that the increased density predicted in the original proposal is much too large. It is concluded that no practical lift is to be expected from the effusion process. Any attainable lift would be severely limited by the stringent materials requirements.

CONCLUSIONS

The theoretical study of the effusion phenomenon, combined with the laboratory evaluation program and the search for microporous media to satisfy the effusion process requirements, has led to the following conclusions:

1. There are no microporous media presently available which will permit an effusion process to take place at atmospheric pressure.

2. Although the production of microporous media with the desired hole diameter is presently obtainable, the production of material with the required thickness is beyond the present state-of-the-art. Even if the thickness requirements could be met, the circuitous nature of the pore channels makes it impossible to achieve effusive flow. The thickness of the microporous media required to test for lift by the effusion process at atmospheric pressure approaches atomic dimensions. Material of this thickness is impractical for the application considered here.

3. The tube model calculation set an upper limit on lift, a limit which is much smaller than the lift predicted in the contract proposal (Report 516, included in the text). It is believed that the low calculated values of lift combined with the stringent materials requirements for effusion fail to justify a more detailed analysis of the feasibility of producing lift by means of the effusion process.

DISCUSSION

INTRODUCTION

The Hayes Corporation Engineering Report Number 516 (29 February 1960) was the basis for the contract proposal which resulted in the award of Contract DA-44-177-TC-697 by the U. S. Army Transportation Research Command, Fort Eutis, Virginia. The contract supported this theoretical and experimental study of the phenomenon of gaseous effusion as applied to a lift system. The period of performance of the contract was from September 26, 1960 through April 25, 1961.

Since the Hayes Engineering Report No. 516 contains the appropriate concepts, derivations, and calculations for this theoretical work, it is herein presented as an introduction to this final report.

EFFUSION LIFTING SYSTEM

Engineering Report Number 516
29 February 1960

FOREWORD

This report on an "Effusion Lifting System" is an effort to show the feasibility of utilizing a well known physical phenomenon (effusion) in a practical manner in order to achieve propulsion and/or lift.

Since effusion is a microscopic process, different from macroscopic mass flow processes, the forces of interest cannot be calculated by the usual aerodynamical techniques. Instead, one must resort to the statistical calculation of the net number of molecules added to a region (which is "bounded" by other molecules) and compute the increased force achieved by using the product of the area and the increased pressure. The increased pressures are small and are not, from the macroscopic point of view, bounded. This results in a gradual displacement of molecules from the increased pressure region. It can be said that the overall process is one of "molecular migration" rather than "molecular streaming".

The numbers appearing in this report are arbitrary; and any other set of parameters could have been used in the calculation. The values that should be chosen for the most efficient process is an objective in a proposed study program.

The ultimate practical uses of this theory in a system and the comparison of such a system with other devices

cannot be projected with any confidence at this time. It is hoped that as a result of a theoretical and experimental study such questions can be answered.

INTRODUCTION

The ideas expressed in this report were obtained from the classical kinetic molecular theory of gases. Originally, it was felt that perhaps some new or novel application of this theory could be made in the field of high-lift or vertical take-off and landing devices. Certainly, methods in current use in this field leave much to be desired although, in many respects, they are very satisfactory. The goal that was taken in this study was the re-examination of kinetic molecular theory to obtain different approaches to the problem of achieving high lift. This goal was subdivided into methods by which the normal statistical behavior of molecules could be influenced to provide preferential flow directions that either would yield less than normal energy input to produce the same effect or would give a more convenient configuration to produce the same effect.

This report describes one of the methods that appears to be theoretically feasible. It is based upon effusion theory which is discussed below. It should be pointed out that even though a practical configuration is described that utilizes the theory, the materials specified (as far as is known) are not now available; however, such materials are just beyond the present state-of-the-art. It is the present unavailability of materials which makes quantitative testing of the theory rather difficult; however, it is possible with current materials to perform some qualitative tests. This is being planned at the present time.

EFFUSION THEORY

If one considers the flow of gas through an opening in a dividing section between two closed containers at different pressures, the theory that is used to compute quantities of interest depend upon the size of the opening. If the opening is very large compared to the mean free path of the molecules (that average distance a molecule travels between collisions) ordinary hydrodynamical theory is used; if the opening is small when compared to the mean free path, effusion theory must be employed. As the hole size is increased from the small to the large, an intermediate type flow occurs.

Now consider the particular case when the flow of molecules is through holes that are small compared to the mean free path of the molecules. According to classical theory, the molecules, independently of one another, must come out in the form of a molecular stream each molecule moving with the speed it had when it came up to the opening. The loss of molecules now and then through the opening should affect the other molecules in the gas only slightly and this disturbance will be removed by the interactions of the other molecules in the neighborhood of the hole. These interactions always tend to maintain an equilibrium state. If there is a gas on each side of the hole, a process of effusion will take place in both directions independently of the other gas.

In a mass of gas in complete equilibrium, take a small plane area $\triangle S$. There are molecules crossing this area in each direction equally and continually. According to Maxwell-Boltzmann statistics, if there are n particles per unit volume, then

$$4\pi n A_v^2 e^{-\beta^2 v^2} dv \qquad (1)$$

are moving with speeds in the range between v and v + dv. n is the number of particles per unit volume;

$$A = \beta^3/\pi^{3/2}; \beta^2 = m/2kT; \qquad (2)$$

m is the molecular mass; and k is the Boltzmann constant. The net flow across $\triangle S$ is zero, but if one considers the number crossing from one side only, these molecules would compose an "effusive stream". The number crossing per unit area per unit time is defined as the random current density N.

These molecules are moving in all directions and to calculate the number crossing $\triangle S$ from one side only we consider the fraction of them incident on $\triangle S$ in directions which lie within a solid angle dw. Of these molecules, as many will cross during a time, $\triangle t$, as lie at the beginning of $\triangle t$ within a cylinder standing on $\triangle S$ as a base and having a slant height $v \triangle t$ and, therefore, a volume $\triangle S v \triangle t \cos \theta$.

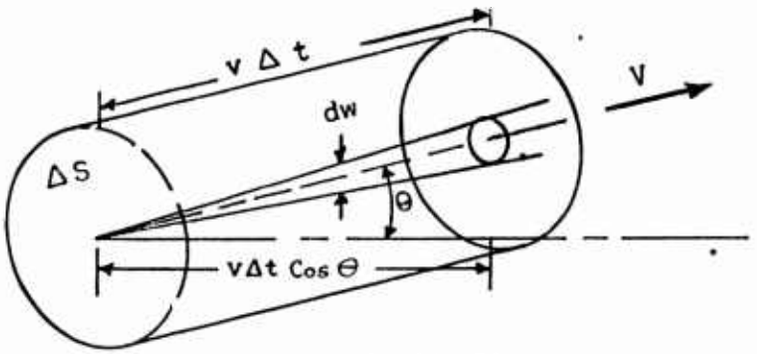

Figure 1. Velocity Diagram

The number, n', in this cylinder is, at the beginning of Δt,

$$n' = 4\pi n \; A \; v^2 e^{-\beta^2 v^2} \; dv \; \Delta S \; v \; \Delta t \; \cos\theta \qquad (3)$$

Therefore, if this is divided by ΔS, Δt, and 4π, the number crossing ΔS per unit area per unit time with speeds in the range v and v + dv becomes for a unit solid angle

$$n \; A \; v^3 e^{-\beta^2 v^2} \; \cos\theta \; dv$$

To obtain the random current density per unit solid angle j, this expression is integrated over all speeds.

$$j = \int_0^\infty n \; A \; v^3 \; e^{-\beta^2 v^2} \; \cos\theta \; dv \qquad (4)$$

Integrating by parts gives $\int_0^\infty v^3 \; e^{-\beta^2 v^2} \; dv = \frac{1}{2\beta^4}$ (5)

and j becomes

$$j = \frac{1}{2\beta^4} \; n \; A \; \cos\theta \qquad (6)$$

In spherical co-ordinates (with the normal to ΔS as the polar axis) an element of solid angle is given by

$$dw = \sin\theta \; d\theta \; d\phi \qquad (7)$$

The current density in dw is then

$$dN = j \; d \; w. \qquad (8)$$

Now an integration of dN over a hemisphere leads to the total random current density N.

$$N = \frac{1}{2\beta^4} \; n A 2 \int_0^{\pi} \int_0^{\frac{\pi}{2}} \text{Cos } \theta \text{ sin } \theta \, d\theta \, d\phi \qquad (9)$$

Since

$$\int_0^{\frac{\pi}{2}} \text{Cos } \theta \text{ sin } \theta \, d\theta = \frac{1}{2} \qquad (10)$$

the result is $N = \frac{\pi}{2} \frac{nA}{\beta 4}$ or $N = \frac{1}{4} n \bar{v}$ (11)

where $\bar{v}$ is the mean molecular speed is given by .

$$\bar{v} = \frac{2}{\sqrt{\pi}} \frac{1}{\beta} = 2 \sqrt{\frac{2kT}{\pi M}} \qquad (12)$$

According to this equation for N the rate of molecular flow in either direction across $\triangle S$ is the same as if the gas were moving bodily across it with a speed equal to one-fourth the mean speed of the molecules. This applies to a hole as well as the body of the gas.

In order to see what effect this theory would yield for possible applications, consider a container with a base that is of porous material the porosity of which is such that the ratio of opened to closed area is 1:10. A "mixing region" may be taken just under the container that has a volume equal to the area of the base times one mean free path. It appears that if a sufficient number of molecules can be added to this volume in the length of time that it takes a molecule to travel one mean free path, there should be a pressure increase since the pressure is proportional to the number of molecules. Taking the altitude of this volume to be one mean free path effectively confines the added molecules in the time element considered. Actually, the choice of one mean free path as the height of the mixing region was arbitrary; since the molecules entering the mixing region do so at all angles relative to the base of the container, this distance averaged could be somewhat smaller than one mean free path.

For the purpose of making an illustrative calculation, assume the following: A container having a cross section of one square foot and a vertical dimension very large compared to the mean free path; a pressure, P_1, and a

temperature, T_1, within the container of two atmospheres and 300°K, respectively; external to the container, ambient pressure, P_2, of one atmosphere and ambient temperature, T_2, equal to T_1; a porous base in the container with the sum of the pore area to be one-tenth the total area and the pore diameter to be one-tenth the mean free path; and a pumping system that supplies air in sufficient quantities to the container.

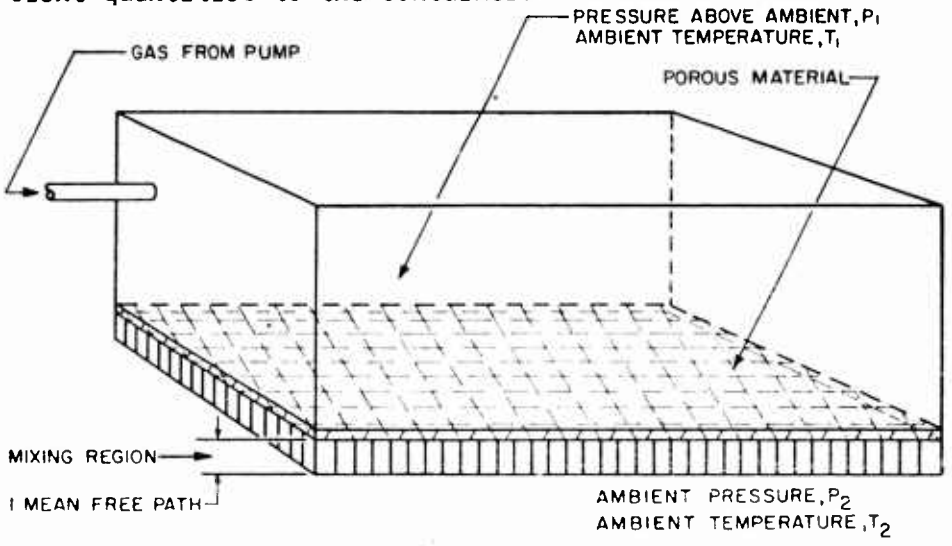

Figure 2. Effusion Chamber

Using the Maxwell-Boltzmann expression for mean free path within the container,

$$\bar{\lambda} = \frac{1}{\sqrt{2}\,\pi\, n\, \sigma}, \qquad (13)$$

when L is the mean free path, n is the density of particles, and σ is the molecular diameter. L is found to be 5.97×10^{-6} cm at 0° C. Correcting this using L proportional to $T^{\alpha + \frac{1}{2}}$ at constant pressure (α for air = 0.79),(Reference 20, page 149) the value of L at 27° C is 6.74×10^{-6} cm.

This gives 6.74×10^{-7} cm as the average pore diameter. The average molecular speed at the temperature, T_1, is

$$\bar{v} = \frac{2}{\sqrt{\pi}} \sqrt{\frac{2kT}{m}} = \frac{2}{\sqrt{\pi}} \sqrt{\frac{2R_M T}{M}} \qquad (14)$$

where R_M is the universal gas constant per gram molecular weight and M is the molecular weight

$$\bar{v} = \frac{2}{\sqrt{\pi}} \left[\frac{2 \times 83.15 \times 10^6 \times 300}{28.96}\right]^{\frac{1}{2}} \text{ cm/sec} \quad (15)$$

$$\bar{v} = 4.69 \times 10^4 \text{ cm/sec} \quad (16)$$

Therefore, the net rate of particle effusion across the porous material is given by

$$N_{net} = N_1 - N_2 = \frac{1}{4} \bar{v} (n_1 - n_2) \quad (17)$$

$$= \frac{1}{4} \times 4.69 \times 10^4 (4.888 \times 10^{19} - 2.444 \times 10^{19})$$

$$= 2.866 \times 10^{23} \text{ molecules/cm}^2\text{/sec}$$

The total area of the base is one square foot or 930 square centimeters. The pore area is one-tenth of this or 93 square centimeters. Therefore, the average excess of particles N_{ex} in the mixing region due to the effusion process is the product of the net rate of particle effusion, the average time

$$\frac{\bar{\lambda}}{\bar{v}}$$

that a particle remains in the mixing region, and the pore area.

$$N_{ex} = N_{net} \times \frac{\bar{\lambda}}{\bar{v}} \times \text{Area} \quad (18)$$

$$= 2.866 \times 10^{23} \text{ molecules/cm}^2\text{/sec} \times \frac{6.74 \times 10^{-6} \text{ cm}}{4.69 \times 10^4 \text{ cm/sec}} \times 93 \text{ cm}^2$$

$$= 3.84 \times 10^{15} \text{ molecules}$$

The volume V_M of the mixing region is equal to 930 square centimeters times $\bar{\lambda}$ which gives 6.27×10^{-3} cubic centimeters. The number of particles initially in the mixing region is given by

$$n_2 V_M = 6.27 \times 10^{-3} \text{ cm}^3 \times 2.444 \times 10^{19} \text{ molecules/cm}^3$$

$$= 15.3 \times 10^{16} \text{ molecules} \quad (19)$$

Therefore the ratio of the total number of molecules to the initial number of molecules in the mixing region is

$$\frac{15.3 \times 10^{16} + .384 \times 10^{16}}{15.3 \times 10^{16}} = 1.025 \quad (20)$$

Since in a perfect gas the pressure is directly proportional to the particle density, the above ratio gives an increase of pressure equal to 0.368 lb/in^2 or 53 lb/ft^2.

The mass flow rate to achieve this differential pressure may be computed by taking N_{Net}, the number of particles per cm^2 per second effusing from the container and multiplying by the total pore area:

$$\text{Mass/time} = N_{Net} A_p$$

$$\dot{M} = 2.866 \times 10^{23} \times 93 \tag{21}$$

$$\dot{M} = 266.5 \times 10^{23} \text{ molecules/sec}$$

or
$$\dot{M} = \frac{266.5 \times 10^{23} \text{ molecules/sec}}{6.023 \times 10^{23} \text{ molecules/mole}} \times 28.6 \text{ gm/Mole} \tag{22}$$

$$= 1265.5 \text{ gm/sec}$$

$$= 2.78 \text{ lb/sec}$$

At the pressures and temperature assumed, this would require input power of 114 Horsepower per square foot of lifting surface.

This effusion theory has been verified for conditions different than those assumed above and for applications that did not include lifting devices. Because of the lack of suitable materials in the past, experiments on effusion were conducted using reduced pressure so as to increase the mean free path and thereby, since pore size is proportional to $\bar{\lambda}$, to increase the required pore size. As stated previously, efforts are continuing to find a suitable material that will, at least, give qualitative verification of this theory.

THEORETICAL PHASE

The initial work accomplished in the theoretical phase of the Effusion Research Program consisted in part of calculating such quantities as molecular flow rates, pressure increase, and heat transfer rates. These calculations, based directly upon the ideas set forth in Report 516 above, will be found in the appendixes. It is believed that in each case sufficient explanation is included for proper understanding.

Materials Difficulties

During the first part of the program, reference materials pertaining to the kinetic theory of gases and to the effusion process were obtained. It subsequently became apparent from these references that a true experimental test of the lift theory could not be conducted with the porous materials obtained for the experiments. One of the reasons for this was that no material available was sufficiently thin to allow a true effusion process to take place. As is pointed out in Report 516 above, effusion takes place when the hole diameters are much smaller than the mean free path of the gas. However, in addition, the thickness must be much smaller than the hole diameter (Reference 26, page 22). For example, Knudsen (Reference 20, page 65) in work on effusion reported in 1909, used a hole roughly 0.025 mm. in diameter in a platinum strip 0.0025 mm. thick. His work confirmed effusion theory when the gas pressure was low enough that the mean free path of the gas was at least 10 times the diameter of the hole. Consequently, it is reasonable to assume that if the effusion-lift theory is to be tested at atmospheric pressure where the mean free path is approximately 10^{-5} cm., the hole diameter should be about 10^{-6} cm. and the thickness required is about 10^{-7}cm., which is of the order of atomic diameters.

The materials tested in the experimental phase of the Effusion Research Program met the pore diameter requirements, but ranged in thickness from about 15×10^{-3} cm. to about 0.15 cm. These materials obviously did not meet the thickness requirements for tests at atmospheric pressures. In fact, there is not presently available any porous material with the necessary thickness and it appears impossible to produce a material this thin which would be strong enough to withstand any appreciable pressure differential. In addition, the circuitous nature of the channels through even the thinnest porous media makes it impossible to achieve effusive flow, regardless of the pressures employed.

The relationships between mean free path, hole diameter, and thickness of the effusion material were used to estimate roughly an upper limit to the lift which might be obtained with presently available materials. For example, the thinnest porous material available is about 0.001 inch thick. This corresponds to a minimum mean free path in air of 0.1 inch or 0.254 cm. This in turn sets the maximum operating pressure inside the effusion chamber at approximately 4×10^{-5} atmospheres. Since it is unreasonable to

expect the lift to be greater than the magnitudes of the pressures involved, 4×10^{-5} atmospheres represents the upper limit of lift attainable.

These considerations led to the termination of the experimental phase of the effusion research program as of January 25, 1961. The theoretical phase was continued to study the validity of the lift theory and also to define better the materials characteristics best suited to demonstrate the lift effect.

This work has turned up several weaknesses in the original ideas involved in the lift theory as presented in Report 516.

Mixing-Region Concept And Mass Flow

A fundamental weakness is in the use of the "mixing-region" concept. The theory predicts a lift-pressure arising from the presence of excess molecules in the "mixing-region" adjacent to the external effusion surface. Reference to the theory indicates that this excess concentration is calculated by assuming that the molecules appearing in the mixing region because of the net effusive flow migrate out after spending an average time $\bar{\lambda}/\bar{v}$ in the mixing region. The length of the mixing region is taken as equal to $\bar{\lambda}$. These assumptions require that, on the average, these molecules speed out of the mixing region at a rate:

$$\frac{\text{Distance}}{\text{Time}} = \frac{\bar{\lambda}}{\frac{\bar{\lambda}}{\bar{v}}} = \bar{v} \quad \text{cm/sec} \qquad (23)$$

In the calculation made in Report 516, $\bar{v}$, the average molecular speed for air in the ambient region, is given as 4.69×10^4 cm/sec. This value is much too high for molecular "migration". More reasonable values, that is, those associated with diffusion, are of the order of 100 cm/hr. (Reference 26, page 66).

In addition to the weaknesses in the "mixing-region" concept, another shortcoming in the original theory is evident. This is the failure to take into consideration the effect of macroscopic mass flow of any excess molecules present in the region adjacent to the external effusion surface. The mass flow away from the external effusion surface would accompany any pressure increase in that region. Mass flow would be of much greater importance than diffusion in determining the average-excess concentration in this region.

Tube Model

The difficulties discussed above necessitated a re-examination of the effusion process as a means of producing lift. As a result, a new method,

which takes into account mass flow, was utilized to establish roughly upper limits to lift due to the external effect predicted in Report 516. The physical model used to make the calculations consists of an effusion chamber to which is attached a hollow cylindrical tube, as indicated in the diagram below.

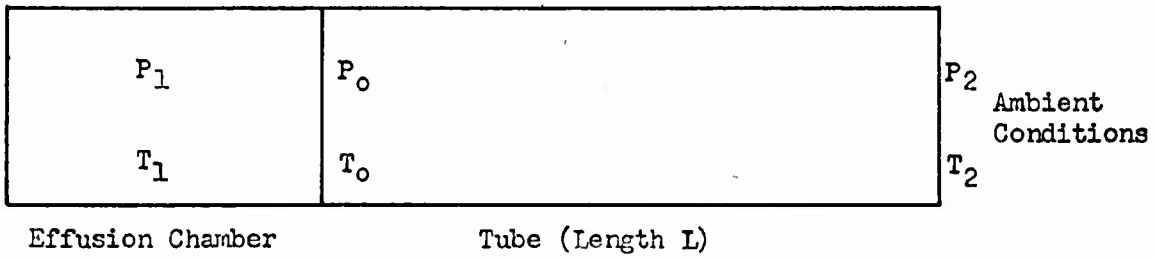

Figure 3. Effusion-Chamber with Tube

The effusion chamber is imagined as cylindrical also, permitting the tube, which is open at both ends, to surround completely the effusion surface. The calculations involve determining the value of P_o, which is the pressure at the external effusion surface, when steady-state flow conditions are achieved for various values of P_1, T_1, P_2, T_2 and L. P_o may then be compared with P_2 to indicate the pressure increase available.

The fundamental equation sets the net effusive flow rate (terms on left) equal to the rate of flow in the tube (term on right)

$$\frac{1}{4} n_1 \bar{v}_1 A^1 - \frac{1}{4} n_o \bar{v}_o A^1 = \frac{a^4 (P_o + P_2)(P_o - P_2)}{(2)(8)\eta k T L} \div \pi a^2 \quad (24)$$

The first and second terms on the left-hand side of the equation are effusion rates (molecules per second per square centimeter of effusion surface) out and into the effusion chamber, respectively. The term on the right-hand side of the equation is the well-known Poiseuille flow term, (Reference 26, page 47), giving in this case the molecular flow rate per unit cross-sectional area through a cylindrical tube of radius a and length L. P_o and P_2 represent the gas pressure at the ends of the tube. T is the temperature of the gas in the tube and η is the gas viscosity at temperature T. Maxwellian velocity distributions are assumed at both sides of the effusion surface, the internal conditions (P_1, T_1) being maintained by a suitable pumping mechanism. The calculations assume air as the gas used.

Appendix V contains a tabulation of the results of the calculations based upon the tube model.

Range and Method of Calculation

The calculations of P_o tabulated in Appendix V cover the following ranges:

L (cm.) = 50, 100

P_1 (atm.) = 0.0001, 0.001, 0.1, 2, 4

P_2 (atm.) = 0.000001, 0.00001, 0.0001, 0.001, 0.01, 1.0

T_1 (^oK) = 100, 273, 600

T_2 (^oK) = 100, 273, 300

T_o was calculated by the following scheme to reflect to some extent the effect of heat transfer to the tube:

for $T_1 = T_2$ $\quad T_o = 1.2\ T_2$

for $T_1 > T_2$ $\quad T_o = 1.2\ T_2$

for $T_1 < T_2$ $\quad T_o = T_2$

T, the temperature of the gas in the tube was taken as:

$$T = \frac{T_2 + T_o}{2} \qquad (25)$$

η, the viscosity, was taken to correspond to T. The above schemes for setting the values for T_o and T are somewhat arbitrary, however, it was found that the absolute values of P_o calculated from equation 24 are not highly sensitive to changes in T_o and T. The following table shows for one case the slight difference resulting from variations of T_o and T:

L (Cm.)	P_1 (Atm.)	P_2 (Atm.)	T_1 (^oK)	T (^oK)	η (Poises)	T_o (^oK)	T_2 (^oK)	P_o (Dynes/cm^2)
50	2	1	273	100	75×10^{-6}	120	100	1.0132001×10^6
50	2	1	273	100	188×10^{-6}	300	300	1.0132003×10^6

Discussion of Data

The general effect of decreasing L in the calculations is to yield lower values of P_o. Thus, the values of $(P_o - P_2)$ represent upper limits for the lift obtainable when effusion takes place directly into the ambient region.

For the same ambient and effusion chamber temperatures and pressures (not tabulated) used in the calculation of the Hayes Engineering Report 516, the tube-model equation above yields for L equal to 100 centimeters a P_o value of 1.0132001×10^6 dynes per square centimeter, an increase over ambient of about 0.00001%. This is to be compared with the 2.5% increase calculated by using the mixing-region concept under the same conditions.

These calculations utilize:

Tube Model	Report 516
$P_1 = 2$ Atm.	$P_1 = 2$ Atm.
$P_2 = 1$ Atm.	$P_2 = 1$ Atm.
$T_1 = T_2 = T_o = 300^oK$	$T_1 = T_2 = 300^oK$
$\eta = 188 \times 10^{-6}$ poises	
$L = 100$ cm.	

The greatest values of pressure differential $(P_o - P_2)$ obtainable from the data in Appendix V is 2.044×10^3 dynes per square centimeter, which equals 2.017×10^{-3} atmospheres or 4.27 pounds per square foot. This value is obtained by use of the following data:

T_o (^oK)	=	300
P_1 (Atm.)	=	4
T_1 (^oK)	=	100
P_2 (Atm.)	=	1/1000
T (^oK)	=	300^oK
η (Poises)	=	188×10^{-6}
T_2 (^oK)	=	273
L (Cm.)	=	100
P_o (dynes/cm^2)	=	3.0622717×10^3

The calculated value of lift equal to 4.27 pounds per square foot is not realistic because of the pressures involved in the calculations. As discussed above, no material is available, and probably none could be made to permit effusive flow at a pressure differential of four atmospheres.

For $P_1 = 10^{-4}$ atmospheres and $P_2 = 10^{-6}$ atmospheres, conditions roughly meeting the upper pressure limit imposed by the thickness of presently available materials, a value of $(P_o - P_2)$ equal to 12.89 dynes per square centimeter or .027 pound per square foot if obtained from the calculation using the tube-model equation. The following data are involved in the calculation:

T_o	(^oK)	=	300
P_1	(Atm.)	=	1
T_1	(^oK)	=	100
P_2	(Atm.)	=	1
T	(^oK)	=	300
η	(Poises)	=	188×10^{-6}
T_2	(^oK)	=	273
L	(Cm.)	=	100
P_o	(dynes/cm^2)	=	13.904749

EFFUSION TEST APPARATUS

A preliminary analysis of the effusion process indicated that it would be desirable to prove or disprove, by laboratory experimentation, the existence of a gross lift effect due to the effusion of gases through microporous media. The decision to test various microporous media required that two things be done. First, attempts had to be made to locate media with the optimum microporous characteristics. Second, an instrument had to be designed which would allow detecting any gross lift effect that might be exhibited as a result of gases effusing through various microporous media. An apparatus was designed and fabricated for this purpose.

Design Characteristics

The effusion test apparatus consists of three principal parts; namely, (1) a gas-flow, pressure-indicating and control panel, (2) a plenum and microporous-media-supporting chamber, and (3) a device for measuring the force resulting from the effusion process. These three components were designed to meter the flow of gas through the microporous media, to indicate the pressure within the plenum chamber immediately before the gas passes through the porous media, and to indicate the magnitude and direction of any force acting upon the media under test.

The control panel shown in Figure 4 has as a composite part of it a flow meter which registers a flow of air from 0 to 4400 standard cubic inches per minute for a gas with a specific gravity of 1.0 and measured at 14.7 pounds per square inch at a temperature of 70° F. Also a part of the panel are two pressure regulators, one of which regulates the high pressure to a plenum tank and air filter behind the panel and the other of which controls the pressure to the plenum chamber holding the porous media. There is a pressure gauge associated with the pressure regulator on the high pressure side of the line. There are three pressure measuring instruments associated with the low pressure air directed to the porous media under test. These instruments are a dial pressure gauge, a mercury manometer, and a water manometer. Each of the three pressure measuring decives are connected to a pressure probe within the plenum test chamber immediately upstream from the location where the microporous test media are placed.

The principal part of the effusion test apparatus is the effusive-lift test chamber. This part of the apparatus is the rectangular box attached to a long bar as shown in Figure 4. A more detailed view of this portion of the test apparatus is shown in Figures 5 through 9. Figure 5 shows the air inlet tubes and support frame for the air diffuser plate. The diffuser plate is shown in Figure 6. Placed upon the diffuser plate is the support frame upon which the microporous media are placed. The plenum chamber is divided into four compartments because of the limited size of the microporous media obtainable. The support

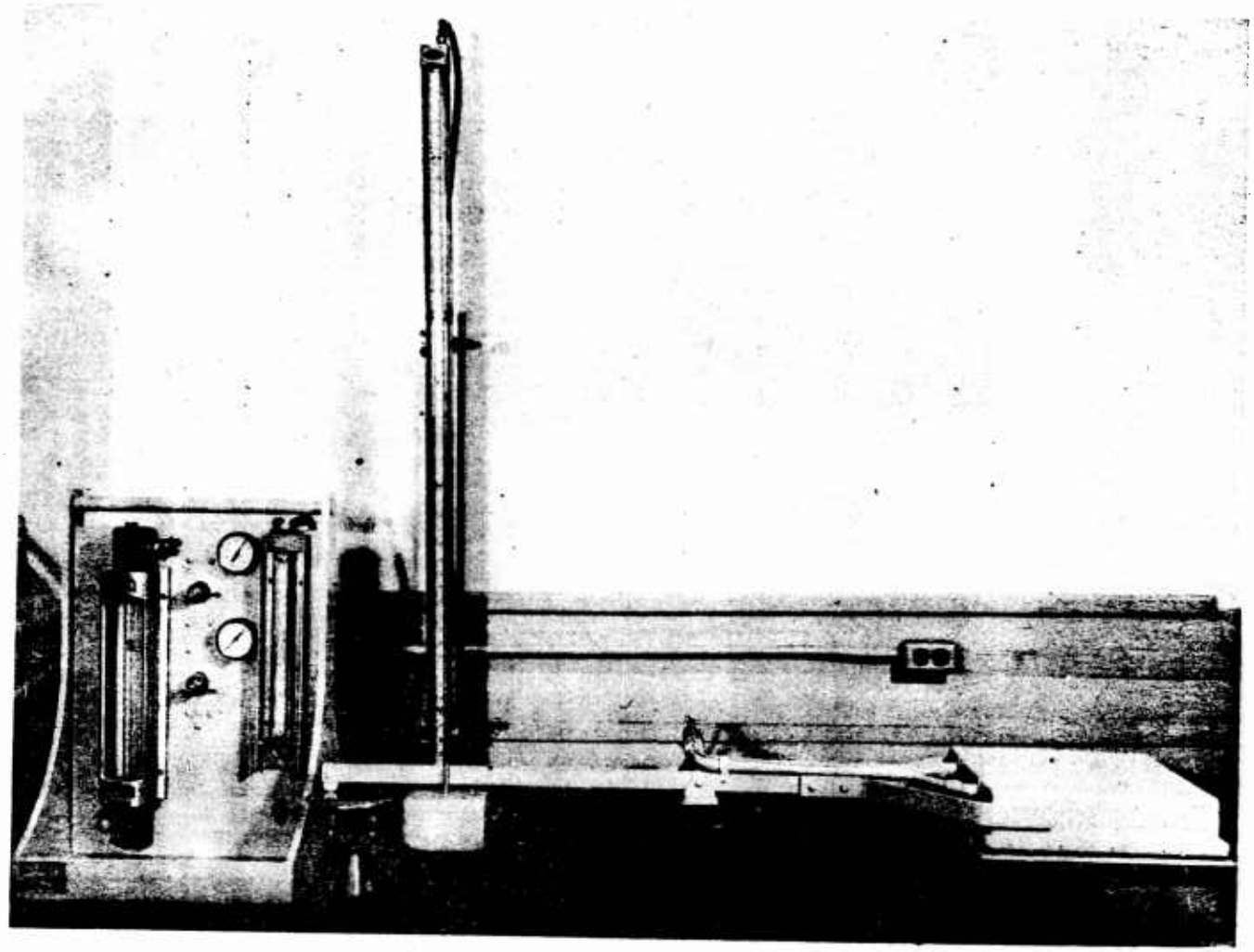

Figure 4. Effusion Test Apparatus.

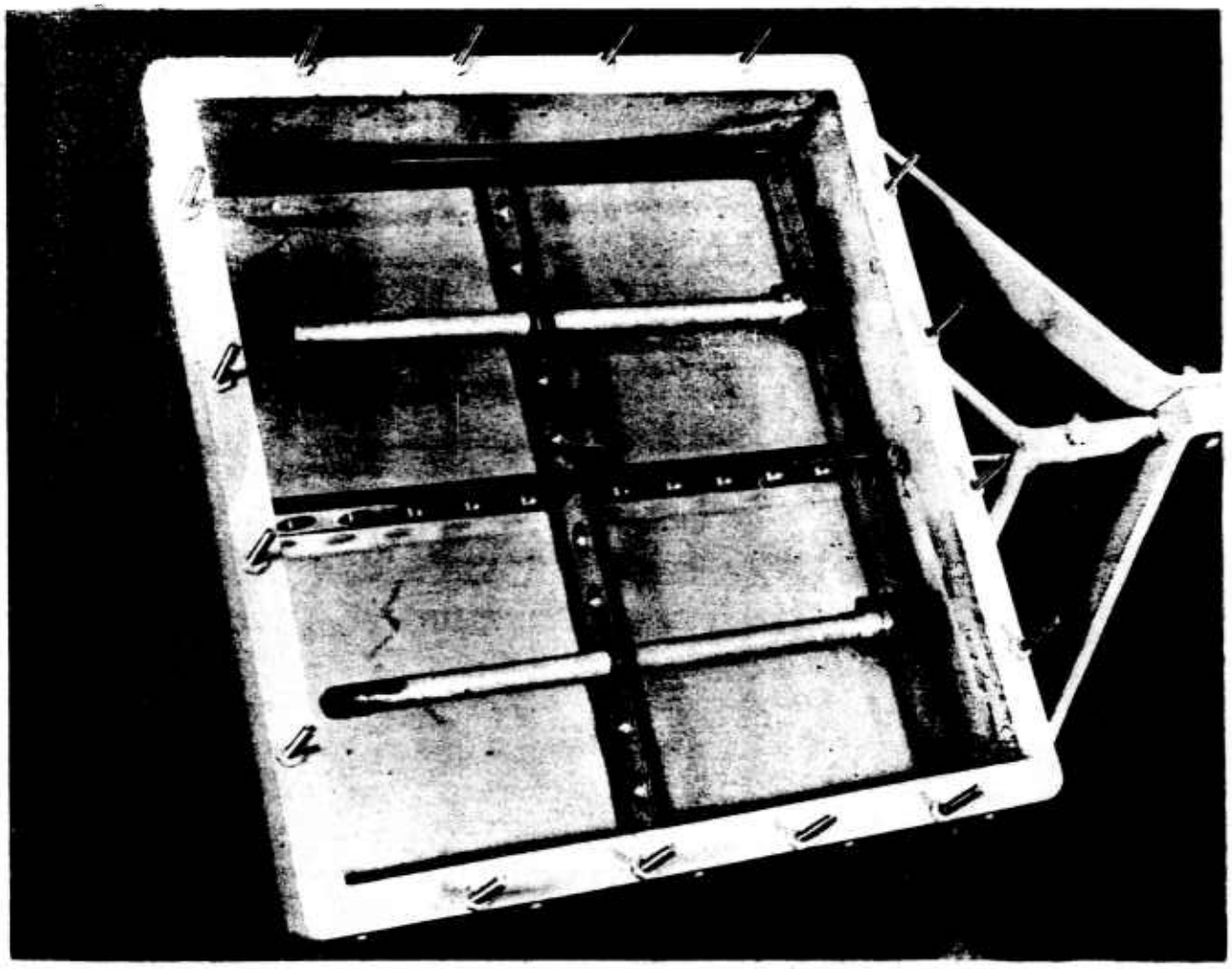

Figure 5. Air Distribution Tubes Within the Test Chamber of the Effusion Test Apparatus.

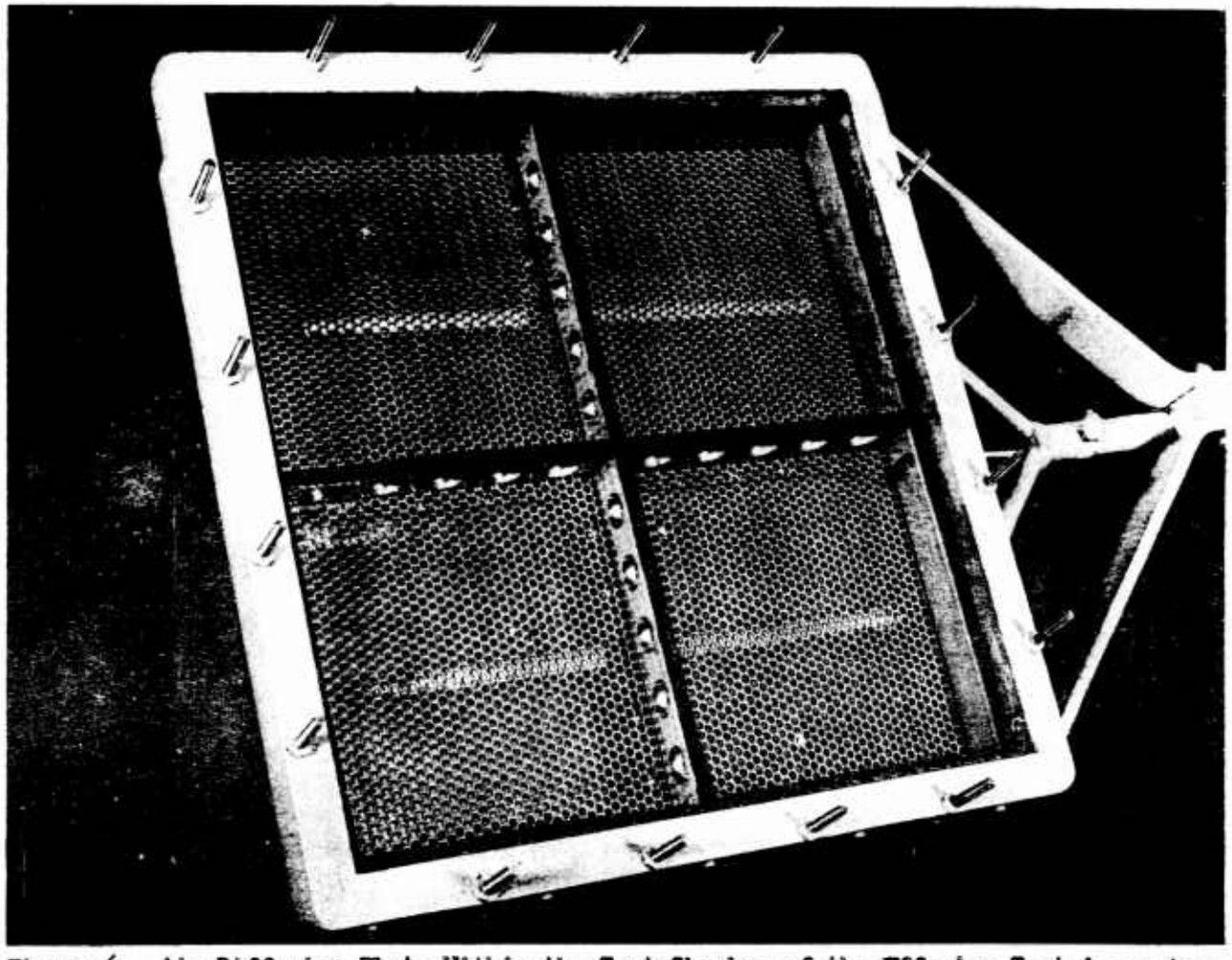

Figure 6. Air Diffusion Plate Within the Test Chamber of the Effusion Test Apparatus.

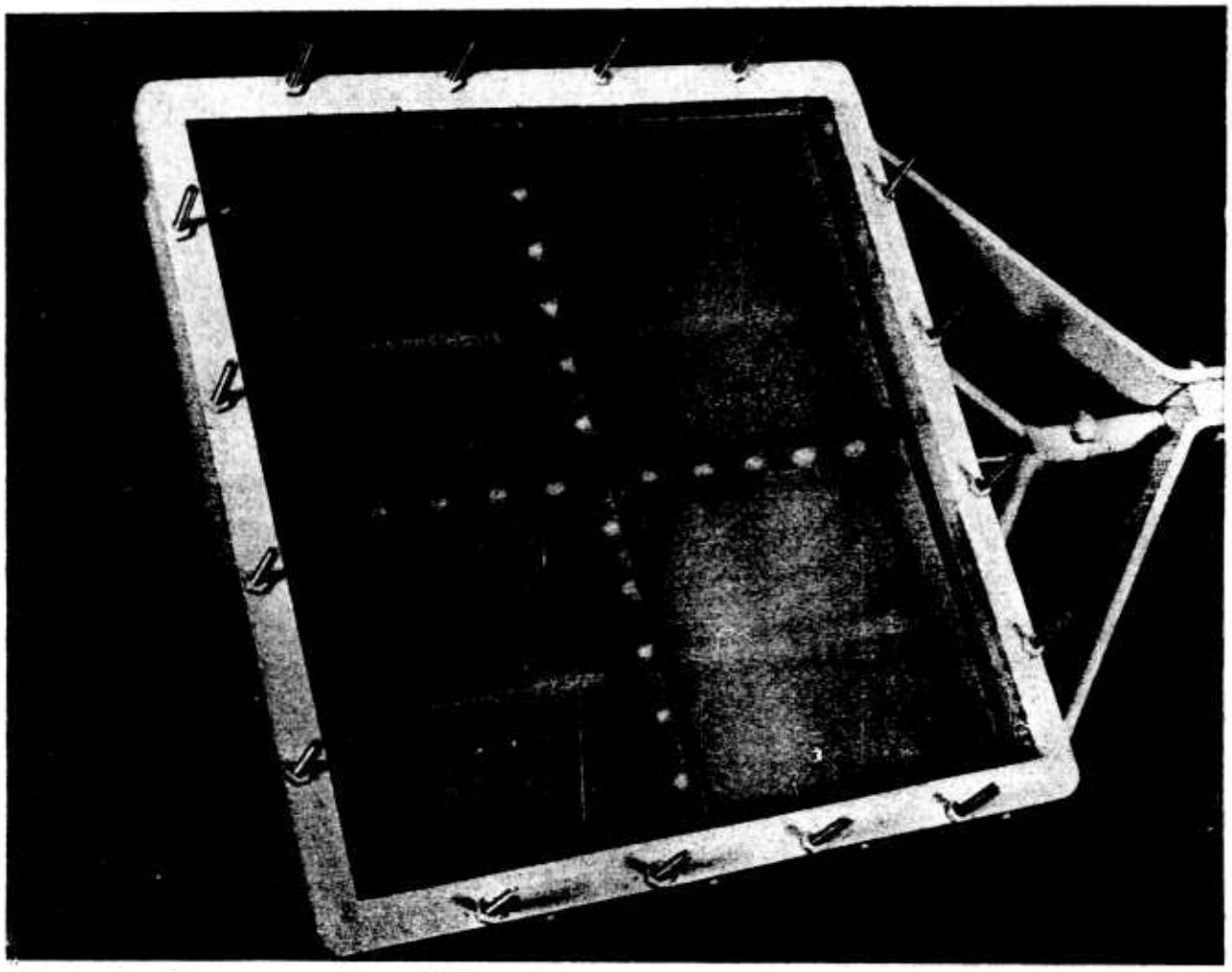

Figure 7. Microporous Glass Within the Test Chamber of the Effusion Test Apparatus.

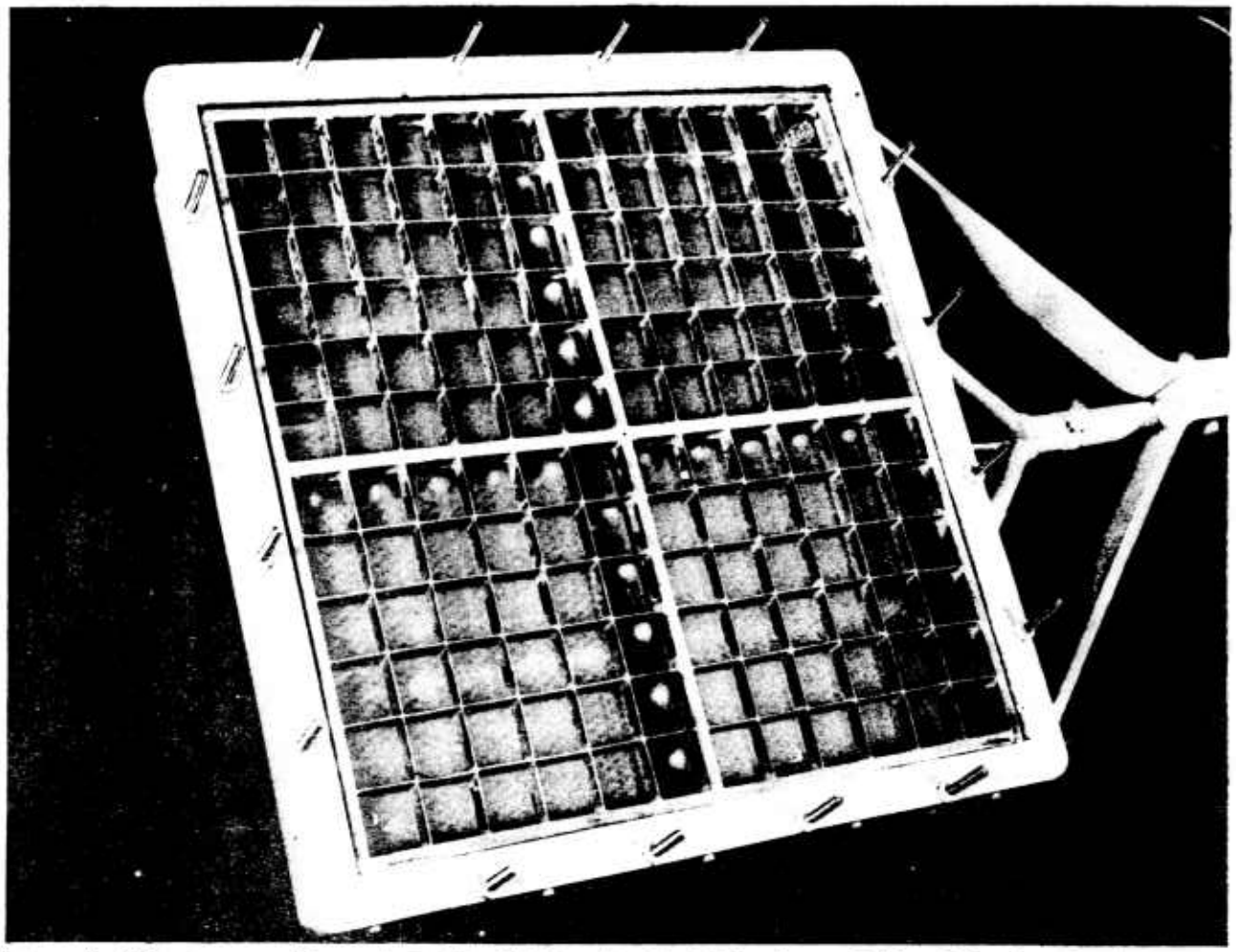

Figure 8. Microporous Support Grill Within the Test Chamber of the Effusion Test Apparatus.

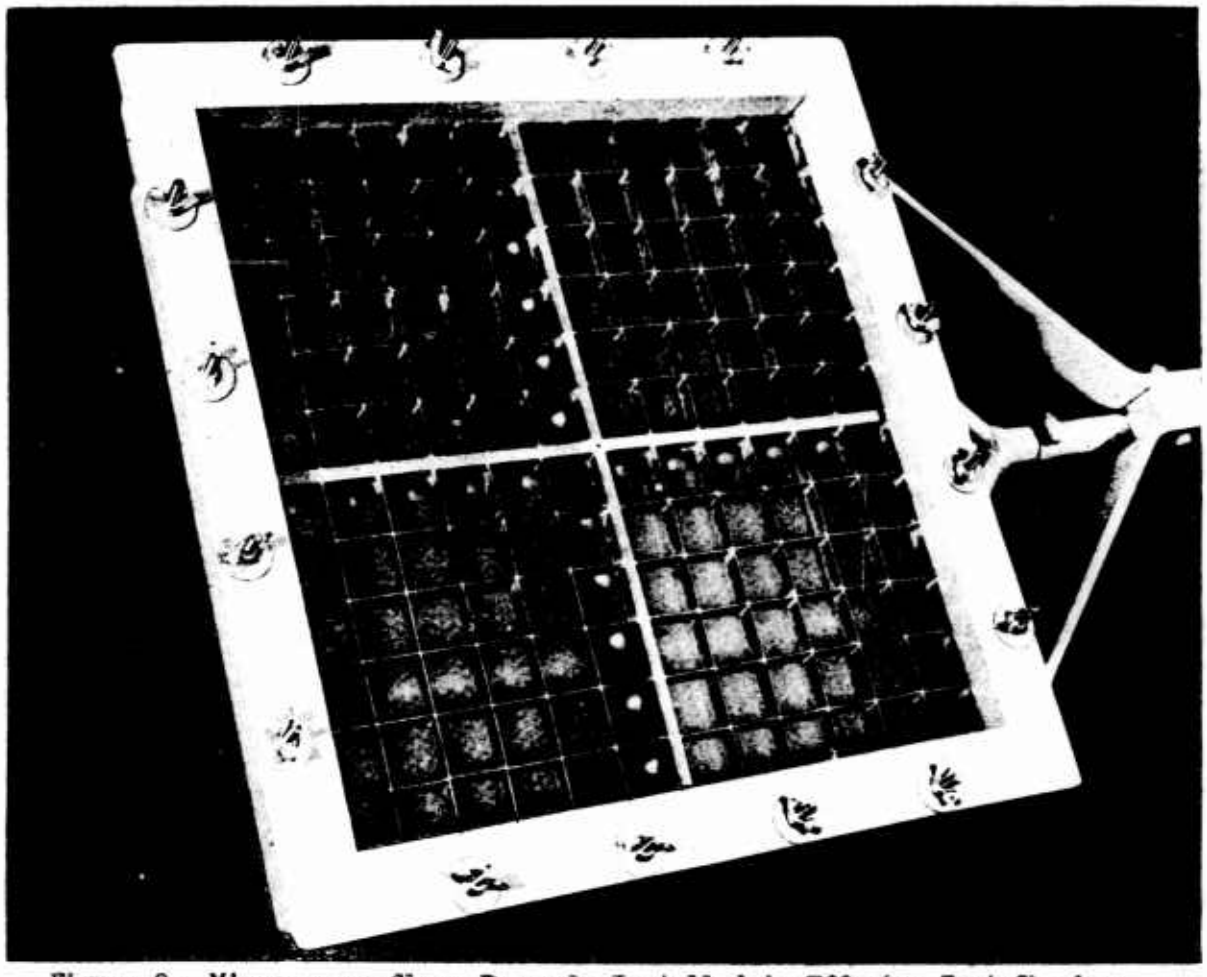

Figure 9. Microporous Glass Properly Installed in Effusion Test Chamber

frame allows space for four square sections of porous media measuring 6½ inches on each side, which consequently allows a total effective test area of one square foot. Figure 7 shows the manner in which the four panels of porous material fit into the framework of the test chamber. The particular medium shown in this figure is that of the Vycor code 7930 microporous glass. Figure 8 illustrates the manner in which the one inch square grill support fits over the medium being tested. The overall dimensions of the test chamber provide effective open area of one square foot. Figure 9 shows the way the whole unit is held firmly together by means of a square frame and 16 wing nuts.

The method of holding the porous glass, sintered stainless steel and nickel as shown in Figure 9 was not adequate for holding the porous cellulosic medium in the test chamber. Figures 10 and 11 illustrate the technique employed to hold the extremely fragile microporous cellulosic medium in place under test. Because of the area occupied by the support grill, the effective test area was reduced 35% by the circular matrix medium used in Figure 10 and only 18% by the square matrix grill used in Figure 11. This means of supporting the fragile, thin cellulose sheet was most successful.

The lift measuring technique employed consisted of balancing the test chamber on one end of a lever arm as shown in Figure 4. The opposite end of the balanced arm was allowed to rest on the weighing pan of a trip-beam balance. This arrangement provided an adequately sensitive means of measuring the force exerted on the microporous medium as a result of gases effusing through the microporous medium. The measuring technique was found to give a reproducible sensitivity of 0.1 gram.

Operating Characteristics

After the microporous medium was securely placed within the test chamber, the counterbalance on the lever arm opposite the test chamber was adjusted in such a manner as to place the trip-beam balance in a neutral position. The balance reading was then recorded. The flow of air through the system was regulated in stages to allow taking readings of the air flow, test-chamber air pressure, and balance deflection at each stage of adjustment. Most measurements were taken by increasing the pressure to specified inches of water or mercury, holding the pressure at that level while readings were taken of the air flow and the balance deflection. The pressure was increased step-wise until the pressure limit of the test chamber was reached or until the fracture limit of the microporous medium was attained. Each microporous medium was tested a sufficient number of times to be sure of obtaining reproducible results.

MICROPOROUS EFFUSION MEDIA

The principal problem associated with the materials phase of the project

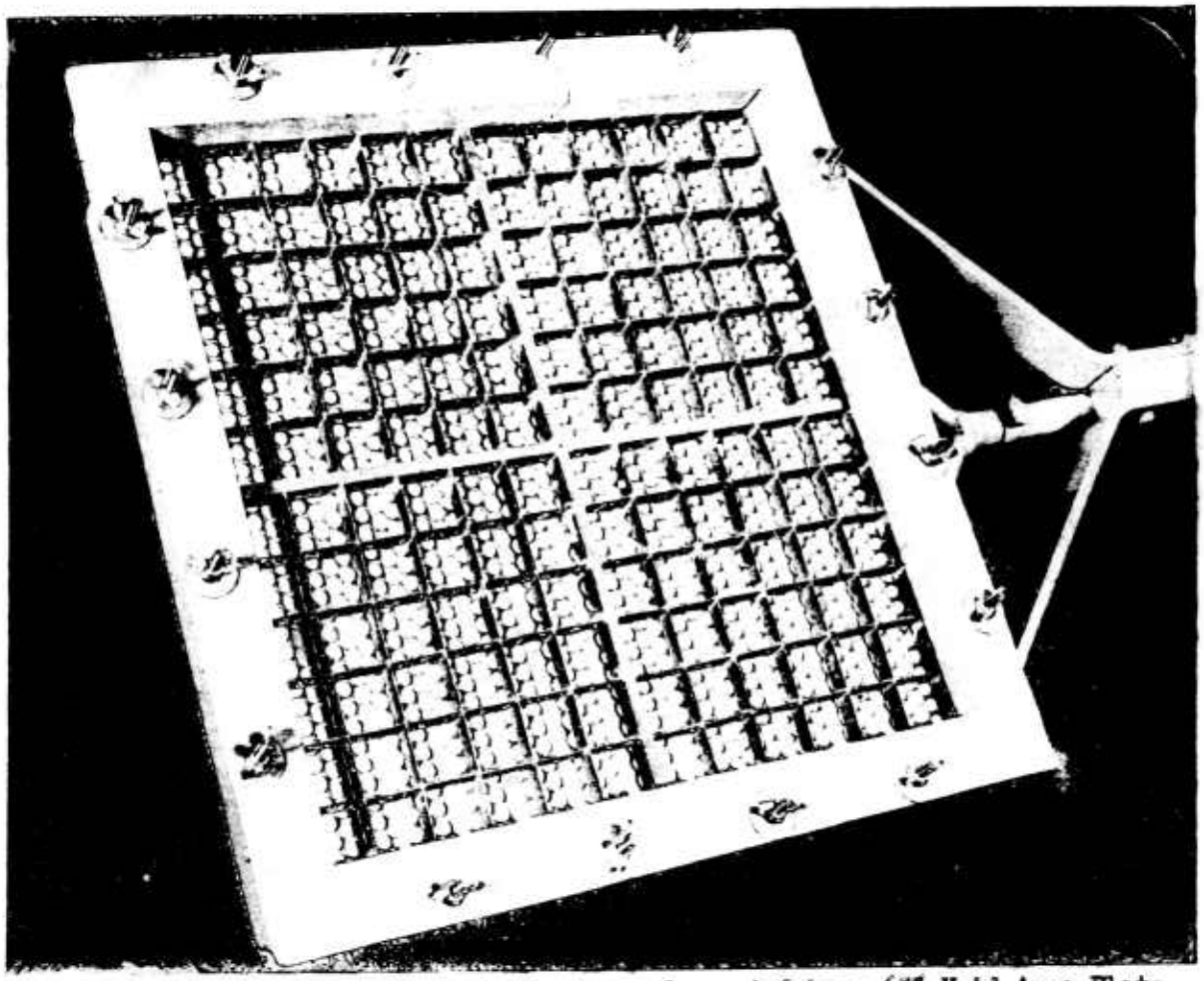

Figure 10. Microporous Cellulosic Membrane Supported by a 65% Void Area Plate in Effusion Test Chamber.

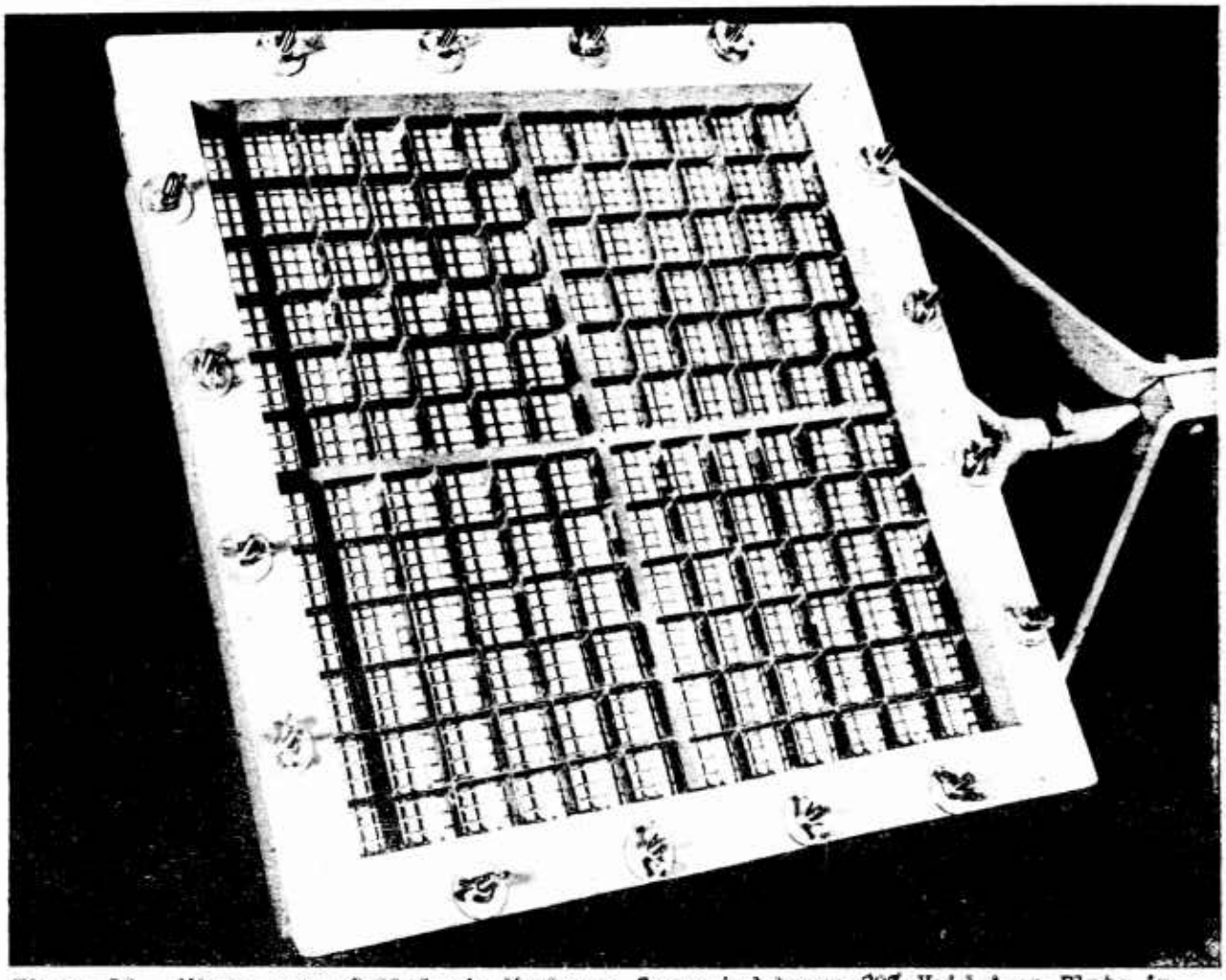

Figure 11. Microporous Cellulosic Membrane Supported by an 82% Void Area Plate in Effusion Test Chamber

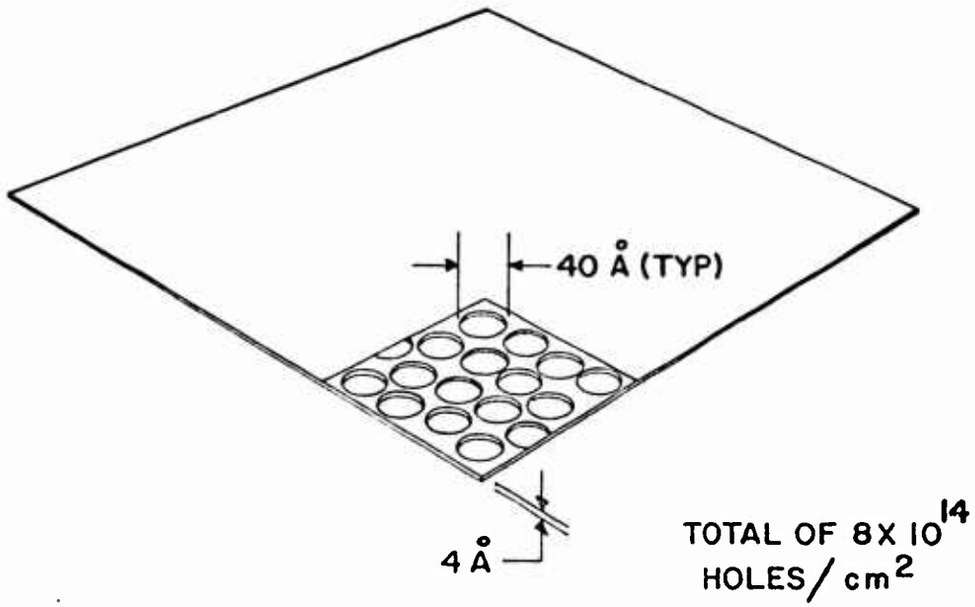

Figure 12. Ideal Porous Medium Characteristics for Effusion at Atmospheric Pressure.

was that of obtaining microporous media with the optimum characteristics to exhibit properly a reaction force resulting from the effusion process. The theoretical investigation conducted concurrently with the materials-selection work suggested certain appropriate microporous characteristics. These optimum characteristics were reviewed in detail with the prospective manufacturers of microporous media.

Materials Selection Criteria

In negotiating with manufacturers of microporous media, five factors were involved. These five characteristics were the ideal sought in order to meet properly the conditions required for obtaining a gross lift effect by the effusion process.

1. The microporous medium should possess pore diameters within the range of 30 to 60 angstroms at the surface of the medium. The pore paths through the medium should be tubular and as perpendicular to the surface as possible, rather than assuming a circuitous path which would offer greater resistance to gas flow through the material.

2. The porosity should be such that there are a minimum of 8×10^{14} holes/cm^2 or a minimum of 10% void area at the surface of the medium. The higher the pore population, the more effectively the microporous medium can serve to meet our established objectives.

3. The flow rate of gas through the medium should be the maximum obtainable with the pore characteristics listed above. Ideally this value should be 2.8 lbs/ft^2/sec.

4. The medium should possess sufficient strength to withstand an absolute pressure differential of one atmosphere. However, the material should be as thin as possible.

5. The porous medium must be in flat sheet form for the application involved. It is desirable that the sheets be as large as possible.

The illustration found in Figure 12 graphically depicts the ideal porous medium desired in order to exhibit adequately the optimum effusion reaction at atmospheric pressure.

Materials Procurement

In an effort to find the optimum microporous medium, nineteen different companies and four consultants in the field were contacted. The following is a list of these contacts.

1. Aircraft Porous Media, Inc.
   Glen Cove, New York

2. ASCO Sintering Corporation
   7799 Telegraph Road
   Los Angeles 22, California

3. Barnstead Still & Sterilizer Co.
   2 Lanesville Terrace
   Boston 31, Massachusetts

4. Bendix Aviation Corporation
   Filter Division
   Madison Heights, Michigan

5. Briggs Filtration Company
   River Road
   Washington 16, D. C.

6. Charles Hardy, Inc.
   420 Lexington Avenue
   New York 17, New York

7. Corning Glass Works
   Corning, New York

8. Cuno Engineering Corporation
   Meriden, Connecticut

9. ESB-Reeves Corporation
   323 West Glenside Avenue
   Glenside, Pennsylvania

10. Gelman Instrument Company
    Chelsea, Michigan

11. Harman Equipment Company
    Los Angeles, California

12. Halex Corporation
    2120 Fairmont Avenue
    Reading, Pennsylvania

13. Hercules Powder Company
    Wilmington, Delaware

14. Isocyanate Products, Inc.
    P. O. Box 1681
    Wilmington, Delaware

15. Linde Company
P. O. Box 44
Tonawanda, New York

16. Millipore Filter Corporation
Bedford, Massachusetts

17. Mott Metallurgical Corporation
272 Huyshope Avenue
Hartford 14, Connecticut

18. Purolator Products, Inc.
Rahway, New Jersey

19. United States Rubber
Textile Division
1230 Avenue of the Americas
New York 20, New York

20. Mr. Henry Marsh
Former Chief of Army Research
(Consultant)

21. Dr. Thomas C. Franklin
Baylor University
Department of Chemistry
Waco, Texas
(Consultant)

22. Dr. S. Loeb
University of California
Department of Engineering
Los Angeles 24, California
(Consultant)

23. Mr. A. J. Langhammer
2343 Crooks Road
Royal Oaks, Michigan
(Consultant)

As a result of these contacts four companies supplied microporous media which were used in the laboratory-evaluation phase of this project. The characteristics of the materials supplied by these companies are itemized in Table 1.

TABLE 1

CHARACTERISTICS OF MICROPOROUS MEDIA TESTED

Suppliers	Aircraft Porous Media, Inc.	Corning Glass Works	Mott Metallurgical Corporation	Millipore Filter Corporation
Composition of Porous Medium	Nickel Sintered to Wire Mesh Backing	Code 7930 Vycor Glass	Laminated Stainless Steel	Cellulosic Membrane
Thickness of Porous Medium	0.047"	0.060"	0.005" Fine 0.063" Course	150 Microns
Dimensions of Porous Plates	6½" x 6½"	6½" x 6½"	6½" x 6½"	12" Circles
Pore Population of Porous Medium	Approximately 1.6×10^{11} Holes/cm^2	Approximately 2×10^{12} Holes/cm^2	Approximately 8×10^{10} Holes/cm^2	Approximately 6.4×10^{11} Holes/cm^2
Pore Dimensions of Porous Medium	Uncertain	30-60 Angstroms	Uncertain	80-120 Angstroms
Pore Path Through Medium	Extremely Circuitous	Randomly Tubular	Extremely Circuitous	Randomly Tubular
Percent Void Volume of Medium	Approximately 10%	28%	Less Than 10%	80-85%
Density of Porous Medium	Approximately 8.0 Gms/cm^2	1.5 Gms/cm^2	Approximately 7.4 Gms/cm^2	Unknown
Air Flow Through Medium	Approximately 442.7 SCFM/ft^2	37.8 SCIM/ft^2	Approximately 38.7 SCFM/ft^2	4.01 CFM/ft^2 @ 13.5 psi & 25° C
Water Flow Through Medium	Unknown	0.00065 ml/ cm^2/Atmos./ hour	Unknown	1.1 cc/cm^2/min @ 13.5 psi & 25° C
Maximum Temperature Endurance, °F	1100° F	1742° F	1650° F	257° F
Degree of Hygroscopicity	Negligible	Extremely Hygroscopic	Negligible	Fairly Hygroscopic
Strength of Porous Medium	Ductile & Strong	Fairly Brittle	Fragile for Sintered Metal	Extremely Fragile
Manufacturing Technique	Sintering Granular Nickel	Caustic Leaching of Vycor Glass	Sintering Granular S.S.	Paper Manufacturing Technique

LABORATORY EVALUATION PROCEDURE

The laboratory evaluation consisted of placing the four types of microporous materials obtained into the testing apparatus previously described and checking for indications of a force resulting from the effusion of gases through the media.

Installation of Microporous Media

Extreme precautions had to be exercised in placing the microporous media into the effusion test apparatus. This was particularly true in the case of the 150 micron thick cellulosic material and the 1.5 millimeter-thick porous glass plates. The sintered stainless steel and nickel composing the effusion surface of these two types of material were also fragile, and had to be handled with care. Once the samples were in place within the test apparatus there was very little trouble encountered in testing the various media.

Test-Apparatus Check-Out

The first step in checking the installed microporous media within the effusion test apparatus was to check for leaks within the system. The smallest leak in any area of the test chamber was found to exhibit a reaction force, depending upon the direction of the jet of escaping gas. After all leaks were stopped, the microporous materials were tested in a stepwise fashion described in a preceding section of this report.

EXPERIMENTAL RESULTS

The purpose of the laboratory evaluation phase of this project was to determine whether or not a gross lift effect would be exhibited as a result of the effusion process. Table 1, previously referred to, shows the flow obtained through the four microporous media tested. All materials were subjected to air flow and pressure in a stepwise fashion as previously described. None of the four microporous media tested exhibited a lift force greater than 0.1 gram (the sensitivity of the test apparatus). The results of the tests indicate that there was no gross lift effect present at any stage of the testing.

BIBLIOGRAPHY

1. Amberg, C. H., and McIntosh, R., "A Study of Adsorption Hysteresis by Means of Length Changes of A Rod of Porous Glass", Canadian Journal of Chemistry, Volume 30, 1952, pp. 1012-1032.

2. Bhatnagar, P. L., Gross, E. P., Krook, M., "A Model for Collision Processes in Gases. I. Small Amplitude Processes in Charged and Neutral One-Component Systems", Physical Review, Volume 94, Number 3, May 1, 1954, pp. 511-525.

3. Buckingham, Edgar & Edwards, J. D., "Efflux of Gases Through Small Orifices", Scientific Papers of the Bureau of Standards, Volume 15, 8 May 1919, pp. 573-622.

4. Clausing, P., "Concerning the Shape of Beams Formed by Molecular Flow", Z. Physik, Volume 66, October 1930, pp. 471-476.

5. Cowling, T. G., Molecules in Motion, First Edition, Harper & Brothers, New York, N. Y., 1960.

6. Dushman, Saul, Scientific Foundations of Vacuum Technique, John Wiley & Sons, Inc., New York, N. Y., 1960.

7. Emmett and Cines, "Adsorption of Argon, Nitrogen and Butane on Porous Glass", Journal of Physical and Colloid Chemistry, Volume 51(6), 1947, pp. 1248.

8. Freeman, R. D., and Search, A. W., "The Effect of Channel Holes on the Force Exerted by Effusing Vapors", Journal of Chemical Physics, Volume 22, April 1954, pp. 762-763.

9. Hagerbaumer and Kammermeyer, "Separation of Azeotropes by Diffusion Through Porous Membranes", Chemical Engineering Progress Symposium No. 10, Collected Research Papers, Volume 50, 1954, pp. 25.

10. Hancher and Kammermeyer, "Semiautomatic Gas Separation Equipment", Analytical Chemistry, Volume 27, 1955, pp. 83.

11. Harris and Emmett, "Physical Adsorption of Nitrogen Toluene Benzene, Ethyl Iodide, Hydrogen Sulfide, Water Vapor, Carbon Disulfide and Pentane on Various Porous and Non-Porous Solids", Journal of Physical and Colloid Chemistry, Volume 53(6), 1949, pp. 811.

12. Harris, Frank E., and Nash, Leonard K., "Microeffusiometry of Gaseous Mixtures", Analytical Chemistry, Volume 22, Number 12, December 1950, pp. 1552-1556.

13. Howard, W. M., "Density Field Flow Through an Orifice", Physics of Fluids, Volume 4(4), 1961, pp. 521-524.

14. Jayner and Emmett, "Differential Heats of Adsorption and Description of Nitrogen on Porous Glass", Journal of American Chemical Society, Volume 70, 1948, pp. 2359.

15. Jeans, J. H., An Introduction to the Kinetic Theory of Gases, First Edition, Cambridge University Press, New York, N. Y., 1940.

16. Jeans, J. H., The Dynamical Theory of Gases, Fourth Edition, Dover Publications, Inc., London, England.

17. Kammermeyer and Brubaker, "Membrane Separation in the Gaseous Phase", Chemical Engineering Progress, November 1954, pp. 560.

18. Katz, "Permanent Hysteresis in Physical Adsorption", Journal of Physical and Colloid Chemistry, Volume 53(8), 1949, pp. 1166.

19. Kennard, E. H., "Entropy, Reversible Processes and Thermo-Couples", Proceedings of National Academy of Science, Volume 18, 1932, pp. 237-245.

20. Kennard, Earle H., Kinetic Theory of Gases, McGraw-Hill Book Company, Inc., New York, N. Y., 1938.

21. Knudsen, Martin, "Molecule Streaming of Hydrogen Through Tubes and the Hot Wire Manometer", Annalen der Physik, Volume 35, May 1911, pp. 389-396.

22. Knudsen, Martin, The Kinetic Theory of Gases, Methuen & Company Ltd., London 1934.

23. Knudsen, Martin, "Experimental Determination of the Pressure of Saturated Mercury Vapor at 0° C Temperature and Higher", Annalen der Physik, Volume IV, Number 29, March 1909, pp. 179-193.

24. Langmuir, Irving, "The Vapor Pressure of Metallic Tungsten", Physical Review, Volumn II, Number 5, November 1913, pp. 329-342.

25. Mayer, Herbert, "The Validity Limits of the Cosine Law for Molecular Flow", Z. Physik, Volume 58, 30 May 1929, pp. 373-385.

26. Present, R. D., Kinetic Theory of Gases, McGraw-Hill Book Company, Inc., New York, N. Y., 1958.

27. Rice, O. K., "Irreversible Processes with Application to Helium II and the Knudsen Effect in Gases", Physical Review, Volume 89, Number 4, February 1953, pp. 793-799.

28. Schwertz, "Fluid Flow Study of Porous Glass", Journal of American Ceramics Society, Volume 32, 1949, pp. 390-393.

29. Sears, G. W., "A Note on the Flow of Gases through Very Fine Tubes", The Journal of Chemical Physics, Volume 22, Number 7, July 1954, pp. 1252-1253.

30. Sutherland, B. P., and Maass, O., "Measurement of the Viscosity of Gases Over a Large Temperature Range", Canadian Journal of Research, Volume 6, 2 March 1932, pp. 428-443.

31. Wessel, Gunter, "Measurement of Steam Pressure and Condensation Coefficient of Iron, Cadmium, and Silver", Z. Physik, Volumn 130, July 1951, pp. 539-548.

32. Wilson, L. H., Sibbitt, W. L., and Jakob, M., "Flow of Gases in Porous Media", Journal of Applied Physics, Volume 22, Number 8, August 1951, pp. 1027-1030.

33. Yates, D. J. C., "The Influence of the Polar Nature of the Adsorbate on Adsorption Expansion", Journal of American Physical Society, Volume 60(5), 1956, pp. 543.

34. Yates, D. J. C., "The Expansion of Porous Glass on the Adsorption of Non Polar Gases", Proceedings of the Royal Society of London, Volume 224, 1954, pp. 526-544.

35. Zartman, I. F., "A Direct Measurement of Molecular Velocities", Physical Review, Volume 37, 15 February 1931, pp. 383-391.

36. Zhdanov, "Comparative Investigation of the Structure of Porous Glass by Adsorption Methods and Under the Electron Microscope", Doklady Akademii Nauk USSR New Series, Volume 82, 1952, pp. 281.

APPENDIX I, CALCULATIONS OF MEAN FREE PATH IN AIR

This appendix contains a formula for determining the mean free path in air. A sample calculation, data table, and two graphs drawn from the data are also included.

$\bar{\lambda}$ CALCULATION FOR AIR

$$\bar{\lambda} = \frac{\eta}{.499 \rho \bar{v}}$$

let .499 be rounded off and written as $\frac{1}{2}$

$$\bar{\lambda} = \left[\frac{2}{mN\bar{v}}\right] \eta$$

where $N = \left[\frac{273^\circ K \; N_{STP}}{1 \text{ atm}}\right] \frac{P}{T}$

$$\bar{v} = 2 \left[\frac{2k}{\pi m}\right]^{\frac{1}{2}} T^{\frac{1}{2}}$$

$$\bar{\lambda} = \left[\frac{1}{m^{\frac{1}{2}} \left(\frac{273^\circ K \; N_{STP}}{1 \text{ atm}}\right) \left(\frac{2k}{\pi}\right)^{\frac{1}{2}}}\right] \left[\eta \, T^{\frac{1}{2}}\right] \frac{1}{P} \qquad (26)$$

SAMPLE CALCULATION OF

$$\bar{\lambda} = (48.11 \times 10^{-24})^{\frac{1}{2}} (273)(2.687 \times 10^{19})(2.76 \times 10^{-16}/\pi)^{\frac{1}{2}} \left[\eta \, T^{\frac{1}{2}}\right] \frac{1}{P}$$

$$\bar{\lambda} = 2.09 \times 10^{-3} \left[\eta \, T^{\frac{1}{2}}\right] \frac{1}{P}$$

where $\eta = 170.8 \times 10^{-6}$ Poises

$T = 273.16^\circ K$

$P = 1$ atm

$$\bar{\lambda} = 2.09 \times 10^{-3} \; (170.8 \times 10^{-6}) \; (273.16)^{\frac{1}{2}}$$

$$\bar{\lambda} = 5.88 \times 10^{-6} \text{ cm} \qquad (27)$$

TABLE 2

$\overline{\lambda}$ DETERMINATION FOR AIR AT 1 ATMOSPHERE PRESSURE

η (Micropoises)	T (°K)	$\overline{\lambda}$ (cm x 10^{-6})
55.1	78.96	1.02
62.7	90.06	1.24
113.0	169.06	3.06
133.3	203.76	3.97
153.9	241.56	4.99
170.8	273.16	5.88
182.7	291.16	6.50
195.8	313.16	7.22
195.8	327.16	7.38
210.2	347.16	8.17
263.8	502.16	12.32
312.3	607.16	16.04
317.5	630.16	16.61
341.3	682.16	18.58
350.1	739.16	19.84
358.3	754.16	20.51
368.6	810.16	21.87
375.0	838.16	22.63
391.6	893.16	24.40
401.4	911.16	25.25
426.3	1023.16	28.42
441.9	1083.16	30.32
464.3	1196.16	33.47
490.6	1307.16	36.96
520.6	1407.16	40.73

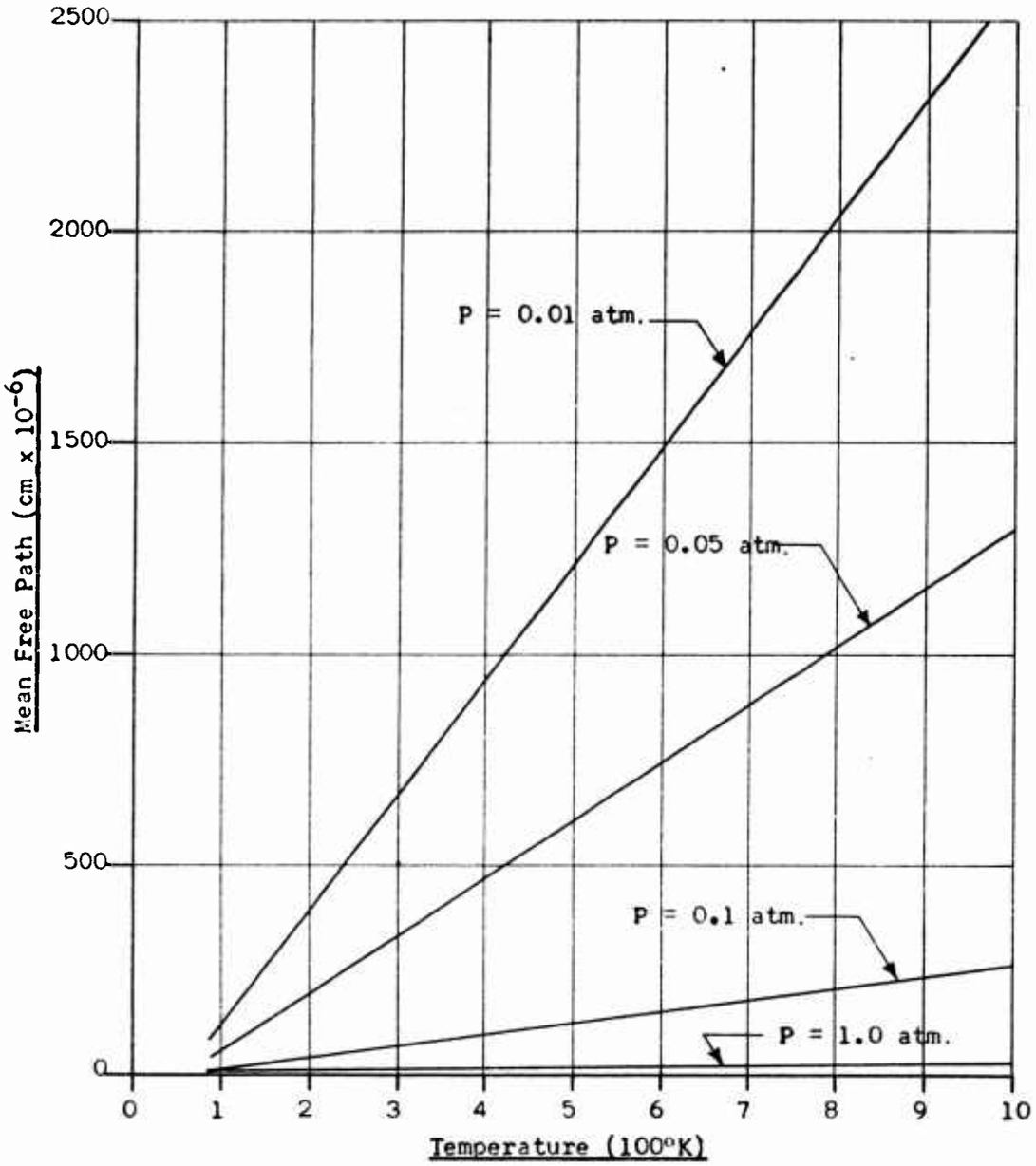

Figure 13. Mean Free Path of Air as a Function of Temperature for P (Atm.) = 0.01, 0.05, 0.1, 1.0.

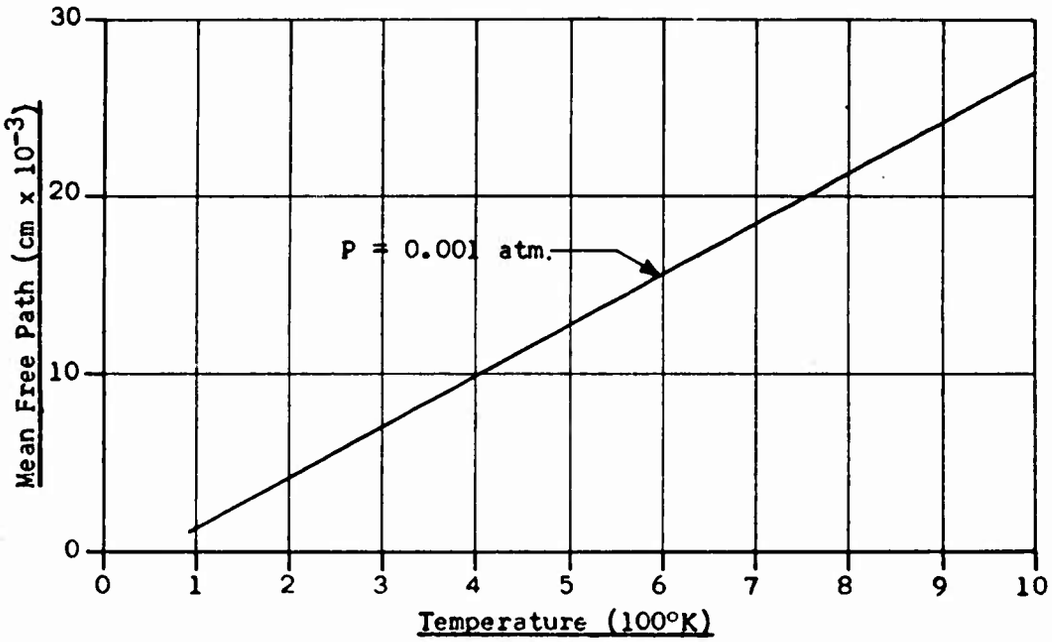

Figure 14. Mean Free Path of Air as a Function of Temperature for P = 0.001 Atm.

APPENDIX II, CALCULATIONS OF MOLECULAR FLOW RATE AND LIFT

This appendix contains derivations and calculated data for molecular flow rates, pressure increases and lift based upon the theory presented in the contract proposal. These calculations were made before the validity of the mixing-region concept was questioned. The mixing-region concept does not enter into the flow rate calculations. These are considered valid for an effusion surface of 1 square foot, 1/10 of which is open area.

The pressure-increase and lift calculations and data are not valid because they depend upon the mixing-region concept. The calculations are included merely to indicate the scope of the early work.

CALCULATIONS OF MOLECULAR FLOW RATE

The molecular flow rate is calculated as follows:

$$\dot{M}_{(\text{molecules}\cdot\text{sec}^{-1})} = N_{net}\, A_p \qquad (28)$$

$$N_{net} = \tfrac{1}{4}\left[n_1\bar{v}_1 - n_2\bar{v}_2\right] \qquad (29)$$

$$N_{net} = \tfrac{1}{4}\left[\frac{n_o T_o}{P_o}\right]\left[2\left(\frac{2R_M}{\pi M}\right)^{\frac{1}{2}}\right]\left[\frac{P_1}{T_1^{\frac{1}{2}}} - \frac{P_2}{T_2^{\frac{1}{2}}}\right] \qquad (30)$$

$$\dot{M}_{(\text{molecules}\cdot\text{sec}^{-1})} = \tfrac{1}{4}\left[\frac{n_o T_o}{P_o}\right]\left[2\left(\frac{2R_M}{\pi M}\right)^{\frac{1}{2}}\right]\left[\frac{P_1}{T_1^{\frac{1}{2}}} - \frac{P_2}{T_2^{\frac{1}{2}}}\right] A_p \qquad (31)$$

Converting to grams per second:

$$\dot{M}_{(\text{gram}\cdot\text{sec}^{-1})} = \dot{M}_{(\text{molecules}\cdot\text{sec}^{-1})}\left[\frac{M\ \text{air}}{A_o}\right] \qquad (32)$$

Converting to pounds per second:

$$\dot{M}_{(\text{lb}\cdot\text{sec}^{-1})} = \dot{M}_{(\text{gram}\cdot\text{sec}^{-1})}\left[2.205 \times 10^{-3}\ \text{lb}\cdot\text{gram}^{-1}\right] \qquad (33)$$

Lift is calculated by assuming that the pressure increase at the external effusion surface is proportional to the number of excess molecules in the "mixing region".

$$\Delta P = \left[\frac{N_{ex}}{n_2 V_M}\right] P_2 \qquad (34)$$

$$N_{ex} = \tfrac{1}{4} \left[n_1 \bar{v}_1 - n_2 \bar{v}_2\right] A_p \left[\bar{\lambda}_2 / \bar{v}_1\right] \text{ excess molecules} \qquad (35)$$

$$n_2 V_M = n_2 A_B \bar{\lambda}_2 \text{ molecules} \qquad (36)$$

P_2 is ambient pressure

TABLE 3

MOLECULAR FLOW RATE

WHERE $T_1 = 100^{\circ}K$ AND $P_1 = 0.5$ ATM.

P_2 (Atm.)	T_2 ($^{\circ}K$)	$\dot{M}$ Mol./sec x 10^{25}	$\dot{M}$ (gm/sec)	$\dot{M}$ (lb/sec)
0.1	100	1.84	885.7	2.0
0.1	200	1.98	950.6	2.1
0.1	273	2.02	973.1	2.1
0.1	300	2.04	979.3	2.2
0.1	400	2.07	996.4	2.2
0.5	100	0.00	0.0	0.0
0.5	200	0.67	324.3	.7
0.5	273	0.91	437.1	1.0
0.5	300	0.97	467.9	1.0
0.5	400	1.15	553.6	1.2
0.9	100	-1.84	-885.7	-2.0
0.9	200	-0.63	-302.0	-0.7
0.9	273	-0.21	- 99.0	-0.2
0.9	300	-0.09	- 43.4	-0.1
0.9	400	0.23	110.7	0.2

TABLE 4
MOLECULAR FLOW RATE
WHERE T_1 = 200°K AND P_1 = 0.5 ATM.

P_2 (Atm.)	T_2 (°K)	$\dot{M}$ Mol./sec x 10^{25}	$\dot{M}$ (gm/sec)	$\dot{M}$ (lb/sec)
0.1	100	1.17	561.4	1.2
0.1	200	1.30	626.3	1.4
0.1	273	1.35	648.9	1.4
0.1	300	1.36	655.0	1.4
0.1	400	1.40	672.2	1.5
0.5	100	-0.67	-324.3	-0.7
0.5	200	0.0	0.0	0.0
0.5	273	0.23	112.8	0.2
0.5	300	0.30	143.7	0.3
0.5	400	0.48	229.3	0.5
0.9	100	-2.52	-1210.0	-2.7
0.9	200	-1.30	- 626.3	-1.4
0.9	273	-0.88	- 423.3	-0.9
0.9	300	-0.76	- 367.7	-0.8
0.9	400	-0.44	- 213.6	-0.5

TABLE 5
MOLECULAR FLOW RATE
WHERE T_1 = 273°K AND P_1 = 0.5 ATM.

P_2 (Atm.)	T_2 (°K)	$\dot{M}$ Mol./sec x 10^{25}	$\dot{M}$ (gm/sec)	$\dot{M}$ (lb/sec)
0.1	100	.93	448.6	1.0
0.1	200	1.07	513.5	1.1
0.1	273	1.11	536.1	1.2
0.1	300	1.13	542.2	1.2
0.1	400	1.16	559.4	1.2
0.5	100	- .91	- 437.0	- 1.0
0.5	200	- .23	- 112.8	- .2
0.5	273	0	0	0
0.5	300	.06	30.9	0.1
0.5	400	.24	116.5	0.3
0.9	100	- 2.75	-1322.8	- 2.9
0.9	200	- 1.54	- 739.1	- 1.6
0.9	273	- 1.11	- 536.1	- 1.2
0.9	300	- 1.00	- 480.5	- 1.1
0.9	400	- .68	- 326.4	- 0.7

TABLE 6
MOLECULAR FLOW RATE
WHERE T_1 = 300°K AND P_1 = 0.5 ATM.

P_2 (Atm.)	T_2 (°K)	$\dot{M}$ Mol./sec x 10^{25}	$\dot{M}$ (gm/sec)	$\dot{M}$ (lb/sec)
0.1	100	.87	417.8	0.9
0.1	200	1.00	482.6	1.1
0.1	273	1.05	505.2	1.1
0.1	300	1.06	511.4	1.1
0.1	400	1.10	528.5	1.2
0.5	100	- .97	- 467.9	- 1.0
0.5	200	- .30	- 143.7	- 0.3
0.5	273	- .06	- 30.9	- 0.1
0.5	300	0	0	0
0.5	400	.18	85.6	0.2
0.9	100	- 2.92	-1353.7	- 3.0
0.9	200	- 1.60	- 770.0	- 1.7
0.9	273	- 1.18	- 566.9	- 1.3
0.9	300	- 1.06	- 511.4	- 1.1
0.9	400	- .74	- 357.2	- 0.8

TABLE 7
MOLECULAR FLOW RATE
WHERE T_1 = 400°K AND P_1 = 0.5 ATM.

P_2 (Atm.)	T_2 (°K)	$\dot{M}$ Mol./sec x 10^{25}	$\dot{M}$ (gm/sec)	$\dot{M}$ (lb/sec)
0.1	100	.69	332.1	0.7
0.1	200	.83	397.0	0.9
0.1	273	.87	419.6	0.9
0.1	300	.89	425.7	0.9
0.1	400	.92	442.9	1.0
0.5	100	- 1.15	- 553.6	- 1.2
0.5	200	- .48	- 229.3	- 0.5
0.5	273	- .24	- 116.5	- 0.3
0.5	300	- .18	- 85.6	- 0.2
0.5	400	0	0	0
0.9	100	- 2.99	-1439.0	- 3.2
0.9	200	- 1.78	- 855.6	- 1.9
0.9	273	- 1.36	- 652.6	- 1.4
0.9	300	- 1.24	- 597.0	- 1.3
0.9	400	- .92	- 442.9	- 1.0

TABLE 8
MOLECULAR FLOW RATE
WHERE T_1 = 500°K AND P_1 = 0.5 ATM.

P_2 (Atm.)	T_2 (°K)	$\dot{M}$ Mol./sec x 10^{25}	$\dot{M}$ (gm/sec)	$\dot{M}$ (lb/sec)
0.1	100	.57	273.7	0.6
0.1	200	.70	338.6	0.7
0.1	273	.75	361.1	0.8
0.1	300	.76	367.3	0.8
0.1	400	.80	384.4	0.8
0.5	100	-1.27	- 612.0	-1.3
0.5	200	- .60	- 287.7	-0.6
0.5	273	- .36	- 174.9	-0.4
0.5	300	- .30	- 144.1	-0.3
0.5	400	- .12	- 58.4	-0.1
0.9	100	-3.11	-1497.7	-3.3
0.9	200	-1.90	- 914.0	-2.0
0.9	273	-1.48	- 711.0	-1.6
0.9	300	-1.36	- 655.4	-1.4
0.9	400	-1.04	- 501.3	-1.1

TABLE 9
MOLECULAR FLOW RATE
WHERE T_1 = 600°K AND P_1 = 0.5 ATM.

P_2 (Atm.)	T_2 (°K)	$\dot{M}$ Mol./sec x 10^{25}	$\dot{M}$ (gm/sec)	$\dot{M}$ (lb/sec)
0.1	100	.48	230.6	0.5
0.1	200	.61	295.4	0.7
0.1	273	.66	318.0	0.7
0.1	300	.67	324.1	0.7
0.1	400	.71	341.3	0.8
0.5	100	- 1.36	- 655.2	- 1.4
0.5	200	- .69	- 330.9	- 0.7
0.5	273	- .45	- 218.1	- 0.5
0.5	300	- .39	- 187.2	- 0.4
0.5	400	- .21	- 101.6	- 0.2
0.9	100	- 3.20	-1540.9	- 3.4
0.9	200	- 1.99	- 957.2	- 2.1
0.9	273	- 1.57	- 754.1	- 1.7
0.9	300	- 1.45	- 698.6	- 1.5
0.9	400	- 1.13	- 544.4	- 1.2

TABLE 10
MOLECULAR FLOW RATE
WHERE T_1 = 700°K AND P_1 = 0.5 ATM.

P_2 (Atm.)	T_2 (°K)	$\dot{M}$ Mol./sec x 10^{25}	$\dot{M}$ (gm/sec)	$\dot{M}$ (lb/sec)
0.1	100	.41	197.0	0.4
0.1	200	.54	261.9	0.6
0.1	273	.59	284.4	0.6
0.1	300	.60	290.6	0.6
0.1	400	.64	307.7	0.7
0.5	100	- 1.43	- 688.7	- 1.5
0.5	200	- .76	- 364.4	- 0.8
0.5	273	- .52	- 251.6	- 0.6
0.5	300	- .46	- 220.7	- 0.5
0.5	400	- .28	- 135.1	- 0.3
0.9	100	- 3.27	-1574.4	- 3.5
0.9	200	- 2.06	- 990.7	- 2.2
0.9	273	- 1.64	- 787.7	- 1.7
0.9	300	- 1.52	- 732.1	- 1.6
0.9	400	- 1.20	- 578.0	- 1.3

TABLE 11
MOLECULAR FLOW RATE
WHERE T_1 = 100°K AND P_1 = 2.0 ATM.

P_2 (Atm.)	T_2 (°K)	$\dot{M}$ Mol./sec x 10^{25}	$\dot{M}$ (gm/sec)	$\dot{M}$ (lb/sec)
0.1	100	8.75	4207.2	9.3
0.1	200	8.88	4272.0	9.4
0.1	273	8.93	4294.6	9.5
0.1	300	8.94	4300.7	9.5
0.1	400	8.98	4317.9	9.5
0.5	100	6.91	3321.4	7.3
0.5	200	7.58	3645.7	8.0
0.5	273	7.82	3758.5	8.3
0.5	300	7.88	3789.4	8.4
0.5	400	8.06	3875.0	8.5
0.9	100	5.07	2435.7	5.4
0.9	200	6.28	3019.4	6.7
0.9	273	6.70	3222.4	7.1
0.9	300	6.82	3278.0	7.2
0.9	400	7.14	3432.2	7.6

TABLE 12
MOLECULAR FLOW RATE
WHERE T_1 = 200°K AND P_1 = 2.0 ATM.

P_2 (Atm.)	T_2 (°K)	$\dot{M}$ Mol./sec x 10^{25}	$\dot{M}$ (gm/sec)	$\dot{M}$ (lb/sec)
0.1	100	6.05	2910.1	6.4
0.1	200	6.19	2974.9	6.6
0.1	273	6.23	2997.5	6.6
0.1	300	6.25	3003.6	6.6
0.1	400	6.28	3020.8	6.7
0.5	100	4.21	2024.3	4.5
0.5	200	4.88	2348.6	5.2
0.5	273	5.12	2461.4	5.4
0.5	300	5.18	2492.3	5.5
0.5	400	5.36	2577.9	5.7
0.9	100	2.37	1138.6	2.5
0.9	200	3.58	1722.3	3.8
0.9	273	4.00	1925.3	4.2
0.9	300	4.12	1980.9	4.4
0.9	400	4.44	2135.0	4.7

TABLE 13
MOLECULAR FLOW RATE
WHERE T_1 = 273°K AND P_1 = 2.0 ATM.

P_2 (Atm.)	T_2 (°K)	$\dot{M}$ Mol./sec x 10^{25}	$\dot{M}$ (gm/sec)	$\dot{M}$ (lb/sec)
0.1	100	5.11	2458.9	5.4
0.1	200	5.25	2523.7	5.6
0.1	273	5.30	2546.3	5.6
0.1	300	5.31	2552.4	5.6
0.1	400	5.34	2569.6	5.7
0.5	100	3.27	1573.2	3.5
0.5	200	3.95	1897.4	4.2
0.5	273	4.18	2010.2	4.4
0.5	300	4.24	2041.0	4.5
0.5	400	4.42	2126.7	4.7
0.9	100	1.43	687.4	1.5
0.9	200	2.64	1271.1	2.8
0.9	273	3.07	1474.2	3.2
0.9	300	3.18	1529.7	3.4
0.9	400	3.50	1683.9	3.7

TABLE 14
MOLECULAR FLOW RATE
WHERE T_1 = 300°K AND P_1 = 2.0 ATM.

P_2 (Atm.)	T_2 (°K)	$\dot{M}$ Mol./sec x 10^{25}	$\dot{M}$ (gm/sec)	$\dot{M}$ (lb/sec)
0.1	100	4.86	2335.4	5.1
0.1	200	4.99	2400.3	5.3
0.1	273	5.04	2422.8	5.3
0.1	300	5.05	2429.0	5.4
0.1	400	5.09	2446.1	5.4
0.5	100	3.01	1449.7	3.2
0.5	200	3.69	1774.0	3.9
0.5	273	3.92	1886.8	4.2
0.5	300	3.99	1917.6	4.2
0.5	400	4.17	2003.3	4.4
0.9	100	1.17	564.0	1.2
0.9	200	2.39	1147.7	2.5
0.9	273	2.81	1350.7	3.0
0.9	300	2.92	1406.3	3.1
0.9	400	3.25	1560.4	3.4

TABLE 15
MOLECULAR FLOW RATE
WHERE T_1 = 400°K AND P_1 = 2.0 ATM.

P_2 (Atm.)	T_2 (°K)	$\dot{M}$ Mol./sec x 10^{25}	$\dot{M}$ (gm/sec)	$\dot{M}$ (lb/sec)
0.1	100	4.14	1992.9	4.4
0.1	200	4.28	2057.7	4.5
0.1	273	4.33	2080.3	4.6
0.1	300	4.34	2086.4	4.6
0.1	400	4.37	2103.6	4.6
0.5	100	2.30	1107.1	2.4
0.5	200	2.98	1431.4	3.2
0.5	273	3.21	1544.2	3.4
0.5	300	3.28	1575.1	3.5
0.5	400	3.45	1660.7	3.7
0.9	100	.46	221.4	0.5
0.9	200	1.67	805.1	1.8
0.9	273	2.10	1008.2	2.2
0.9	300	2.21	1063.7	2.3
0.9	400	2.53	1217.9	2.7

TABLE 16
MOLECULAR FLOW RATE
WHERE T_1 = 500°K AND P_1 = 2.0 ATM.

P_2 (Atm.)	T_2 (°K)	$\dot{M}$ Mol./sec x 10^{25}	$\dot{M}$ (gm/sec)	$\dot{M}$ (lb/sec)
0.1	100	3.66	1759.1	3.9
0.1	200	3.79	1823.9	4.0
0.1	273	3.84	1846.5	4.1
0.1	300	3.85	1852.7	4.1
0.1	400	3.89	1869.8	4.1
0.5	100	1.82	873.4	1.9
0.5	200	2.49	1197.7	2.6
0.5	273	2.73	1310.4	2.9
0.5	300	2.79	1341.3	3.0
0.5	400	2.97	1426.9	3.1
0.9	100	- .03	- 12.3	.0
0.9	200	1.19	571.4	1.3
0.9	273	1.61	774.4	1.7
0.9	300	1.73	829.9	1.8
0.9	400	2.05	984.1	2.2

TABLE 17
MOLECULAR FLOW RATE
WHERE T_1 = 600°K AND P_1 = 2.0 ATM.

P_2 (Atm.)	T_2 (°K)	$\dot{M}$ Mol./sec x 10^{25}	$\dot{M}$ (gm/sec)	$\dot{M}$ (lb/sec)
0.1	100	3.30	1586.5	3.5
0.1	200	3.43	1651.4	3.6
0.1	273	3.48	1673.9	3.7
0.1	300	3.49	1680.1	3.7
0.1	400	3.53	1697.2	3.7
0.5	100	1.46	700.8	1.5
0.5	200	2.13	1025.1	2.3
0.5	273	2.37	1137.9	2.5
0.5	300	2.43	1168.8	2.6
0.5	400	2.61	1254.4	2.8
0.9	100	- .38	- 184.9	- 0.4
0.9	200	.83	398.8	0.9
0.9	273	1.25	601.8	1.3
0.9	300	1.37	657.4	1.4
0.9	400	1.69	811.5	1.8

TABLE 18
MOLECULAR FLOW RATE
WHERE T_1 = 700°K AND P_1 = 2.0 ATM.

P_2 (Atm.)	T_2 (°K)	$\dot{M}$ Mol./sec x 10^{25}	$\dot{M}$ (gm/sec)	$\dot{M}$ (lb/sec)
0.1	100	3.02	1452.4	3.2
0.1	200	3.16	1517.3	3.3
0.1	273	3.20	1539.8	3.4
0.1	300	3.22	1546.0	3.4
0.1	400	3.25	1563.1	3.4
0.5	100	1.18	566.7	1.2
0.5	200	1.85	891.0	2.0
0.5	273	2.09	1003.8	2.2
0.5	300	2.15	1034.6	2.3
0.5	400	2.33	1120.3	2.5
0.9	100	- .66	- 319.0	- .7
0.9	200	.55	264.7	.6
0.9	273	.97	467.7	1.0
0.9	300	1.09	523.3	1.2
0.9	400	1.41	677.4	1.5

TABLE 19
MOLECULAR FLOW RATE AND LIFT
WHERE P_1 = 1.5 ATM., P_2 = 1 ATM., T_2 = 300°K

T_1 (K°)	$N_{ex}/n_2 V_M$ x 10^{-2}	P (lb/in^2)	Lift (lb/ft^2)	$\dot{M}$ (gm/sec)	$\dot{M}$ (lb/sec)
100	6.92	1.017	146.4	2049.6	4.5
150	3.96	.583	84.0	1438.2	3.2
200	2.56	.377	54.3	1073.6	2.4
250	1.76	.259	37.3	824.9	1.8
273	1.50	.221	31.8	734.2	1.6
300	1.25	.184	26.5	641.3	1.4
350	.90	.132	19.0	498.6	1.1
400	.65	.095	13.7	383.5	.8
450	.46	.067	9.6	288.2	.6
500	.31	.046	6.6	207.6	.5
600	.11	.016	2.3	77.8	.2
700	-.03	-.004	-0.6	-23.1	-.1

TABLE 20

MOLECULAR FLOW RATE AND LIFT

WHERE $P_1 = P_2 = 1$ ATM. AND $T_2 = 300^{\circ}K$

T_1 (K°)	$N_{ex}/n_2 V_M$ x 10^{-2}	P (lb/in^2)	Lift (lb/ft^2)	$\dot{M}$ (gm/sec)	$\dot{M}$ (lb/sec)
100	3.17	.466	67.1	938.9	2.1
150	1.46	.215	31.0	532.3	1.2
200	.69	.101	14.5	288.3	0.6
250	.26	.038	5.5	122.4	0.3
273	.13	.019	2.7	61.9	0.1
300	.00	.000	0.0	0.0	0.0
350	-.17	-.025	-3.6	-95.1	-0.2
400	-.29	-.043	-6.2	-171.8	-0.4
450	-.37	-.055	-7.9	-235.4	-0.5
500	-.44	-.064	-9.2	-289.1	-0.6
600	-.52	-.076	-10.9	-375.7	-0.8
700	-.57	-.083	-12.0	-442.9	-1.0

TABLE 21

MOLECULAR FLOW RATE AND LIFT

WHERE P_1 = 2 ATM., P_2 = 1 ATM., T_2 = 300°K

T_1 (K°)	$N_{ex}/n_2 V_M$ x 10^{-2}	P (lb/in^2)	Lift (lb/ft^2)	$\dot{M}$ (gm/sec)	$\dot{M}$ (lb/sec)
100	10.67	1.569	225.9	3160.4	7.0
150	6.47	.950	136.8	2345.1	5.2
200	4.44	.652	93.9	1859.1	4.1
250	3.26	.479	69.0	1527.4	3.4
273	2.87	.422	60.8	1406.4	3.1
300	2.50	.368	53.0	1282.5	2.8
350	1.97	.290	41.8	1092.3	2.4
400	1.58	.233	33.6	938.9	2.1
450	1.29	.190	27.4	811.9	1.8
500	1.06	.156	22.5	704.4	1.6
600	.73	.108	15.6	531.3	1.2
700	.51	.074	10.7	396.7	.9

TABLE 22
MOLECULAR FLOW RATE AND LIFT
WHERE P_1 = 2.5 ATM., P_2 = 1 ATM., T_2 = 300°K

T_1 (K°)	N_{ex}/N_2 V_M x 10^{-2}	P (lb/in^2)	Lift (lb/ft^2)	$\dot{M}$ (gm/sec)	$\dot{M}$ (lb/sec)
100	14.42	2.120	305.3	4271.0	9.4
150	8.97	1.318	189.8	3251.9	7.2
200	6.31	.928	133.6	2644.4	5.8
250	4.76	.700	100.8	2229.8	4.9
273	4.25	.624	89.9	2078.6	4.6
300	3.75	.551	79.3	1923.8	4.2
350	3.04	.447	64.4	1686.0	3.7
400	2.52	.371	53.4	1494.2	3.3
450	2.13	.312	44.9	1335.4	2.9
500	1.81	.267	38.4	1201.1	2.6
600	1.36	.200	28.8	984.7	2.2
700	1.04	.153	22.0	816.5	1.8

TABLE 23
MOLECULAR FLOW RATE AND LIFT
WHERE P_1 = 3 ATM., P_2 = 1 ATM., T_2 = 300°K

T_1 (K°)	N_{ex}/N_2 V_M x 10^{-2}	P (lb/in^2)	Lift (lb/ft^2)	$\dot{M}$ (gm/sec)	$\dot{M}$ (lb/sec)
100	18.17	2.671	384.6	5381.9	11.9
150	11.47	1.685	242.6	4158.9	9.2
200	8.19	1.204	173.4	3429.9	7.6
250	6.26	.921	132.6	2932.4	6.5
273	5.62	.826	118.9	2750.9	6.1
300	5.00	.735	105.8	2565.1	5.7
350	4.11	.605	87.1	2279.7	5.0
400	3.46	.509	73.3	2049.6	4.5
450	2.96	.435	62.6	1859.1	4.1
500	2.56	.377	54.3	1697.8	3.7
600	1.98	.291	41.9	1438.2	3.2
700	1.58	.232	33.4	1236.3	2.7

TABLE 24
MOLECULAR FLOW RATE AND LIFT
WHERE P_1 = 3.5 ATM., P_2 = 1 ATM., T_2 = 300°K

T_1 (K°)	N_{ex}/N_2 V_M x 10^{-2}	P (lb/in^2)	Lift (lb/ft^2)	$\dot{M}$ (gm/sec)	$\dot{M}$ (lb/sec)
100	21.92	3.223	464.1	6492.4	14.3
150	13.97	2.053	295.6	5065.7	11.2
200	10.06	1.479	213.0	4215.2	9.3
250	7.76	1.141	164.3	3634.8	8.0
273	7.00	1.028	148.0	3423.1	7.5
300	6.25	.919	132.3	3206.3	7.1
350	5.19	.762	109.7	2873.3	6.3
400	4.40	.646	93.0	2604.9	5.7
450	3.79	.558	80.4	2382.6	5.3
500	3.31	.487	70.1	2194.5	4.8
600	2.61	.383	55.2	1891.6	4.2
700	2.11	.311	44.8	1656.1	3.7

TABLE 25

MOLECULAR FLOW RATE AND LIFT

WHERE P_1 = 4 ATM., P_2 = 1 ATM., T_2 = 300°K

T_1 (K°)	N_{ex}/N_2 V_M x 10^{-2}	P (lb/in^2)	Lift (lb/ft^2)	$\dot{M}$ (gm/sec)	$\dot{M}$ (lb/sec)
100	25.67	3.774	543.5	7603.4	16.8
150	16.47	2.421	348.6	5972.8	13.2
200	11.94	1.755	252.7	5000.8	11.0
250	9.26	1.362	196.1	4337.4	9.6
273	8.37	1.230	177.1	4095.5	9.0
300	7.50	1.103	158.8	3847.7	8.5
350	6.26	.920	132.5	3467.2	7.6
400	5.34	.784	112.9	3160.4	7.0
450	4.63	.680	97.9	2906.3	6.4
500	4.06	.597	86.0	2691.3	5.9
600	3.23	.475	68.4	2345.1	5.2
700	2.65	.389	56.0	2076.0	4.6

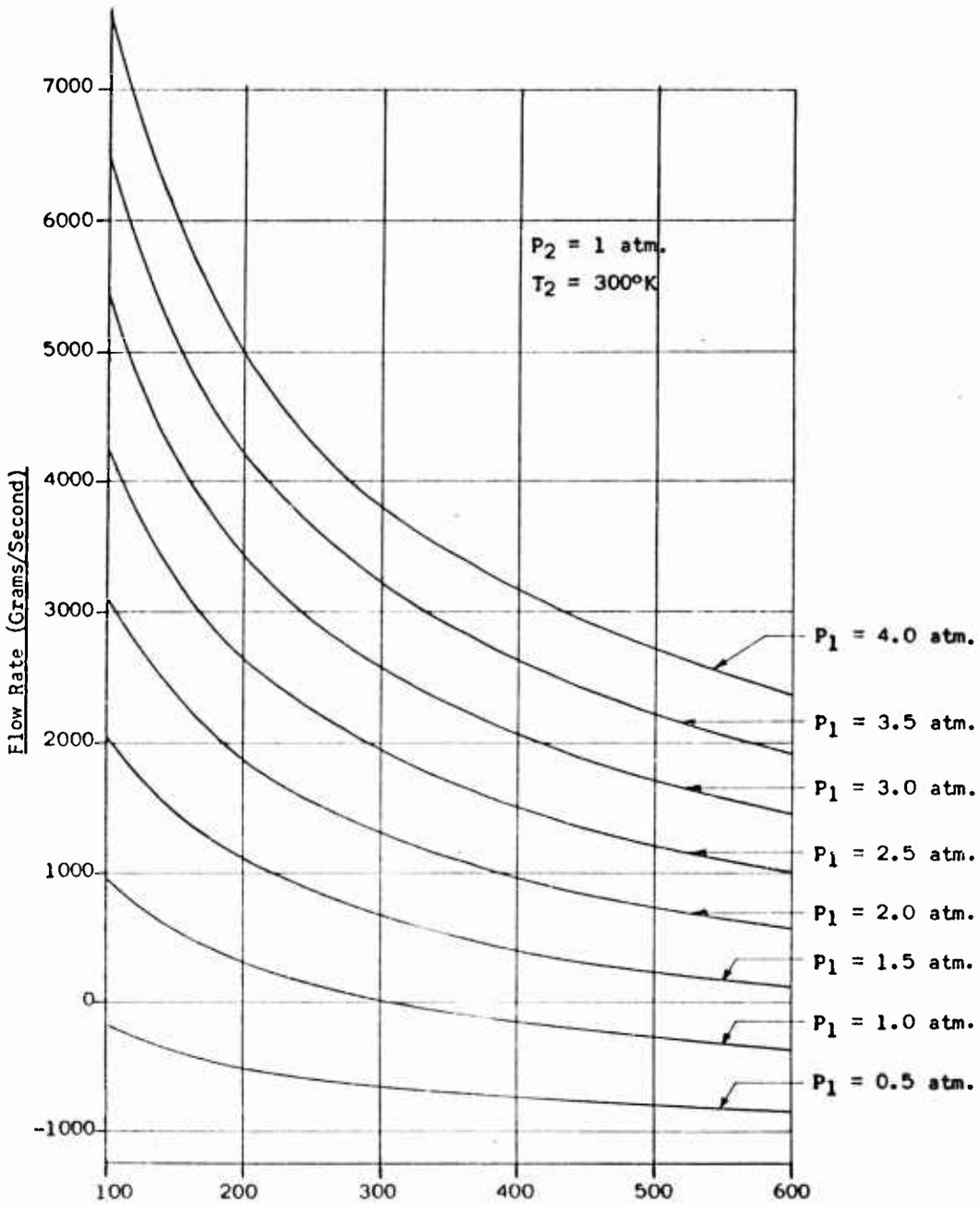

Figure 15. Molecular Flow Rate as a Function of Effusion-Chamber Temperature for P_2 = 1 Atm., T_2 = 300°K.

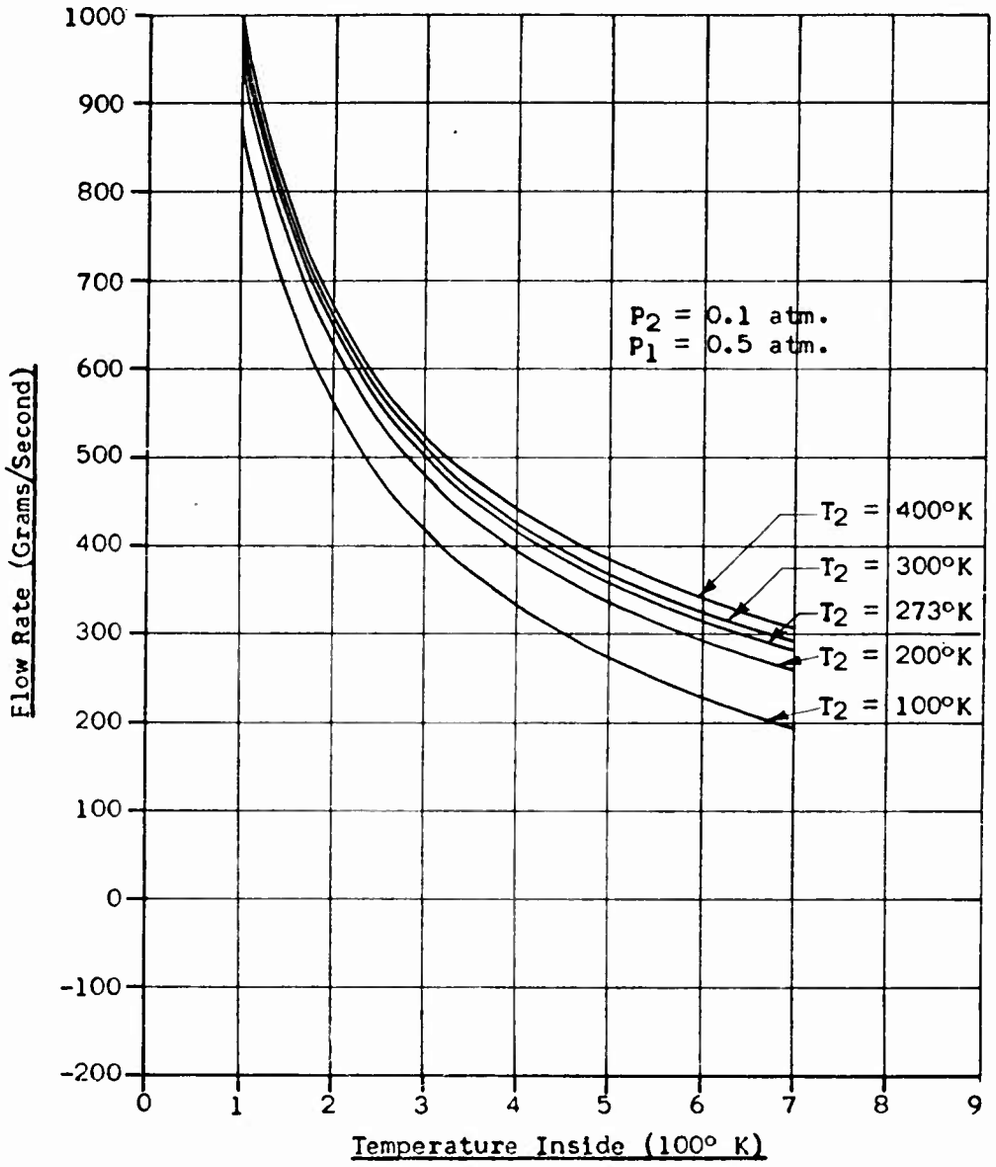

Figure 16. Molecular Flow Rate as a Function of Effusion-Chamber Temperature for P_2 = 0.1 Atm., P_1 = 0.5 Atm.

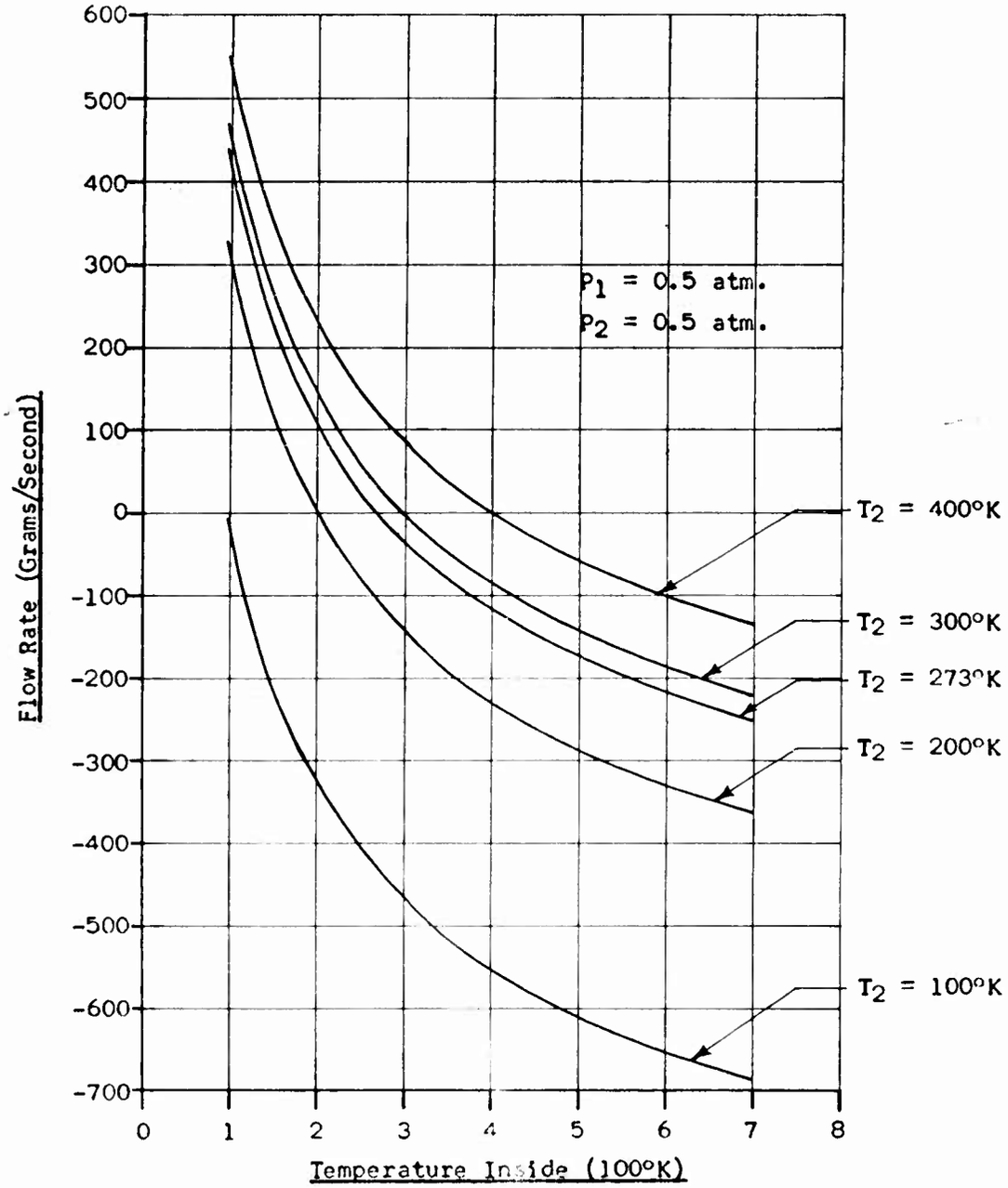

Figure 17. Molecular Flow Rate as a Function of Effusion-Chamber Temperature for P_1 = 0.5 Atm., P_2 = 0.5 Atm.

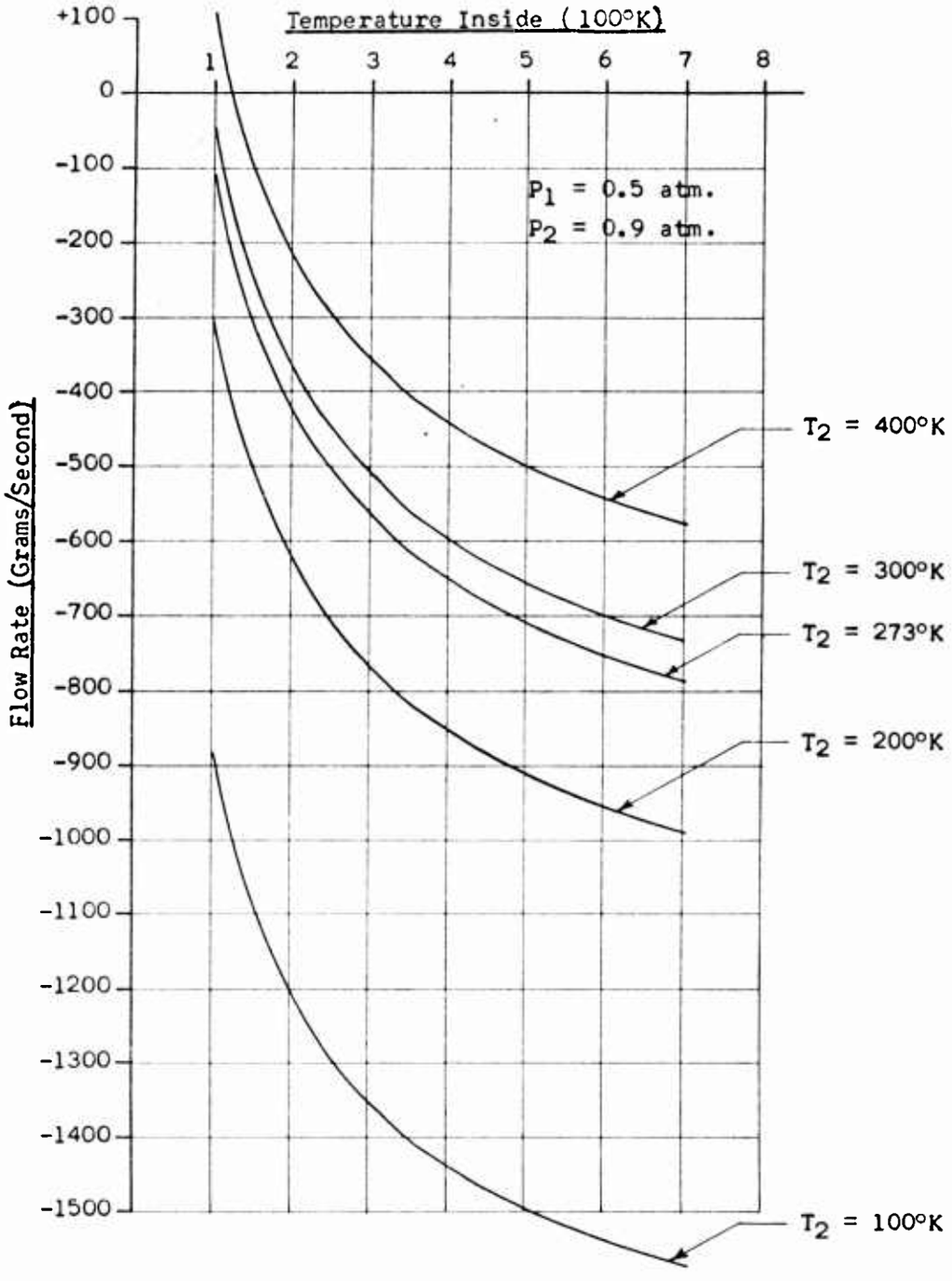

Figure 18. Molecular Flow Rate as a Function of Effusion-Chamber Temperature for P_1 = 0.5 Atm., P_2 = 0.9 Atm.

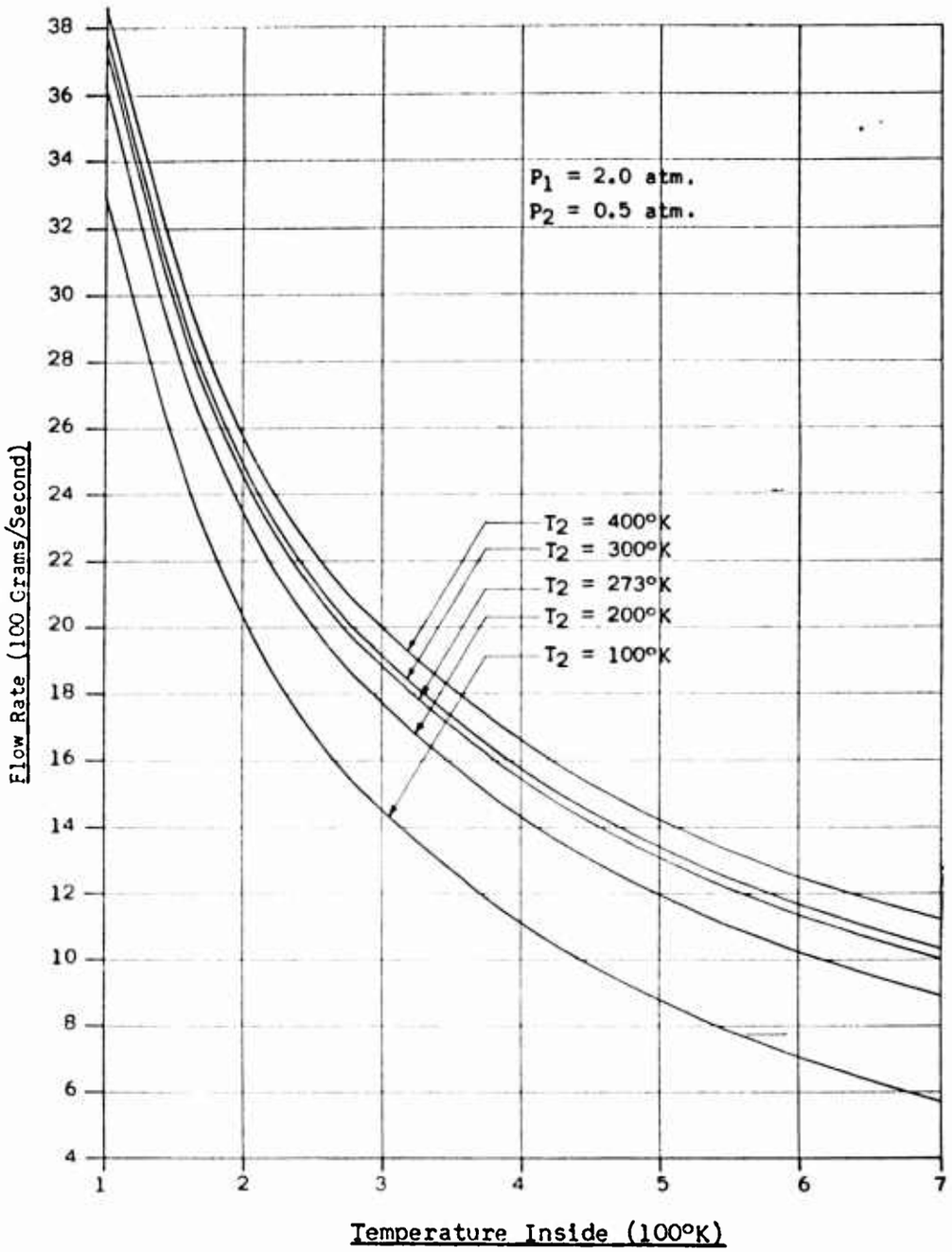

Figure 19. Molecular Flow Rate as a Function of Effusion-Chamber Temperature for P_1 = 2.0 Atm., P_2 = 0.5 Atm.

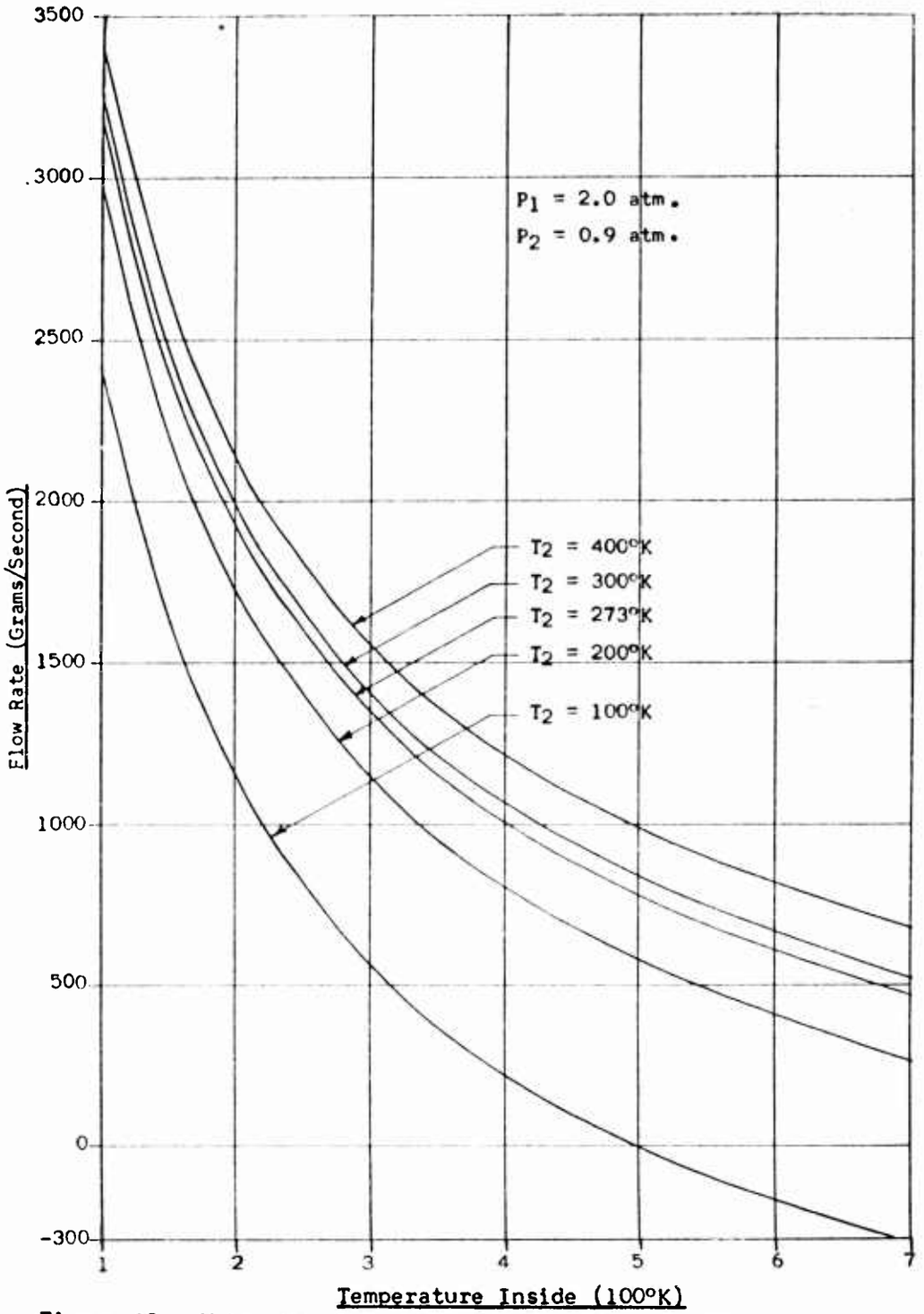

Figure 20. Molecular Flow Rate as a Function of Effusion-Chamber Temperature for P_1 = 2.0 Atm., P_2 = 0.9 Atm.

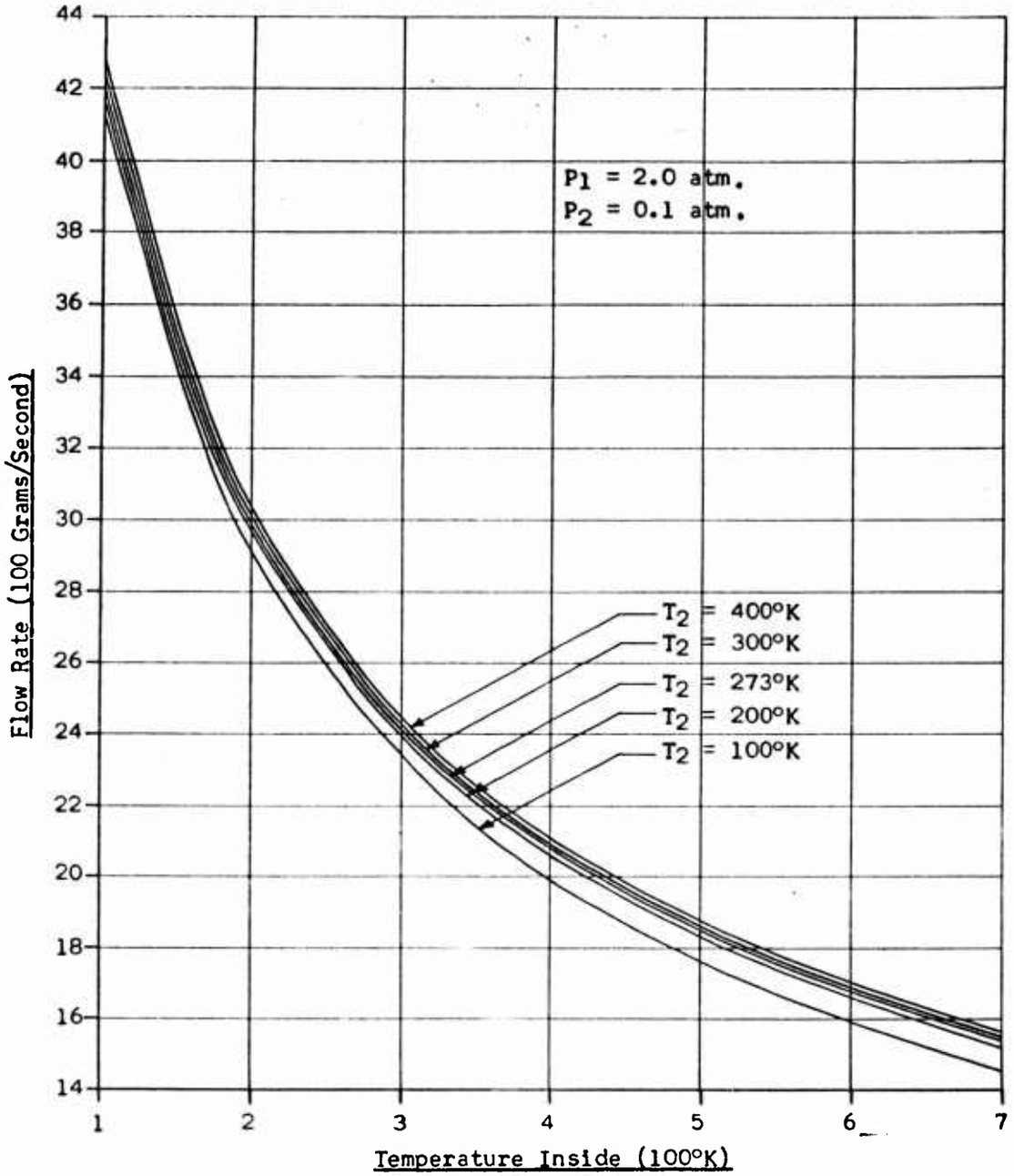

Figure 21. Molecular Flow Rate as a Function of Effusion-Chamber Temperature for P_1 = 2.0 Atm., P_2 = 0.1 Atm.

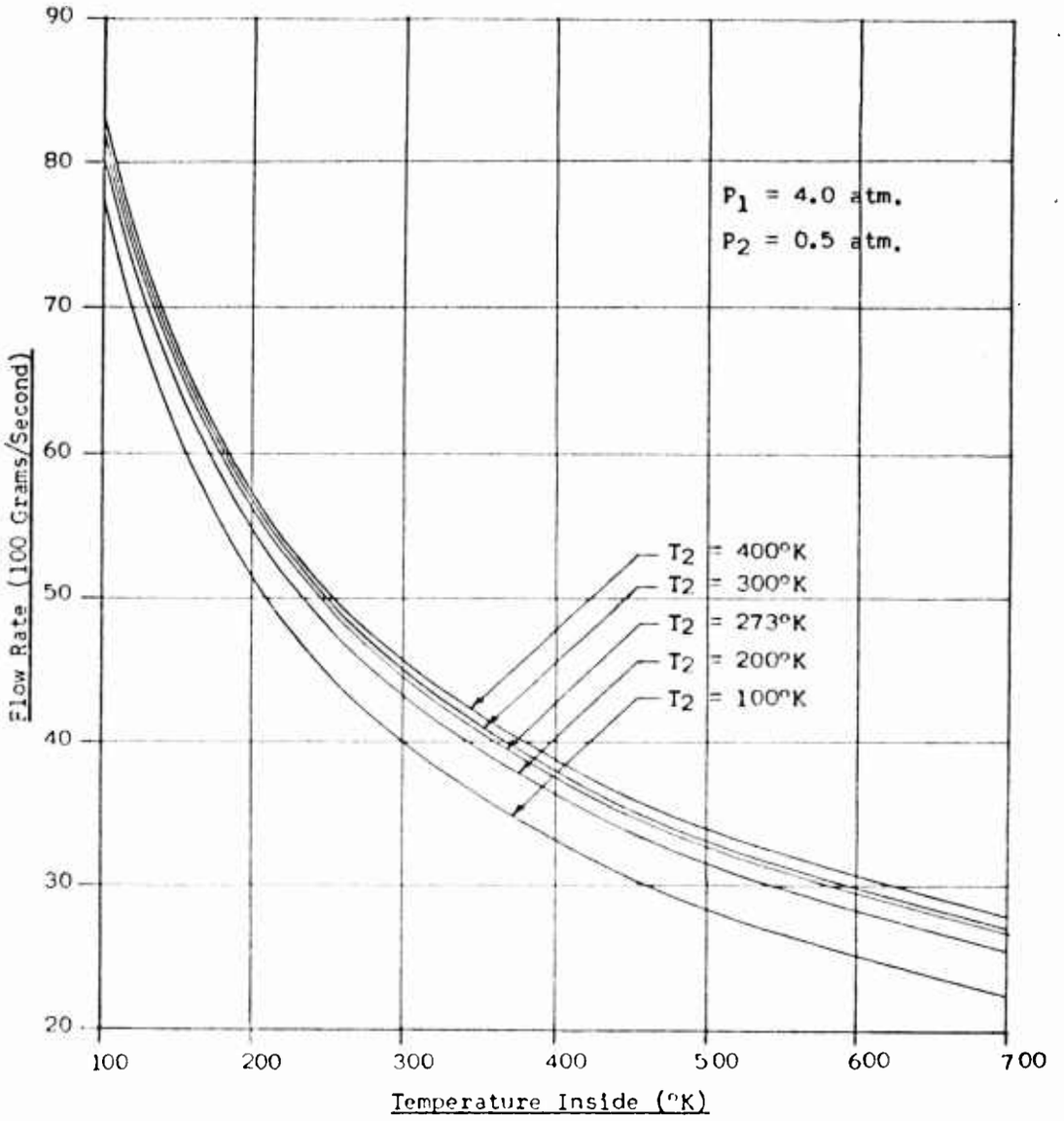

Figure 22. Molecular Flow Rate as a Function of Effusion-Chamber Temperature for P_1 = 4.0 Atm., P_2 = 0.5 Atm.

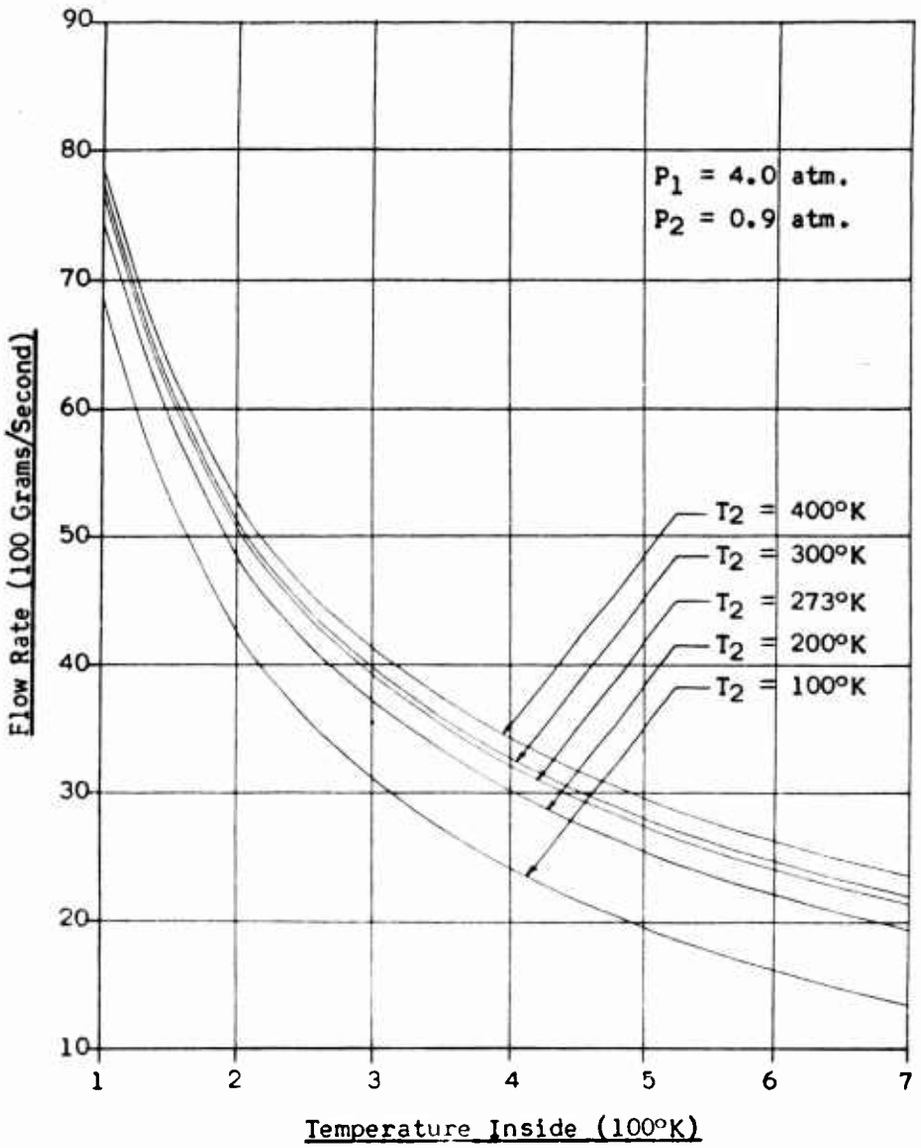

Figure 23. Molecular Flow Rate as a Function of Effusion-Chamber Temperature for P_1 = 4.0 Atm., P_2 = 0.9 Atm.

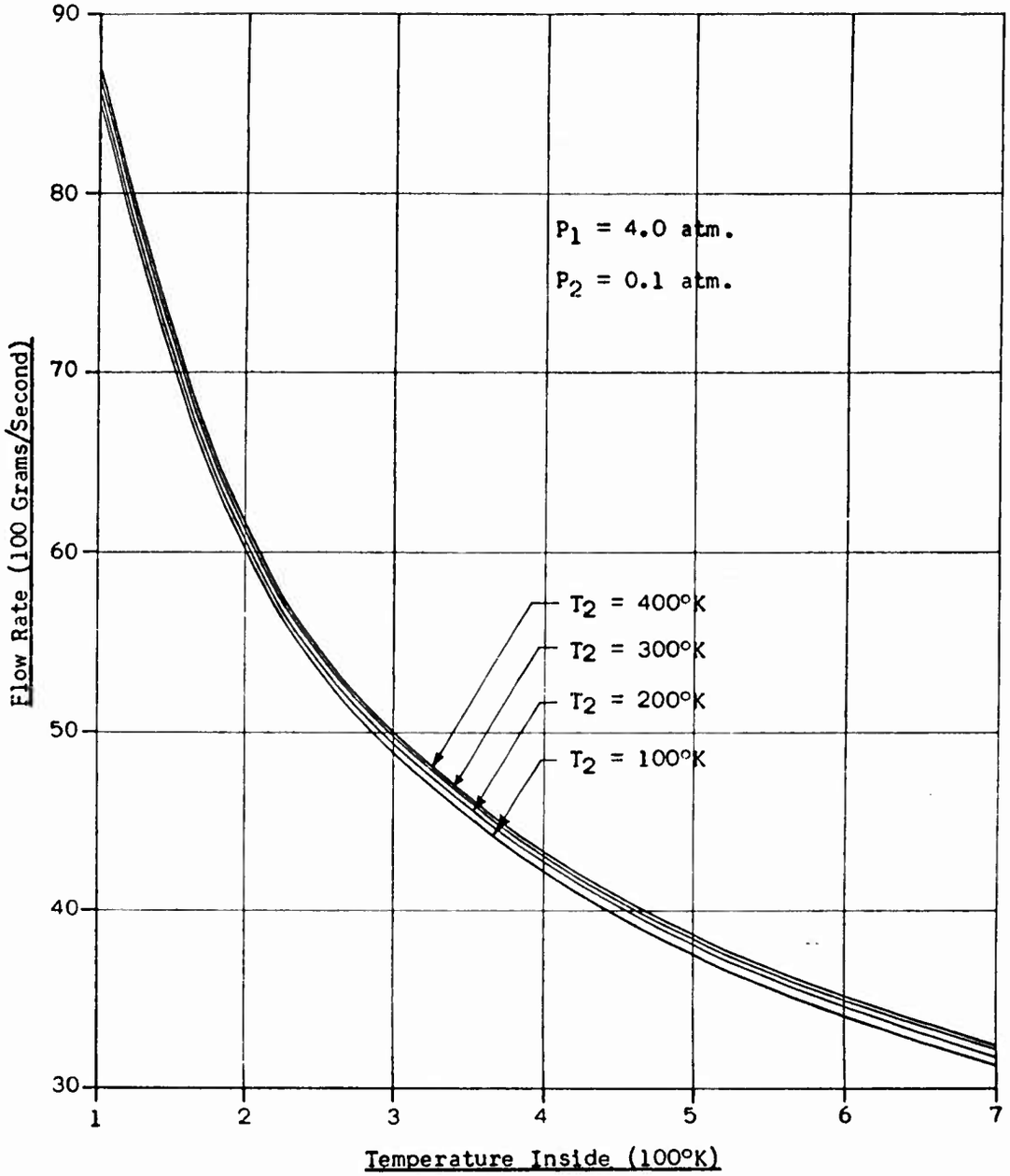

Figure 24. Molecular Flow Rate as a Function of Effusion-Chamber Temperature for P_1 = 4.0 Atm., P_2 = 0.1 Atm.

APPENDIX III, CALCULATIONS OF NET HEAT-TRANSFER RATE THROUGH AN EFFUSION SURFACE

This appendix contains the derivation of the formula used to calculate the net rate at which heat is transferred through an effusion surface whose total area is one square foot, one-tenth of which is hole area. Also included are the calculated data and graphs constructed from the data. The graphs depict horsepower vs. effusion-chamber temperature and also horsepower vs. effusion-chamber pressure.

HEAT-TRANSFER RATE DERIVATION

Determination of net rate of heat transfer through the effusion surface by the effusion process:

Let N_1 be the number of particles effusing out of chamber in unit time per unit area of effusion surface (molecules per cm^2 per second).

$3/2\ kT_1$ = Average kinetic energy of molecules in chamber (37)

$2\ kT_1$ = Average kinetic energy of molecules effusing out (Reference 20, page 64) (38)

$1/2\ kT_1$ = Average excess kinetic energy of molecules leaving chamber (with respect to average inside) (39)

$N_1(1/2)\ kT_1$ = Total excess kinetic energy carried out of chamber (40)

$N_2(2)\ kT_2$ = Total kinetic energy of molecules effusing into chamber (41)

$N_2\ (2kT_2 - 3/2\ kT_1)$ = Total excess kinetic energy added to inside by N_2 molecules (with respect to average inside) (42)

Energy Out-Energy In = Heat energy which must be added to inside to restore original conditions (43)

$$H = N_1\ (1/2\ kT_1) - N_2\ (2\ kT_2 - 3/2\ kT_1) \qquad (\ 44\ )$$

Net heat to be added per unit area of effusion surface per second. (ergs per cm^2 per sec)

To write above equation in terms of temperature and pressure, let:

$$N_1 = n_1 \, (1/4) \, \bar{v}_1 \, A' \qquad (45)$$

Where n_1 = particles per unit volume

$\bar{v}_1$ = average speed of molecules inside

A' = pore area per unit area of effusion surface

$$N_2 = n_2 \, (1/4) \, \bar{v}_2 \, A' \qquad (46)$$

Heat energy per unit area per unit time is given by:

$$H = n_1(1/4)\bar{v}_1 A' \left[1/2 \; kT_1\right] - n_2(1/4)\bar{v}_2 A' \left[2 \; kT_2 - 3/2 \; kT_1\right] \qquad (47)$$

$$\text{Since } \bar{v} = 2 \left(\frac{2kT}{\pi m}\right)^{\frac{1}{2}} = 2 \left(\frac{2k}{\pi m}\right)^{\frac{1}{2}} T^{\frac{1}{2}} \qquad (48)$$

Substitute in equation for $\bar{v}_1$ & $\bar{v}_2$

$$\bar{v}_1 = 2 \left(\frac{2k}{\pi m}\right)^{\frac{1}{2}} T_1^{\frac{1}{2}} \qquad (49)$$

$$\bar{v}_2 = 2 \left(\frac{2k}{\pi m}\right)^{\frac{1}{2}} T_2^{\frac{1}{2}} \qquad (50)$$

$$H = n_1 (1/4) \; 2 \left(\frac{2k}{\pi m}\right)^{\frac{1}{2}} T_1^{\frac{1}{2}} \, A' \left[1/2 \; kT_1\right] -$$

$$n_2 (1/4) \; 2 \left(\frac{2k}{\pi m}\right)^{\frac{1}{2}} T_2^{\frac{1}{2}} \, A' \left[2kT_2 - 3/2kT_1\right] \qquad (51)$$

n_1 & n_2 are molecular densities (molecules per unit volume). Expressing these in terms of pressure and temperature

$$n_1 = \left[\frac{273^{\circ}K \; n_{STP}}{1 \text{ Atm.}}\right] \frac{P_1}{T_1} \qquad (52)$$

$$n_2 = \left[\frac{273^{\circ}K \; n_{STP}}{1 \text{ Atm.}}\right] \frac{P_2}{T_2} \qquad (53)$$

$$H = \left[\frac{273^{\circ}K\ n_{STP}}{1\ Atm.}\right] \frac{P_1}{T_1} \left(\tfrac{1}{2}\right) \left(\frac{2k}{\pi m}\right)^{\frac{1}{2}} T_1^{\frac{1}{2}} A' \left[\tfrac{1}{2} k T_1\right] -$$

$$\left[\frac{273^{\circ}K\ n_{STP}}{1\ Atm.}\right] \frac{P_2}{T_2} \left(\tfrac{1}{2}\right) \left(\frac{2k}{\pi m}\right)^{\frac{1}{2}} T_2^{\frac{1}{2}} A' \left[2 k T_2 - 3/2\ k T_1\right] \quad (54)$$

$$H = \left[\frac{273^{\circ}K\ n_{STP}}{1\ Atm.}\right] P_1 \left(\tfrac{1}{2}\right) \left(\frac{2k}{\pi m}\right)^{\frac{1}{2}} T_1^{-\frac{1}{2}} A' \left[\tfrac{1}{2} k T_1\right] -$$

$$\left[\frac{273^{\circ}K\ n_{STP}}{1\ Atm.}\right] P_2 \left(\tfrac{1}{2}\right) \left(\frac{2k}{\pi m}\right)^{\frac{1}{2}} T_2^{-\frac{1}{2}} A' \left[2 k T_2 - 3/2\ k T_1\right] \quad (55)$$

$$H = \left[\frac{273^{\circ}K\ n_{STP}}{1\ Atm.}\right] \left(\tfrac{1}{2}\right) \left(\frac{2}{\pi m}\right)^{\frac{1}{2}} k^{\frac{3}{2}} A'$$

$$X \left[\tfrac{1}{2} P_1 T_1^{\frac{1}{2}} - P_2 T_2^{-\frac{1}{2}} (2T_2 - 3/2\ T_1)\right] \frac{ergs}{sec\ cm^2} \quad (56)$$

The following conversion factor is used to convert H in ergs/sec·cm^2 to horsepower per square foot:

$$1.245 \times 10^{-7}$$

TABLE 26
NET HEAT TRANSFER THROUGH AN EFFUSION SURFACE
WHEN $T_2 = 100^{\circ}K$ AND $T_1 = 100^{\circ}K$

P_2 (Atm.)	P_1 (Atm.)	H (Erg/sec-cm^2)	HP
0.1	0.5	1.38×10^8	17.2
0.1	1.0	3.10×10^8	38.6
0.1	2.0	6.54×10^8	81.5
0.1	3.0	9.98×10^8	124.4
0.1	4.0	13.43×10^8	167.2
0.5	0.5	0.00×10^8	0.0
0.5	1.0	1.72×10^8	21.4
0.5	2.0	5.16×10^8	64.3
0.5	3.0	8.61×10^8	107.2
0.5	4.0	12.05×10^8	150.1
1.0	0.5	-1.72×10^8	21.4
1.0	1.0	0.00×10^8	0.0
1.0	2.0	3.44×10^8	42.9
1.0	3.0	6.89×10^8	85.8
1.0	4.0	10.33×10^8	128.7
1.5	0.5	-3.44×10^8	-42.9
1.5	1.0	-1.72×10^8	-21.4
1.5	2.0	1.72×10^8	21.4
1.5	3.0	5.16×10^8	64.3
1.5	4.0	8.61×10^8	107.2

TABLE 27
NET HEAT TRANSFER THROUGH AN EFFUSION SURFACE WHEN $T_2 = 100^{\circ}K$ AND $T_1 = 200^{\circ}K$

P_2 (Atm.)	P_1 (Atm.)	H (Erg/sec-cm^2)	HP
0.1	0.5	3.12×10^8	38.9
0.1	1.0	5.56×10^8	69.2
0.1	2.0	10.43×10^8	129.9
0.1	3.0	15.30×10^8	190.5
0.1	4.0	20.16×10^8	251.2
0.5	0.5	5.88×10^8	73.2
0.5	1.0	8.31×10^8	103.5
0.5	2.0	13.18×10^8	164.2
0.5	3.0	18.05×10^8	224.8
0.5	4.0	22.92×10^8	285.5
1.0	0.5	9.32×10^8	116.1
1.0	1.0	11.75×10^8	146.4
1.0	2.0	16.62×10^8	207.1
1.0	3.0	21.49×10^8	267.7
1.0	4.0	26.36×10^8	328.4
1.5	0.5	12.76×10^8	159.0
1.5	1.0	15.20×10^8	189.3
1.5	2.0	20.07×10^8	249.9
1.5	3.0	24.93×10^8	310.6
1.5	4.0	29.80×10^8	371.2

TABLE 28
NET HEAT TRANSFER THROUGH AN EFFUSION SURFACE WHEN $T_2 = 100^{\circ}K$ AND $T_1 = 273^{\circ}K$

P_2 (Atm.)	P_1 (Atm.)	H (Erg/sec-cm^2)	HP
0.1	0.5	4.28×10^8	53.4
0.1	1.0	7.13×10^8	88.8
0.1	2.0	12.82×10^8	159.7
0.1	3.0	18.51×10^8	230.5
0.1	4.0	24.20×10^8	301.4
0.5	0.5	10.06×10^8	125.3
0.5	1.0	12.90×10^8	160.7
0.5	2.0	18.59×10^8	231.6
0.5	3.0	24.28×10^8	302.4
0.5	4.0	29.97×10^8	373.3
1.0	0.5	17.27×10^8	215.1
1.0	1.0	20.11×10^8	250.5
1.0	2.0	25.80×10^8	321.4
1.0	3.0	31.49×10^8	392.2
1.0	4.0	37.18×10^8	463.1
1.5	0.5	24.48×10^8	304.9
1.5	1.0	27.33×10^8	340.4
1.5	2.0	33.01×10^8	411.2
1.5	3.0	38.70×10^8	482.9
1.5	4.0	44.39×10^8	552.9

TABLE 29
NET HEAT TRANSFER THROUGH AN EFFUSION SURFACE
WHEN $T_2 = 100^{\circ}K$ AND $T_1 = 400^{\circ}K$

P_2 (Atm.)	P_1 (Atm.)	H (Erg/sec-cm^2)	HP
0.1	0.5	6.20×10^8	77.2
0.1	1.0	9.64×10^8	120.1
0.1	2.0	16.53×10^8	205.8
0.1	3.0	23.41×10^8	291.6
0.1	4.0	30.30×10^8	377.4
0.5	0.5	17.21×10^8	214.4
0.5	1.0	20.66×10^8	257.3
0.5	2.0	27.54×10^8	343.1
0.5	3.0	34.43×10^8	428.8
0.5	4.0	41.31×10^8	514.6
1.0	0.5	30.98×10^8	386.0
1.0	1.0	34.43×10^8	428.8
1.0	2.0	41.31×10^8	514.6
1.0	3.0	48.20×10^8	600.4
1.0	4.0	55.08×10^8	686.1
1.5	0.5	44.76×10^8	557.5
1.5	1.0	48.20×10^8	600.4
1.5	2.0	55.08×10^8	686.1
1.5	3.0	61.97×10^8	771.9
1.5	4.0	68.86×10^8	857.7

TABLE 30
NET HEAT TRANSFER THROUGH AN EFFUSION SURFACE
WHEN $T_2 = 100^{\circ}K$ AND $T_1 = 500^{\circ}K$

P_2 (Atm.)	P_1 (Atm.)	H (Erg/sec-cm^2)	HP
0.1	0.5	7.64×10^8	95.1
0.1	1.0	11.49×10^8	143.1
0.1	2.0	19.18×10^8	239.0
0.1	3.0	26.88×10^8	334.8
0.1	4.0	34.58×10^8	430.7
0.5	0.5	22.78×10^8	283.8
0.5	1.0	26.63×10^8	331.7
0.5	2.0	34.33×10^8	427.6
0.5	3.0	42.03×10^8	523.5
0.5	4.0	49.73×10^8	619.4
1.0	0.5	41.72×10^8	519.7
1.0	1.0	45.57×10^8	567.6
1.0	2.0	53.27×10^8	663.5
1.0	3.0	60.97×10^8	759.4
1.0	4.0	68.66×10^8	855.3
1.5	0.5	60.65×10^8	755.5
1.5	1.0	64.50×10^8	803.5
1.5	2.0	72.20×10^8	899.4
1.5	3.0	79.90×10^8	995.2
1.5	4.0	87.60×10^8	1091.1

TABLE 31
NET HEAT TRANSFER THROUGH AN EFFUSION SURFACE
WHEN $T_2 = 200^{\circ}K$ AND $T_1 = 100^{\circ}K$

P_2 (Atm.)	P_1 (Atm.)	H (Erg/sec-cm^2)	HP
0.1	0.5	$.50 \times 10^8$	6.3
0.1	1.0	2.23×10^8	27.7
0.1	2.0	5.67×10^8	70.6
0.1	3.0	9.11×10^8	113.5
0.1	4.0	12.55×10^8	156.4
0.5	0.5	-4.36×10^8	-54.4
0.5	1.0	-2.64×10^8	-32.9
0.5	2.0	$.80 \times 10^8$	10.0
0.5	3.0	4.24×10^8	52.8
0.5	4.0	7.69×10^8	95.7
1.0	0.5	-10.45×10^8	-130.2
1.0	1.0	$- 8.73 \times 10^8$	-108.7
1.0	2.0	$- 5.29 \times 10^8$	- 65.8
1.0	3.0	$- 1.84 \times 10^8$	- 23.0
1.0	4.0	1.60×10^8	19.9
1.5	0.5	-16.54×10^8	-206.0
1.5	1.0	-14.82×10^8	-184.5
1.5	2.0	-11.37×10^8	-141.7
1.5	3.0	$- 7.93 \times 10^8$	- 98.8
1.5	4.0	$- 4.49 \times 10^8$	- 55.9

TABLE 32
NET HEAT TRANSFER THROUGH AN EFFUSION SURFACE
WHEN $T_2 = 200^{\circ}K$ AND $T_1 = 200^{\circ}K$

P_2 (Atm.)	P_1 (Atm.)	H (Erg/sec-cm^2)	HP
0.1	0.5	1.95×10^8	24.3
0.1	1.0	4.38×10^8	54.6
0.1	2.0	9.25×10^8	115.2
0.1	3.0	14.12×10^8	175.8
0.1	4.0	18.99×10^8	236.5
0.5	0.5	13.77×10^0	0.0
0.5	1.0	2.43×10^8	30.3
0.5	2.0	7.30×10^8	91.0
0.5	3.0	12.17×10^8	151.6
0.5	4.0	17.04×10^8	212.3
1.0	0.5	-2.43×10^8	-30.3
1.0	1.0	27.54×10^0	0.0
1.0	2.0	4.87×10^8	60.6
1.0	3.0	9.74×10^8	121.3
1.0	4.0	14.61×10^8	181.9
1.5	0.5	-4.87×10^8	-60.6
1.5	1.0	-2.43×10^8	-30.3
1.5	2.0	2.43×10^8	30.3
1.5	3.0	7.30×10^8	91.0
1.5	4.0	12.17×10^8	151.6

TABLE 33
NET HEAT TRANSFER THROUGH AN EFFUSION SURFACE
WHEN T_2 = 200°K AND T_1 = 273°K

P_2 (Atm.)	P_1 (Atm.)	H (Erg/sec-cm^2)	HP
0.1	0.5	2.89×10^8	36.0
0.1	1.0	5.73×10^8	71.4
0.1	2.0	11.42×10^8	142.3
0.1	3.0	17.11×10^8	213.1
0.1	4.0	22.80×10^8	284.0
0.5	0.5	3.08×10^8	38.3
0.5	1.0	5.92×10^8	73.7
0.5	2.0	11.61×10^8	144.6
0.5	3.0	17.30×10^8	215.4
0.5	4.0	22.98×10^8	286.3
1.0	0.5	3.31×10^8	41.2
1.0	1.0	6.15×10^8	76.6
1.0	2.0	11.84×10^8	147.5
1.0	3.0	17.53×10^8	218.3
1.0	4.0	23.22×10^8	289.2
1.5	0.5	3.54×10^8	44.1
1.5	1.0	6.38×10^8	79.5
1.5	2.0	12.07×10^8	150.4
1.5	3.0	17.76×10^8	221.2
1.5	4.0	23.45×10^8	292.1

TABLE 34
NET HEAT TRANSFER THROUGH AN EFFUSION SURFACE
WHEN $T_2 = 200^{\circ}K$ AND $T_1 = 400^{\circ}K$

P_2 (Atm.)	P_1 (Atm.)	H (Erg/sec-cm^2)	HP
0.1	0.5	4.42×10^8	55.0
0.1	1.0	7.86×10^8	97.9
0.1	2.0	14.74×10^8	183.7
0.1	3.0	21.63×10^8	269.4
0.1	4.0	28.52×10^8	355.2
0.5	0.5	8.31×10^8	103.5
0.5	1.0	11.75×10^8	146.4
0.5	2.0	18.64×10^8	232.2
0.5	3.0	25.53×10^8	317.9
0.5	4.0	32.41×10^8	403.7
1.0	0.5	13.18×10^8	164.2
1.0	1.0	16.62×10^8	207.1
1.0	2.0	23.51×10^8	292.8
1.0	3.0	30.39×10^8	378.6
1.0	4.0	37.28×10^8	464.4
1.5	0.5	18.05×10^8	224.8
1.5	1.0	21.49×10^8	267.7
1.5	2.0	28.38×10^8	353.5
1.5	3.0	35.26×10^8	439.2
1.5	4.0	42.15×10^8	525.0

TABLE 35
NET HEAT TRANSFER THROUGH AN EFFUSION SURFACE
WHEN $T_2 = 200^{\circ}K$ AND $T_1 = 500^{\circ}K$

P_2 (Atm.)	P_1 (Atm.)	H (Erg/sec-cm^2)	HP
0.1	0.5	5.55×10^8	69.2
0.1	1.0	9.40×10^8	117.1
0.1	2.0	17.10×10^8	213.0
0.1	3.0	24.80×10^8	308.9
0.1	4.0	32.50×10^8	404.8
0.5	0.5	12.37×10^8	154.1
0.5	1.0	16.22×10^8	202.0
0.5	2.0	23.92×10^8	297.9
0.5	3.0	31.62×10^8	393.8
0.5	4.0	39.31×10^8	489.7
1.0	0.5	20.89×10^8	260.2
1.0	1.0	24.74×10^8	308.2
1.0	2.0	32.44×10^8	404.0
1.0	3.0	40.14×10^8	499.9
1.0	4.0	47.83×10^8	595.8
1.5	0.5	29.41×10^8	366.3
1.5	1.0	33.26×10^8	414.3
1.5	2.0	40.96×10^8	510.2
1.5	3.0	48.66×10^8	606.1
1.5	4.0	56.35×10^8	702.0

TABLE 36
NET HEAT TRANSFER THROUGH AN EFFUSION SURFACE
WHEN $T_2 = 273^{\circ}K$ AND $T_1 = 100^{\circ}K$

P_2 (Atm.)	P_1 (Atm.)	H (Erg/sec-cm^2)	HP
0.1	0.5	$.07 \times 10^8$	0.9
0.1	1.0	1.79×10^8	22.3
0.1	2.0	5.24×10^8	65.2
0.1	3.0	8.68×10^8	108.1
0.1	4.0	12.12×10^8	151.0
0.5	0.5	-6.53×10^8	-81.3
0.5	1.0	-4.81×10^8	-59.9
0.5	2.0	-1.37×10^8	-17.0
0.5	3.0	2.08×10^8	25.9
0.5	4.0	5.52×10^8	68.8
1.0	0.5	-14.78×10^8	-184.1
1.0	1.0	-13.06×10^8	-162.7
1.0	2.0	-9.62×10^8	-119.8
1.0	3.0	-6.17×10^8	-76.9
1.0	4.0	-2.73×10^8	-34.0
1.5	0.5	-23.03×10^8	-286.9
1.5	1.0	-21.31×10^8	-265.5
1.5	2.0	-17.87×10^8	-222.6
1.5	3.0	-14.43×10^8	-179.7
1.5	4.0	-10.98×10^8	-136.8

TABLE 37
NET HEAT TRANSFER THROUGH AN EFFUSION SURFACE
WHEN $T_2 = 273^{\circ}K$ AND $T_1 = 200^{\circ}K$

P_2 (Atm.)	P_1 (Atm.)	H (Erg/sec-cm^2)	HP
0.1	0.5	1.41×10^8	17.6
0.1	1.0	3.84×10^8	47.9
0.1	2.0	8.71×10^8	108.5
0.1	3.0	13.58×10^8	169.2
0.1	4.0	18.45×10^8	229.8
0.5	0.5	-2.69×10^8	-33.5
0.5	1.0	-0.26×10^8	- 3.2
0.5	2.0	4.61×10^8	57.4
0.5	3.0	9.48×10^8	118.1
0.5	4.0	14.35×10^8	178.7
1.0	0.5	-7.81×10^8	-97.4
1.0	1.0	-5.38×10^8	-67.0
1.0	2.0	-0.51×10^8	- 6.4
1.0	3.0	4.35×10^8	54.2
1.0	4.0	9.22×10^8	114.9
1.5	0.5	-12.94×10^8	-161.2
1.5	1.0	-10.51×10^8	-130.9
1.5	2.0	-5.64×10^8	-70.2
1.5	3.0	-0.77×10^8	- 9.6
1.5	4.0	4.10×10^8	51.0

TABLE 38
NET HEAT TRANSFER THROUGH AN EFFUSION SURFACE
WHEN $T_2 = 273^{\circ}K$ AND $T_1 = 273^{\circ}K$

P_2 (Atm.)	P_1 (Atm.)	$\dot{H}$ (Erg/sec-cm^2)	HP
0.1	0.5	2.28×10^8	28.3
0.1	1.0	5.12×10^8	63.8
0.1	2.0	10.81×10^8	134.6
0.1	3.0	16.50×10^8	205.5
0.1	4.0	22.18×10^8	276.3
0.5	0.5	13.77	0.0
0.5	1.0	2.84×10^8	35.4
0.5	2.0	8.53×10^8	106.3
0.5	3.0	14.22×10^8	177.1
0.5	4.0	19.91×10^8	248.0
1.0	0.5	-2.84×10^8	-35.4
1.0	1.0	27.54	0.0
1.0	2.0	5.69×10^8	70.9
1.0	3.0	11.38×10^8	141.7
1.0	4.0	17.07×10^8	212.6
1.5	0.5	-5.69×10^8	-70.9
1.5	1.0	-2.84×10^8	-35.4
1.5	2.0	2.84×10^8	35.4
1.5	3.0	8.53×10^8	106.3
1.5	4.0	14.22×10^8	177.1

TABLE 39
NET HEAT TRANSFER THROUGH AN EFFUSION SURFACE
WHEN T_2 = 273°K AND T_1 = 400°K

P_2 (Atm.)	P_1 (Atm.)	H (Erg/sec-cm^2)	HP
0.1	0.5	3.67×10^8	45.7
0.1	1.0	7.11×10^8	88.6
0.1	2.0	14.00×10^8	174.3
0.1	3.0	20.88×10^8	260.1
0.1	4.0	27.77×10^8	345.9
0.5	0.5	4.57×10^8	56.9
0.5	1.0	8.01×10^8	99.8
0.5	2.0	14.90×10^8	185.5
0.5	3.0	21.78×10^8	271.3
0.5	4.0	28.67×10^8	357.1
1.0	0.5	5.69×10^8	70.9
1.0	1.0	9.14×10^8	113.8
1.0	2.0	16.02×10^8	199.6
1.0	3.0	22.91×10^8	285.3
1.0	4.0	29.79×10^8	371.1
1.5	0.5	6.82×10^8	84.9
1.5	1.0	10.26×10^8	127.8
1.5	2.0	17.15×10^8	213.6
1.5	3.0	24.03×10^8	299.3
1.5	4.0	30.92×10^8	385.1

TABLE 40
NET HEAT TRANSFER THROUGH AN EFFUSION SURFACE
WHEN $T_2 = 273^{\circ}K$ AND $T_1 = 500^{\circ}K$

P_2 (Atm.)	P_1 (Atm.)	H (Erg/sec-cm^2)	HP
0.1	0.5	4.70×10^8	58.5
0.1	1.0	8.55×10^8	106.5
0.1	2.0	16.25×10^8	202.4
0.1	3.0	23.95×10^8	298.3
0.1	4.0	31.64×10^8	394.1
0.5	0.5	3.10×10^8	100.9
0.5	1.0	11.95×10^8	148.8
0.5	2.0	19.65×10^8	244.7
0.5	3.0	27.35×10^8	340.6
0.5	4.0	35.04×10^8	436.5
1.0	0.5	12.35×10^8	153.8
1.0	1.0	16.20×10^8	201.8
1.0	2.0	23.90×10^8	297.7
1.0	3.0	31.60×10^8	393.6
1.0	4.0	39.29×10^8	489.5
1.5	0.5	16.60×10^8	206.8
1.5	1.0	20.45×10^8	254.7
1.5	2.0	28.15×10^8	350.1
1.5	3.0	35.85×10^8	446.5
1.5	4.0	43.55×10^8	542.4

TABLE 41
NET HEAT TRANSFER THROUGH AN EFFUSION SURFACE
WHEN T_2 = 400°K AND T_1 = 100°K

P_2 (Atm.)	P_1 (Atm.)	H (Erg/sec-cm^2)	HP
0.1	0.5	-0.52×10^8	- 6.4
0.1	1.0	1.20×10^8	15.0
0.1	2.0	4.65×10^8	57.9
0.1	3.0	8.09×10^8	100.8
0.1	4.0	11.53×10^8	143.7
0.5	0.5	-9.47×10^8	-117.9
0.5	1.0	-7.75×10^8	- 96.5
0.5	2.0	-4.30×10^8	- 53.6
0.5	3.0	$-.86 \times 10^8$	- 10.7
0.5	4.0	2.58×10^8	32.2
1.0	0.5	-20.7×10^8	-257.3
1.0	1.0	-18.94×10^8	-235.9
1.0	2.0	-15.49×10^8	-193.0
1.0	3.0	-12.05×10^8	-150.1
1.0	4.0	-8.61×10^8	-107.2
1.5	0.5	-31.85×10^8	-396.7
1.5	1.0	-30.12×10^8	-375.2
1.5	2.0	-26.68×10^8	-332.3
1.5	3.0	-23.24×10^8	-289.5
1.5	4.0	-19.80×10^8	-246.6

TABLE 42
NET HEAT TRANSFER THROUGH AN EFFUSION SURFACE
WHEN $T_2 = 400^{\circ}K$ AND $T_1 = 200^{\circ}K$

P_2 (Atm.)	P_1 (Atm.)	H (Erg/sec-cm^2)	HP
0.1	0.5	$.71 \times 10^8$	8.9
0.1	1.0	3.15×10^8	39.2
0.1	2.0	8.02×10^8	99.9
0.1	3.0	12.89×10^8	160.5
0.1	4.0	17.75×10^8	221.1
0.5	0.5	$- 6.17 \times 10^8$	- 76.9
0.5	1.0	$- 3.74 \times 10^8$	- 46.6
0.5	2.0	1.13×10^8	14.1
0.5	3.0	6.00×10^8	74.7
0.5	4.0	10.87×10^8	135.4
1.0	0.5	-14.78×10^8	-184.1
1.0	1.0	-12.35×10^8	-153.8
1.0	2.0	$- 7.48 \times 10^8$	- 93.1
1.0	3.0	$- 2.61 \times 10^8$	- 32.5
1.0	4.0	2.26×10^8	28.2
1.5	0.5	$- 23.39 \times 10^8$	-291.3
1.5	1.0	$- 20.95 \times 10^8$	-261.0
1.5	2.0	$- 16.08 \times 10^8$	-200.3
1.5	3.0	$- 11.21 \times 10^8$	-139.7
1.5	4.0	$- 6.35 \times 10^8$	- 79.0

TABLE 43
NET HEAT TRANSFER THROUGH AN EFFUSION SURFACE
WHEN $T_2 = 400^{\circ}K$ AND $T_1 = 273^{\circ}K$

P_2 (Atm.)	P_1 (Atm.)	H (Erg/sec-cm^2)	HP
0.1	0.5	1.50×10^8	18.7
0.1	1.0	4.34×10^8	54.1
0.1	2.0	10.03×10^8	125.0
0.1	3.0	15.72×10^8	195.8
0.1	4.0	21.41×10^8	266.7
0.5	0.5	$- 3.88 \times 10^8$	- 48.3
0.5	1.0	$- 1.03 \times 10^8$	- 12.9
0.5	2.0	4.65×10^8	58.0
0.5	3.0	10.34×10^8	128.8
0.5	4.0	16.03×10^8	199.7
1.0	0.5	-10.60×10^8	-132.0
1.0	1.0	$- 7.76 \times 10^8$	- 96.6
1.0	2.0	$- 2.07 \times 10^8$	- 25.7
1.0	3.0	3.62×10^8	45.1
1.0	4.0	9.31×10^8	116.0
1.5	0.5	-17.32×10^8	-215.8
1.5	1.0	-14.48×10^8	-180.3
1.5	2.0	$- 8.79 \times 10^8$	-109.5
1.5	3.0	$- 3.10 \times 10^8$	- 38.6
1.5	4.0	2.59×10^8	32.2

TABLE 44
NET HEAT TRANSFER THROUGH AN EFFUSION SURFACE
WHEN $T_2 = 400^{\circ}K$ AND $T_1 = 400^{\circ}K$

P_2 (Atm.)	P_1 (Atm.)	H (Erg/sec-cm^2)	HP
0.1	0.5	2.75×10^8	34.3
0.1	1.0	6.20×10^8	77.2
0.1	2.0	13.08×10^8	163.0
0.1	3.0	19.97×10^8	248.7
0.1	4.0	26.85×10^8	334.5
0.5	0.5	0.0	0.0
0.5	1.0	3.44×10^8	42.9
0.5	2.0	10.33×10^8	128.7
0.5	3.0	17.21×10^8	214.4
0.5	4.0	24.10×10^8	300.2
1.0	0.5	$- 3.44 \times 10^8$	- 42.9
1.0	1.0	0.0	0.0
1.0	2.0	6.89×10^8	85.8
1.0	3.0	13.77×10^8	171.5
1.0	4.0	20.66×10^8	257.3
1.5	0.5	$- 6.89 \times 10^8$	- 85.8
1.5	1.0	$- 3.44 \times 10^8$	- 42.9
1.5	2.0	3.44×10^8	42.9
1.5	3.0	10.33×10^8	128.7
1.5	4.0	17.21×10^8	214.4

TABLE 45
NET HEAT TRANSFER THROUGH AN EFFUSION SURFACE
WHEN $T_2 = 400^{\circ}K$ AND $T_1 = 500^{\circ}K$

P_2 (Atm.)	P_1 (Atm.)	H (Erg/sec-cm^2)	HP
0.1	0.5	3.68×10^8	45.8
0.1	1.0	7.53×10^8	93.7
0.1	2.0	15.22×10^8	189.6
0.1	3.0	22.92×10^8	285.5
0.1	4.0	30.62×10^8	381.4
0.5	0.5	2.99×10^8	37.2
0.5	1.0	6.84×10^8	85.2
0.5	2.0	14.54×10^8	181.1
0.5	3.0	22.23×10^8	276.9
0.5	4.0	29.93×10^8	372.8
1.0	0.5	2.13×10^8	26.5
1.0	1.0	5.98×10^8	74.4
1.0	2.0	13.68×10^8	170.3
1.0	3.0	21.37×10^8	266.2
1.0	4.0	29.07×10^8	362.1
1.5	0.5	1.27×10^8	15.8
1.5	1.0	5.12×10^8	63.7
1.5	2.0	12.81×10^8	159.6
1.5	3.0	20.51×10^8	255.5
1.5	4.0	28.21×10^8	351.4

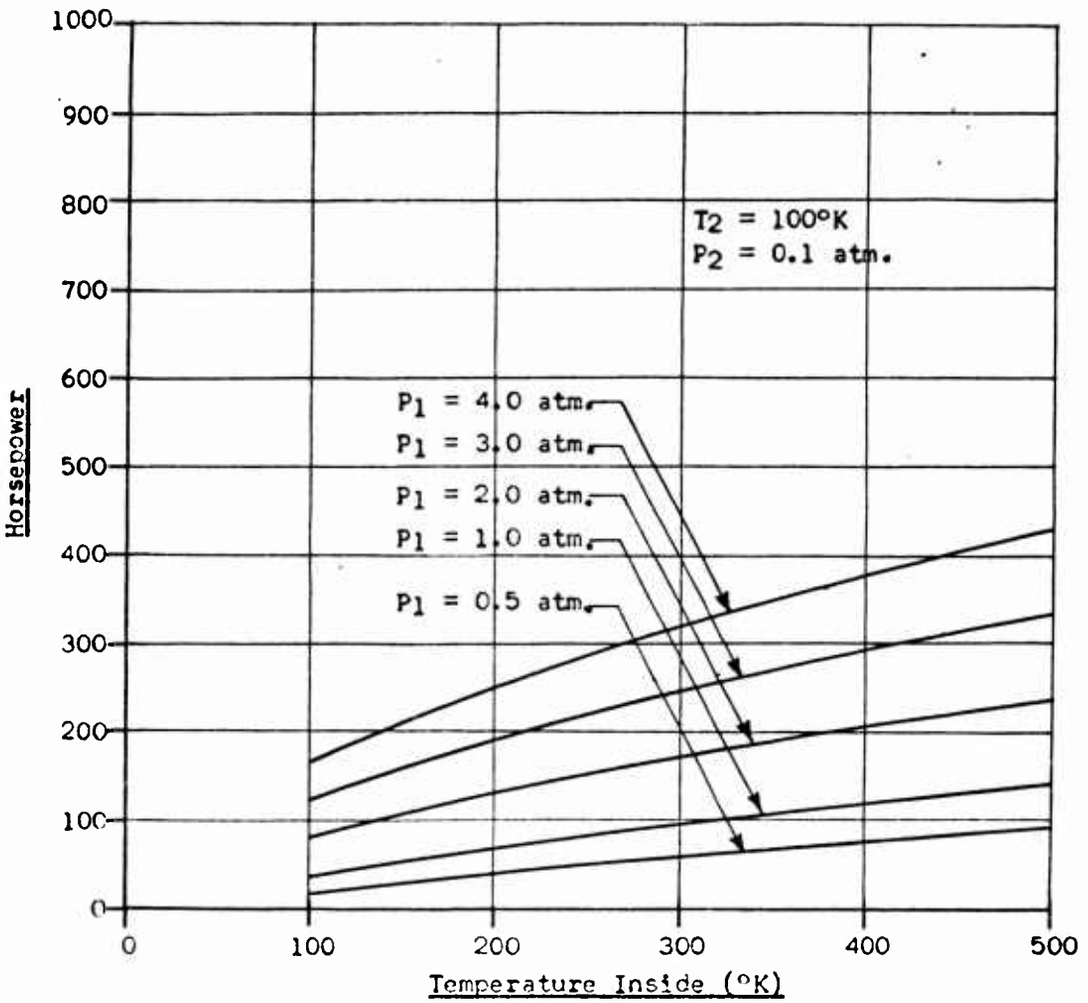

Figure 25. Horsepower as a Function of Effusion-Chamber Temperature for P_2 = 0.1 Atm., T_2 = 100°K.

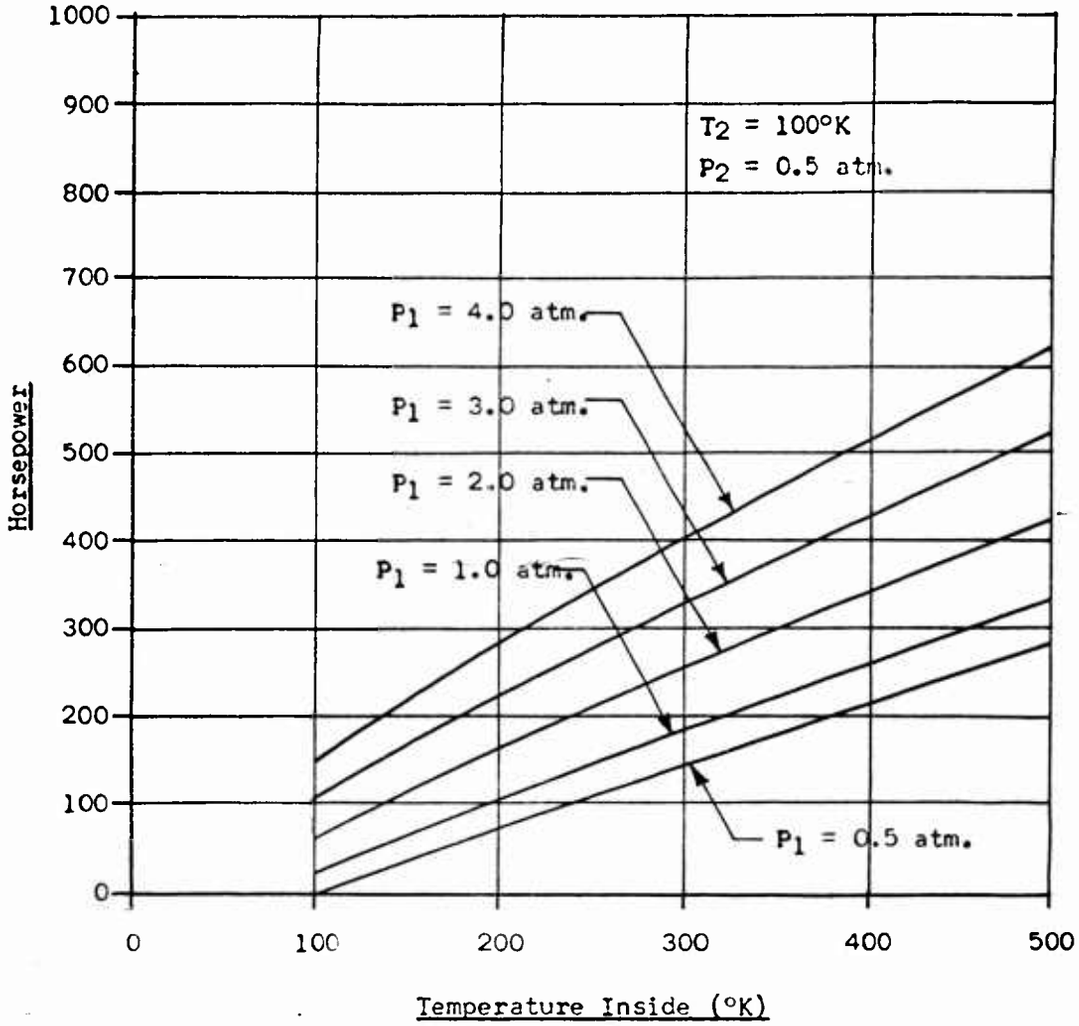

Figure 26. Horsepower as a Function of Effusion-Chamber Temperature for P_2 = 0.5 Atm., T_2 = 100°K.

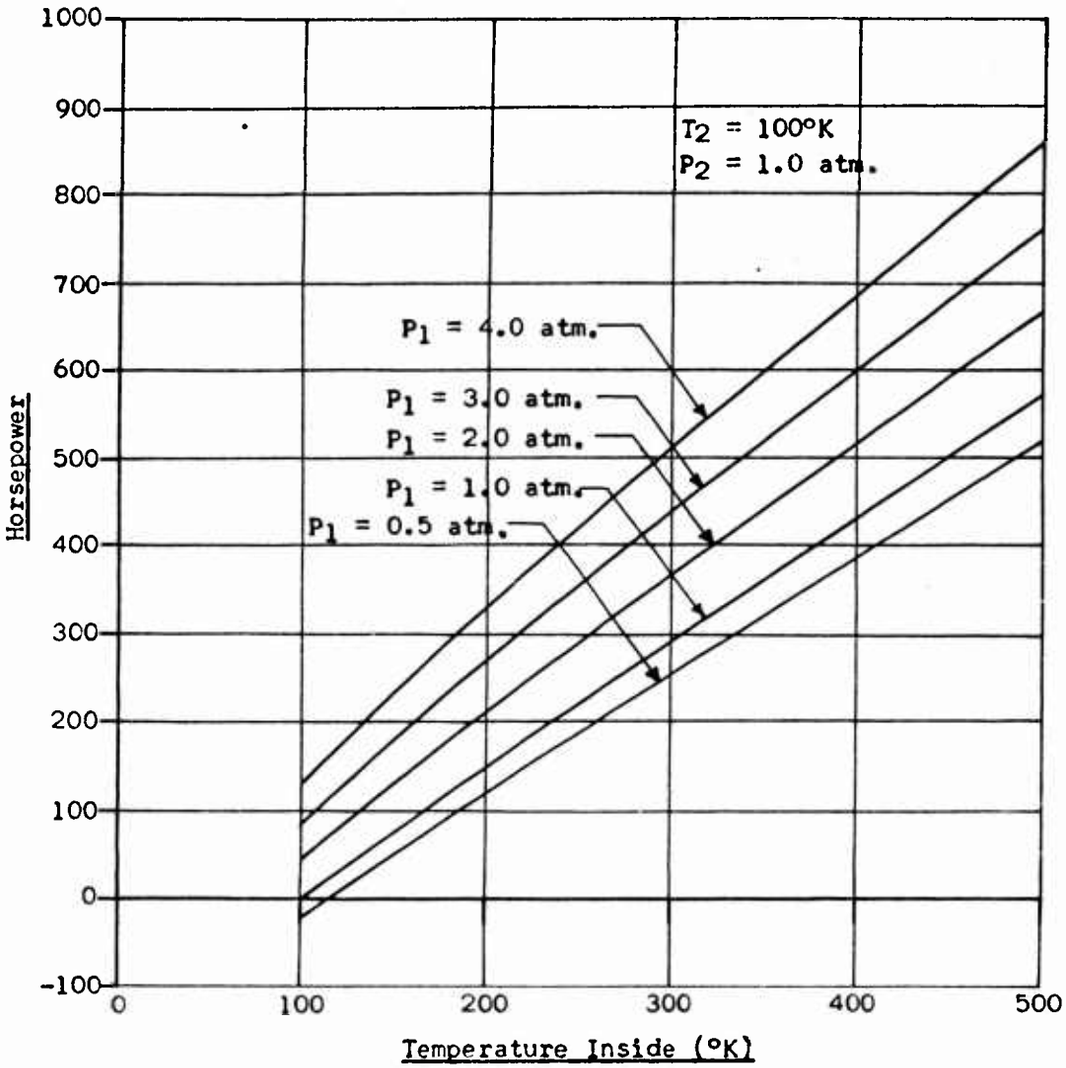

Figure 27. Horsepower as a Function of Effusion-Chamber Temperature for P_2 = 1.0 Atm., T_2 = 100°K.

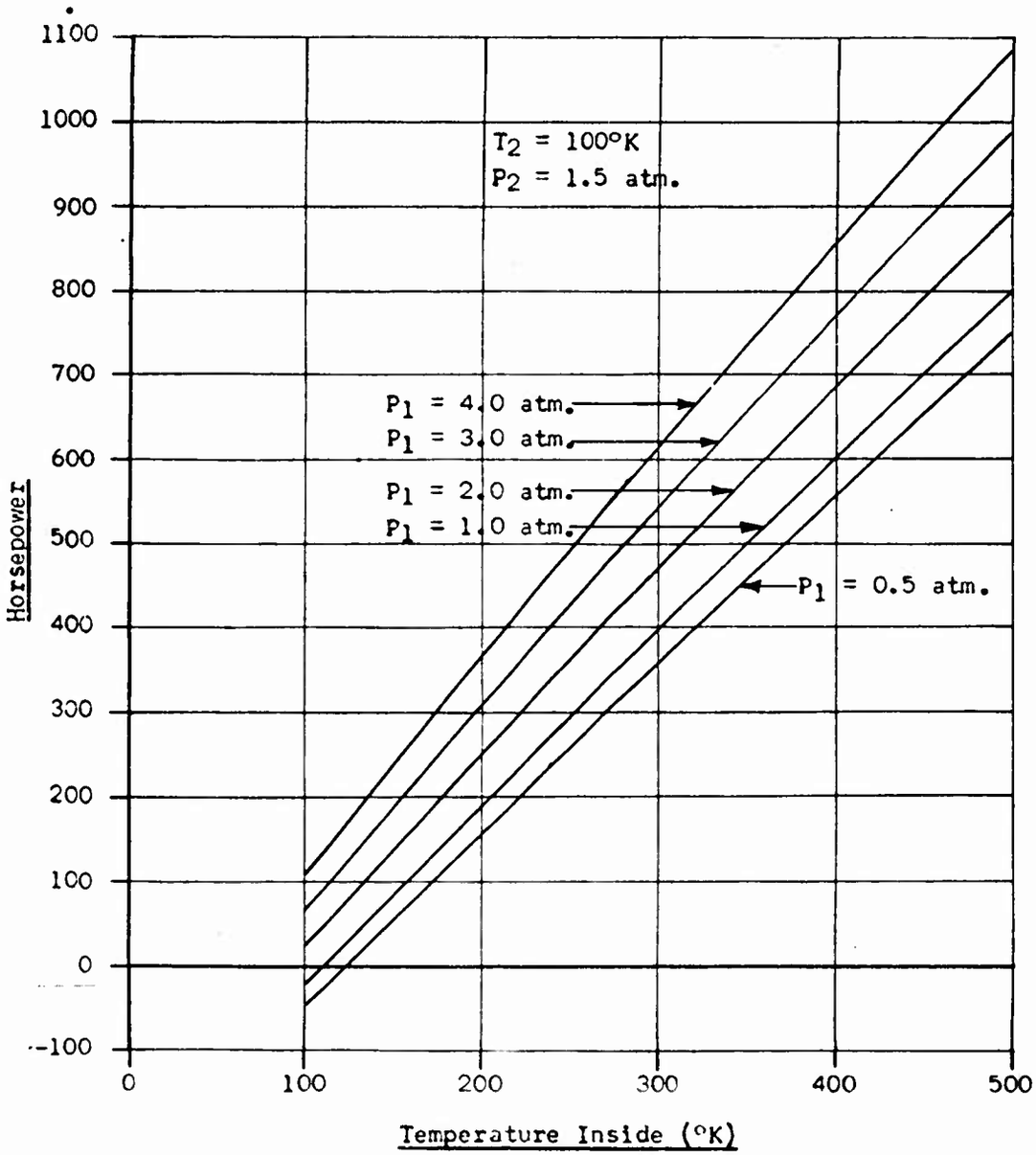

Figure 28. Horsepower as a Function of Effusion-Chamber Temperature for P_2 = 1.5 Atm., T_2 = 100°K.

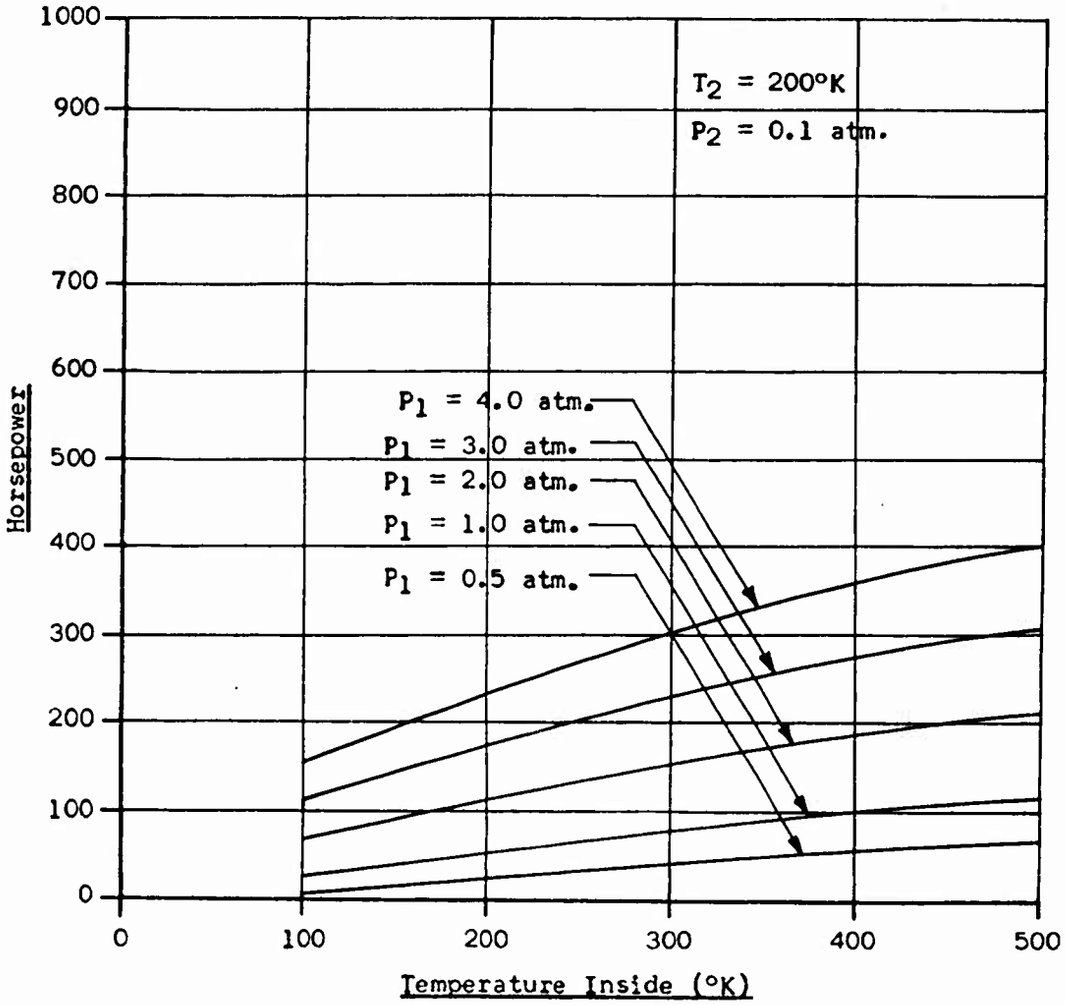

Figure 29. Horsepower as a Function of Effusion-Chamber Temperature for P_2 = 0.1 Atm., T_2 = 200°K.

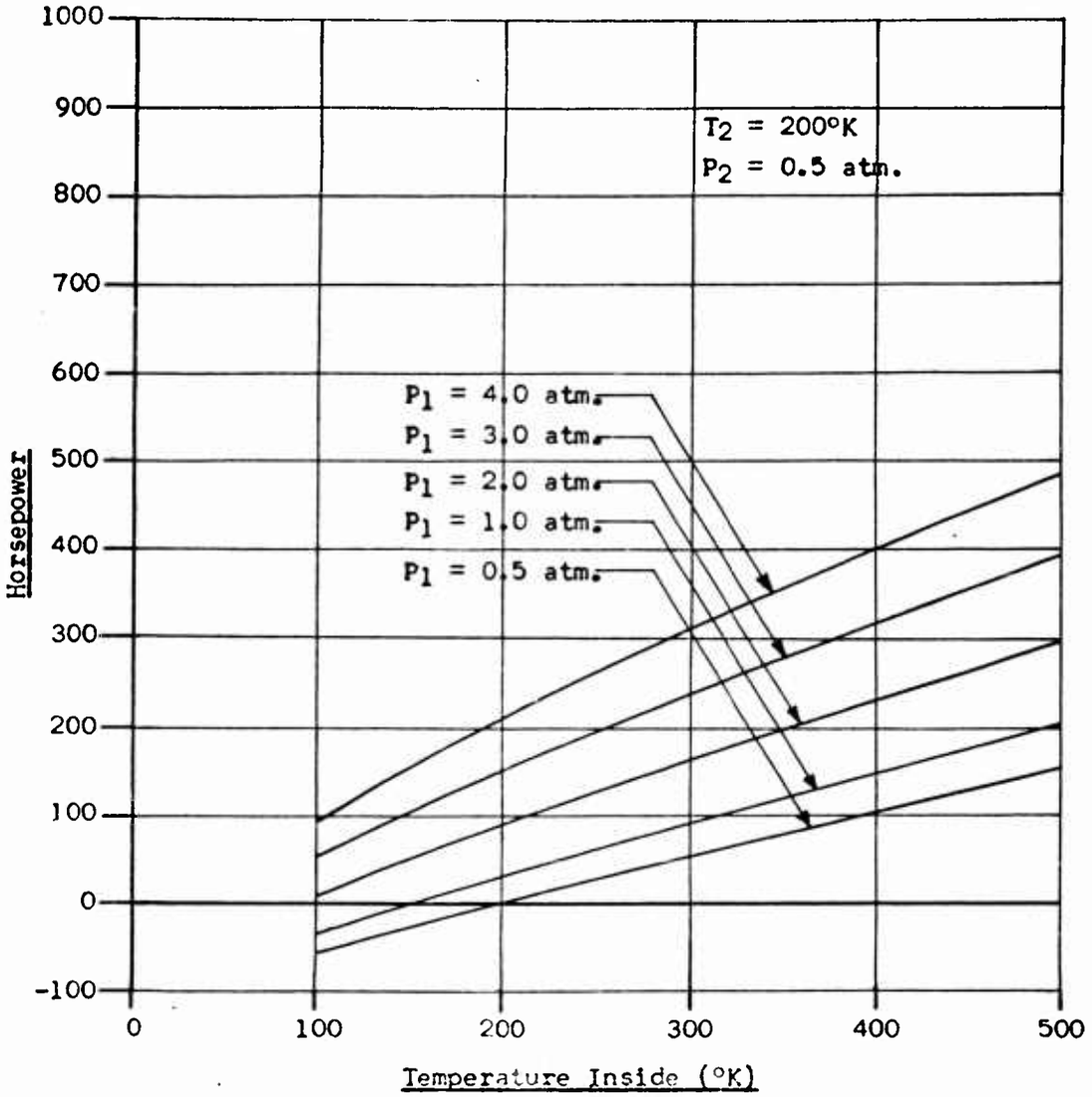

Figure 30. Horsepower as a Function of Effusion-Chamber Temperature for P_2 = 0.5 Atm., T_2 = 200°K.

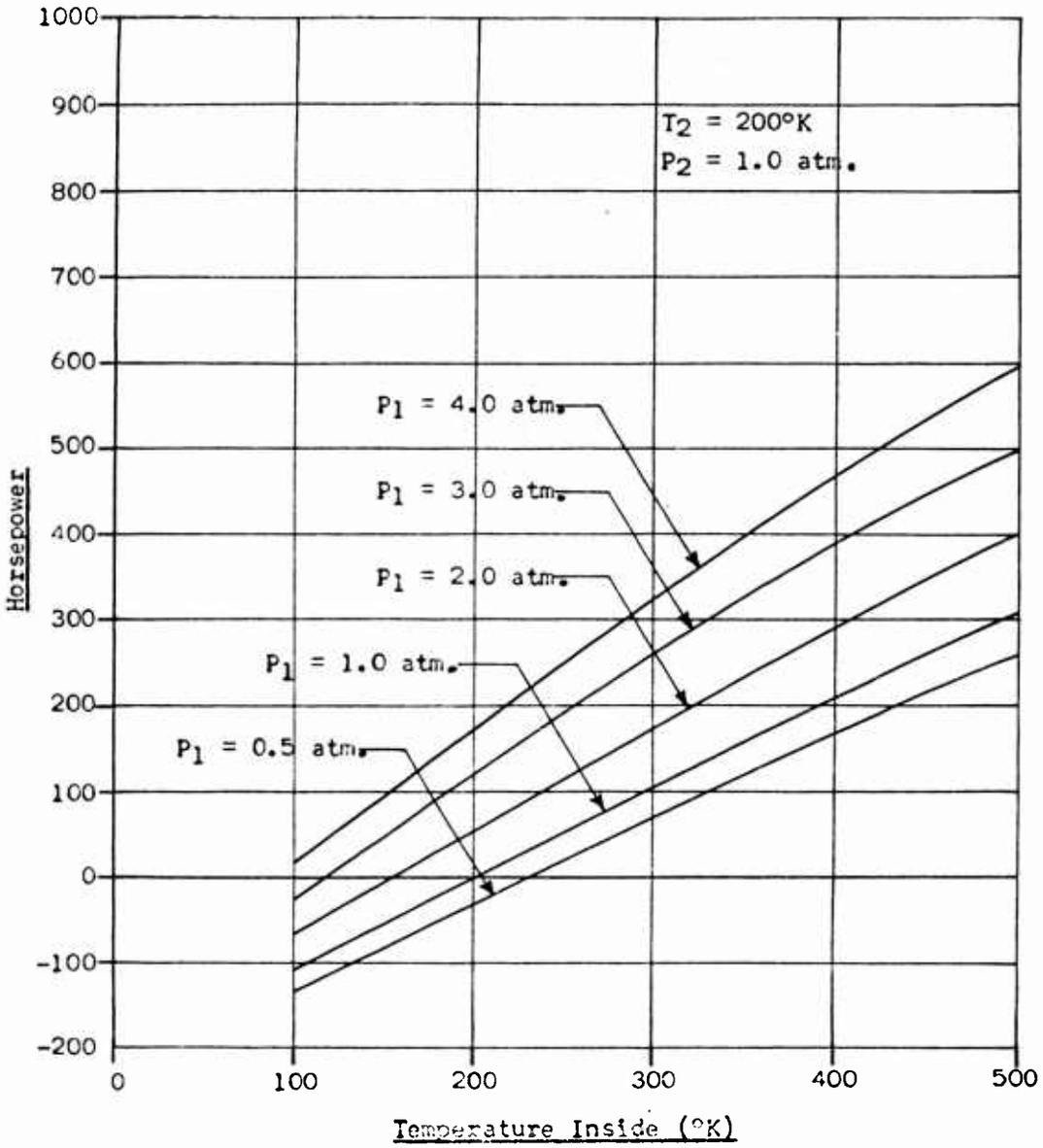

Figure 31. Horsepower as a Function of Effusion-Chamber Temperature for P_2 = 1.0 Atm., T_2 = 200°K.

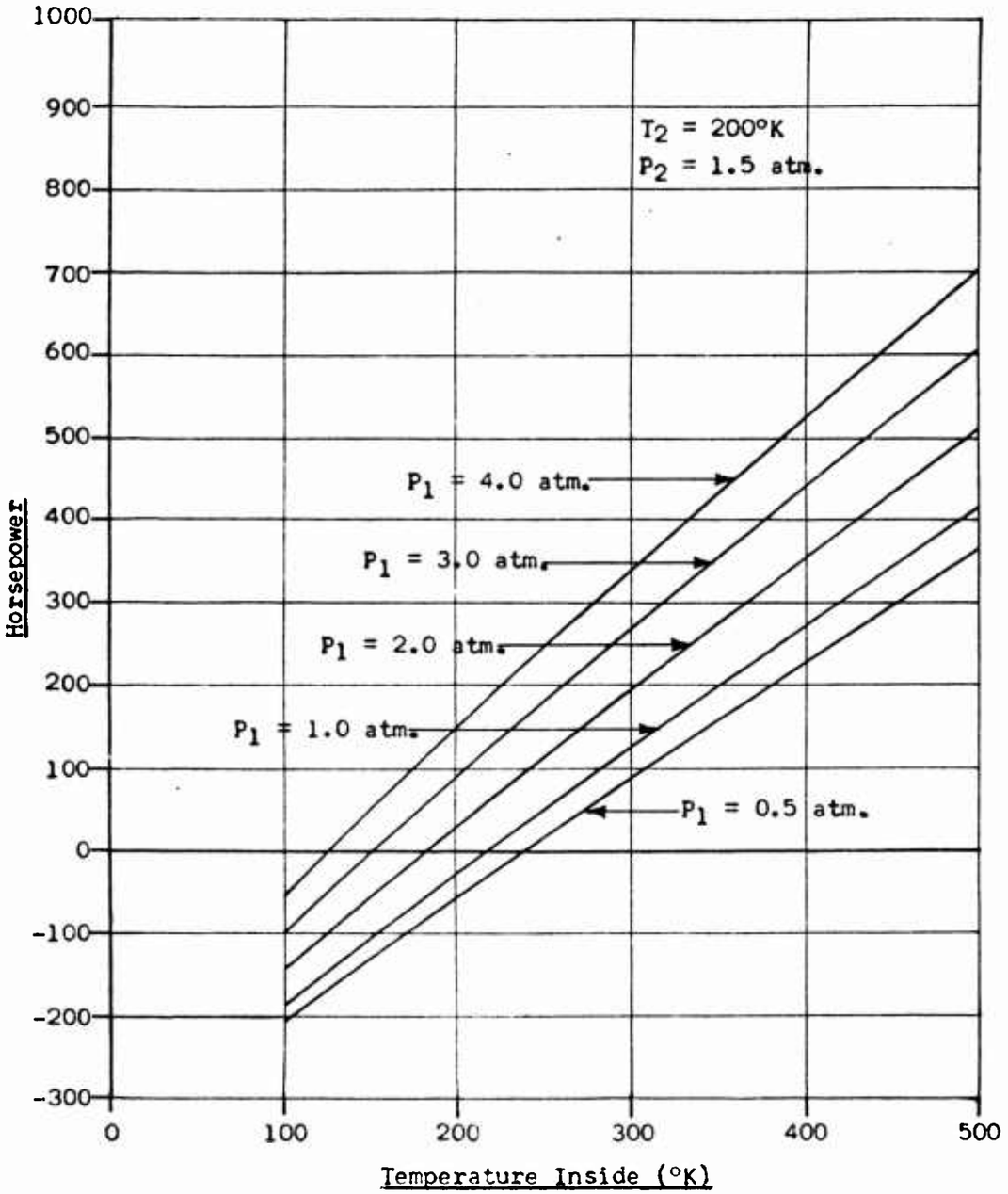

Figure 32. Horsepower as a Function of Effusion-Chamber Temperature for P_2 = 1.5 Atm., T_2 = 200°K.

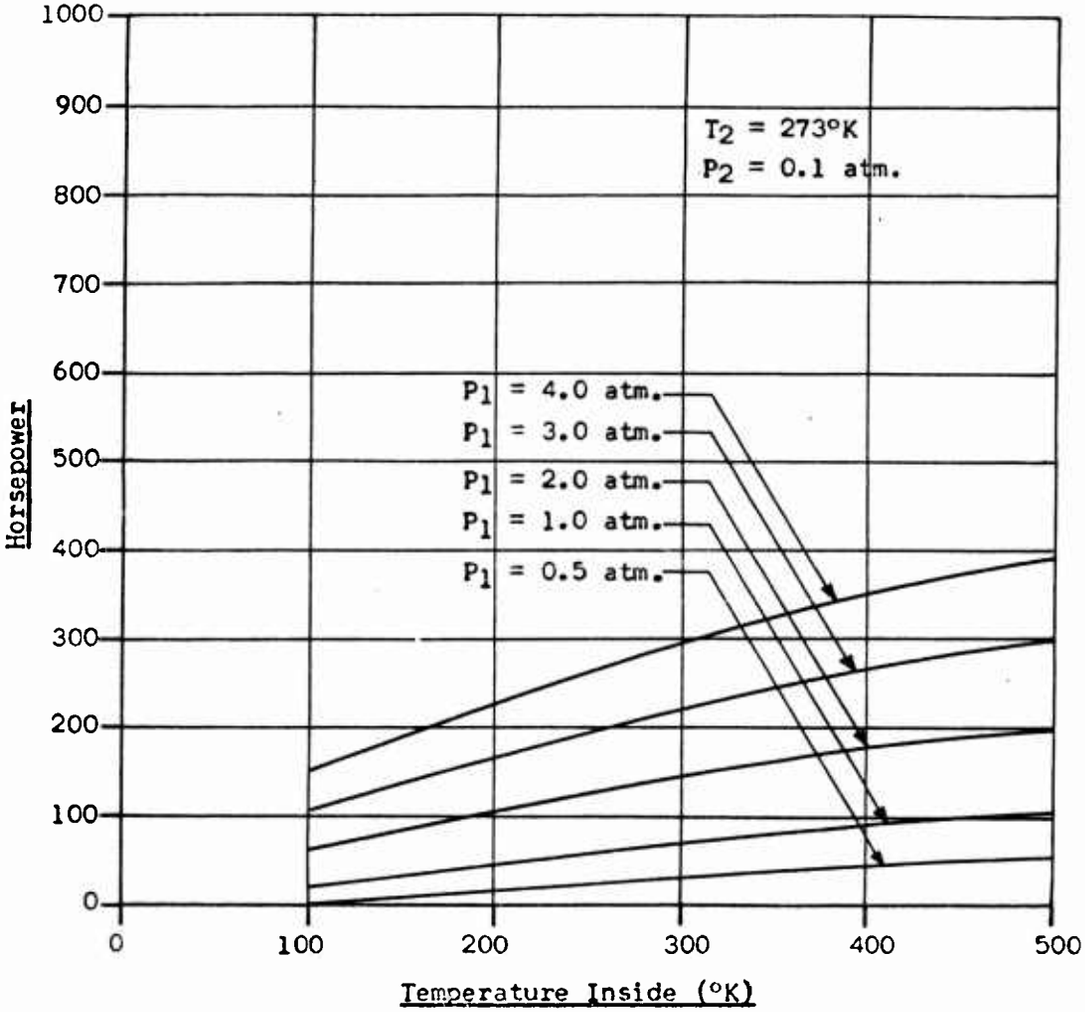

Figure 33. Horsepower as a Function of Effusion-Chamber Temperature for P_2 = 0.1 Atm., T_2 = 273°K.

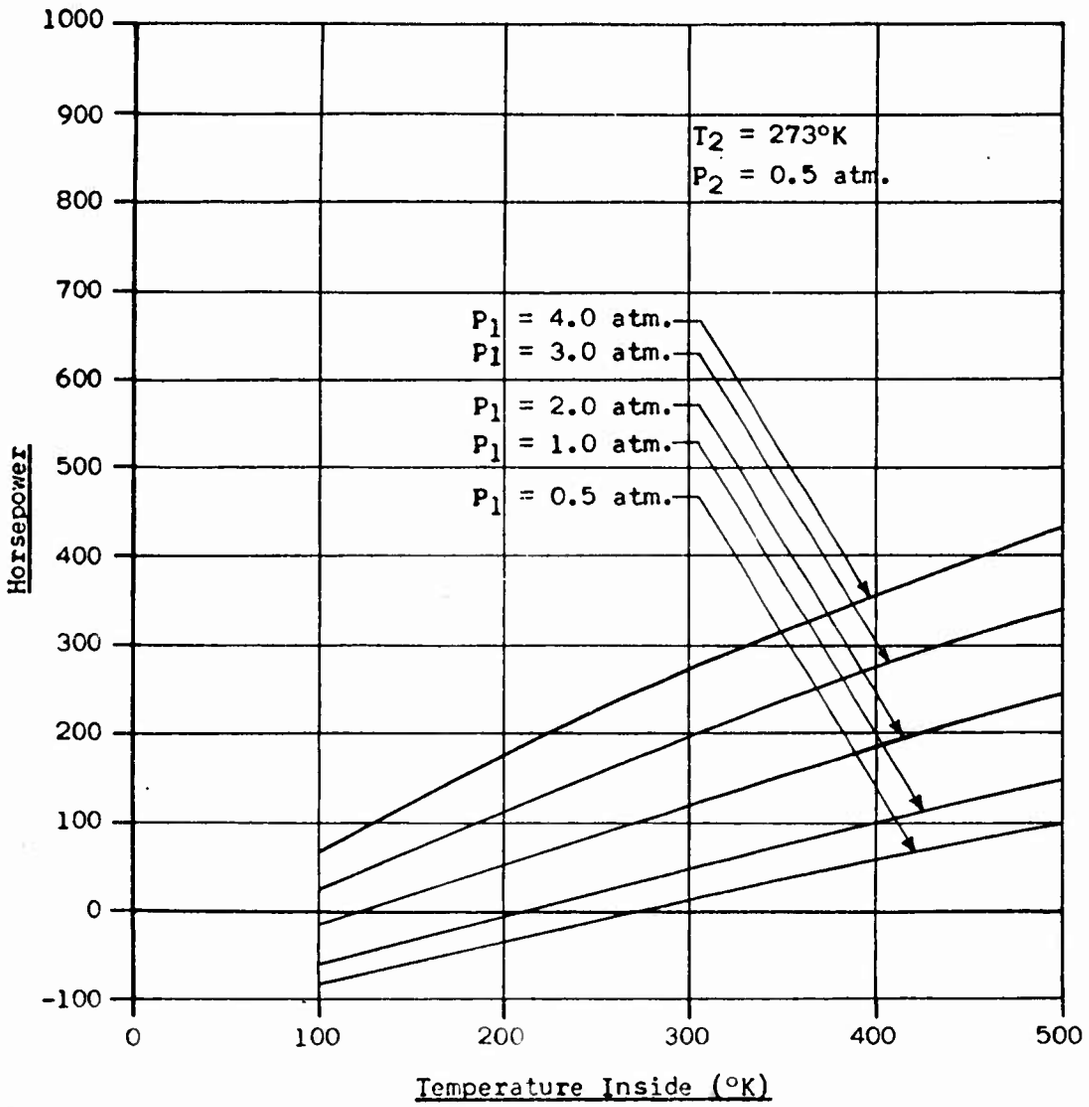

Figure 34. Horsepower as a Function of Effusion-Chamber Temperature for P_2 = 0.5 Atm., T_2 = 273°K.

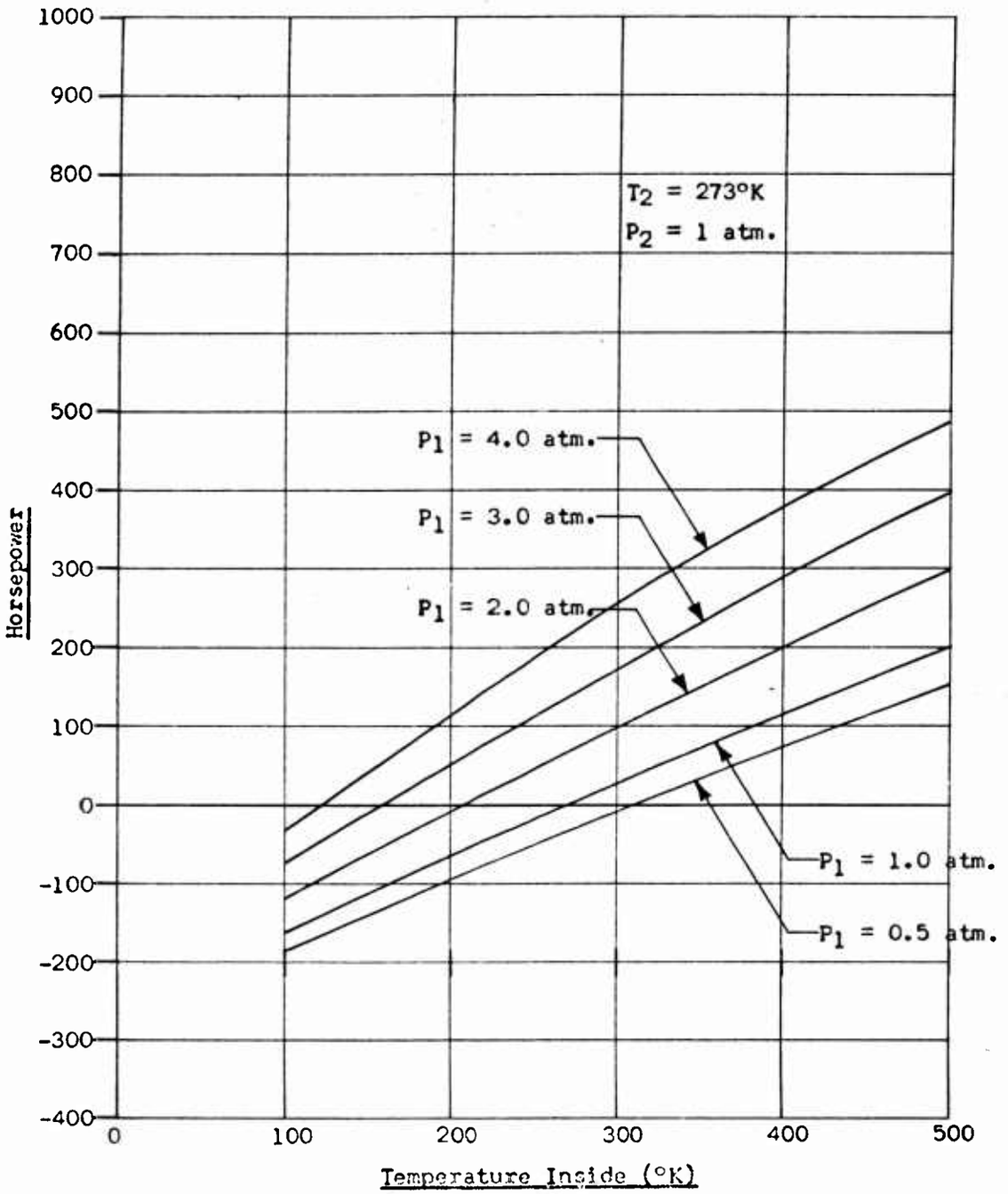

Figure 35. Horsepower as a Function of Effusion-Chamber Temperature for P_2 = 1 Atm., T_2 = 273°K.

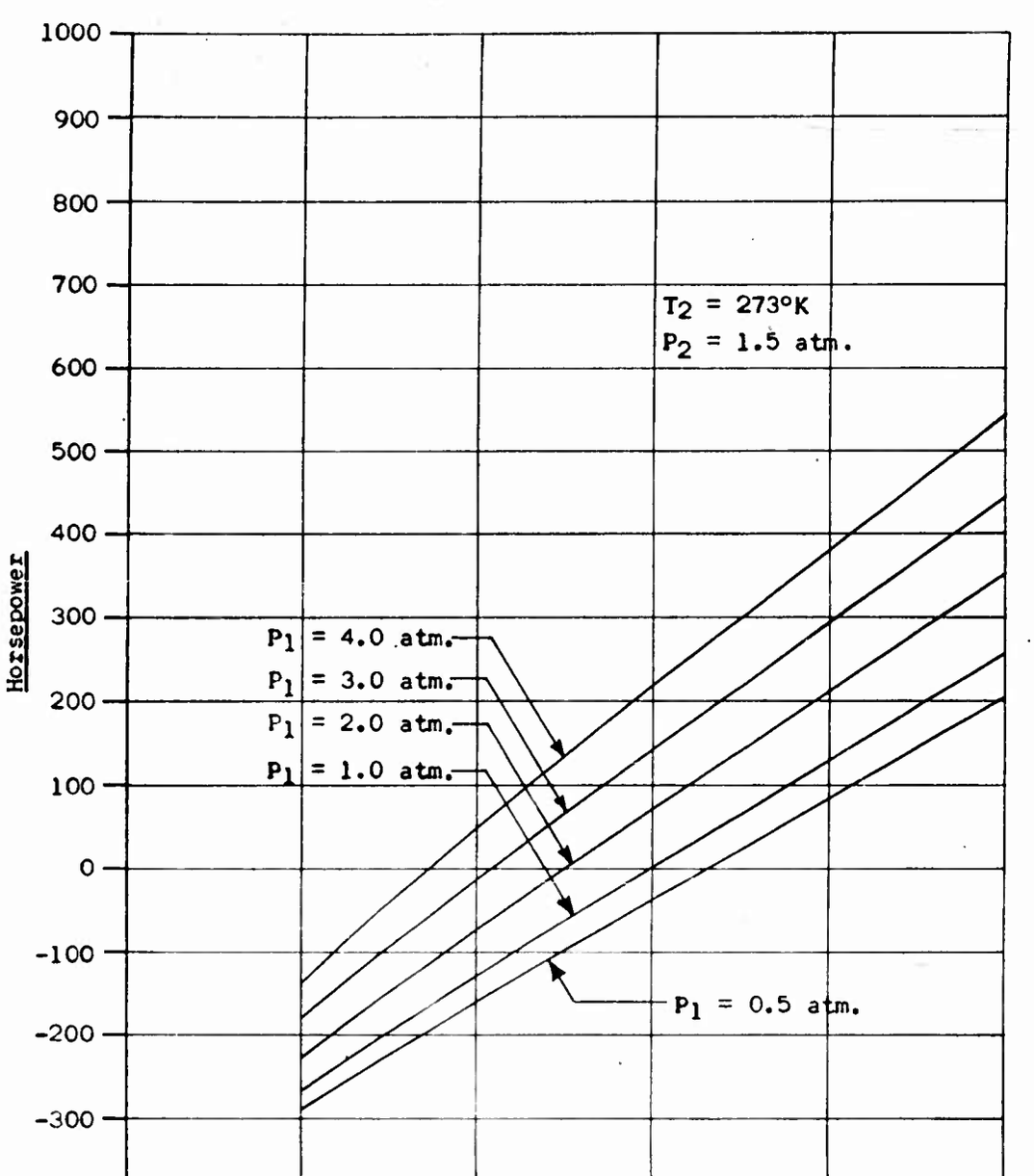

Figure 36. Horsepower as a Function of Effusion-Chamber Temperature for P_2 = 1.5 Atm., T_2 = 273°K.

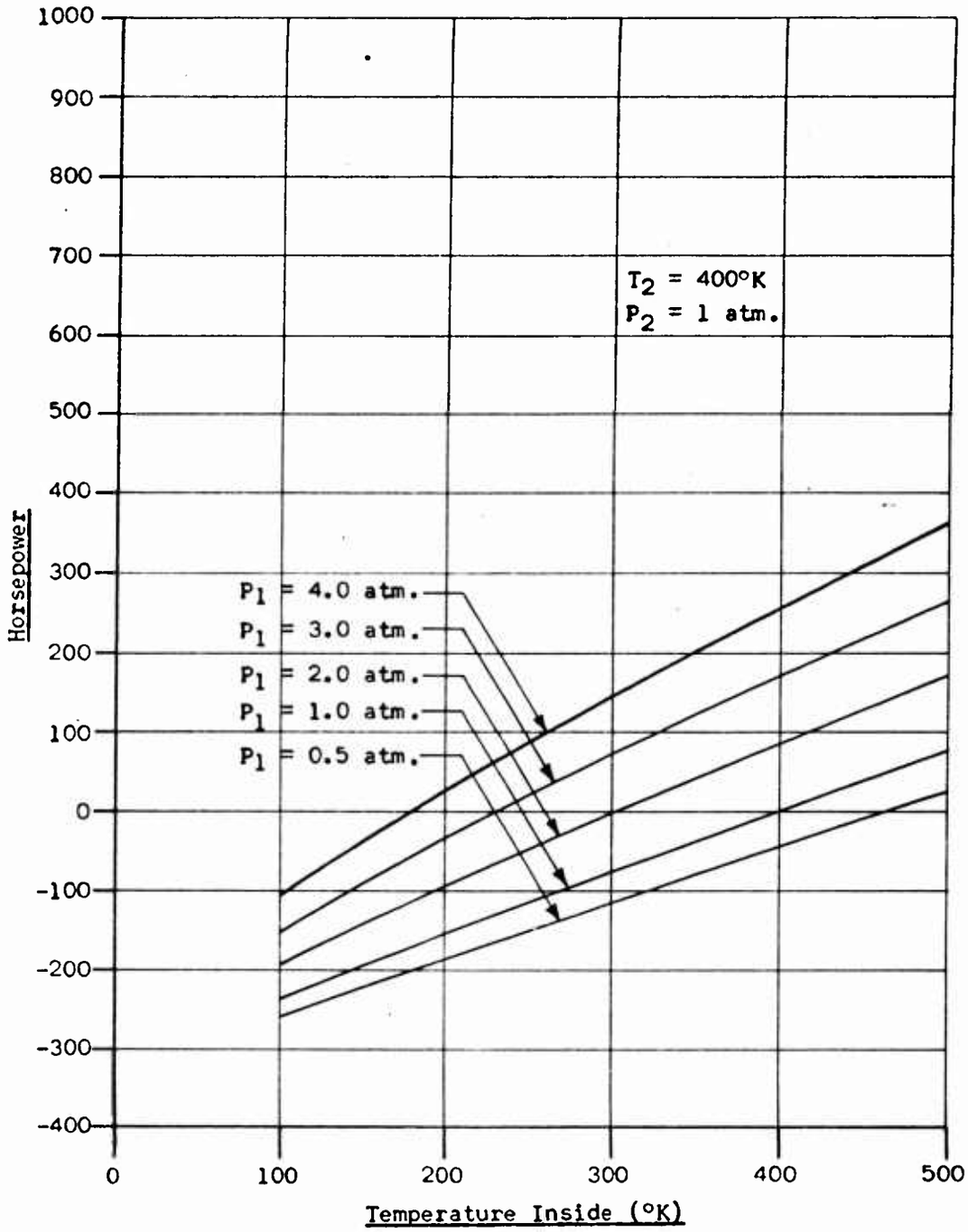

Figure 38. Horsepower as a Function of Effusion-Chamber Temperature for P_2 = 1 Atm., T_2 = 400°K.

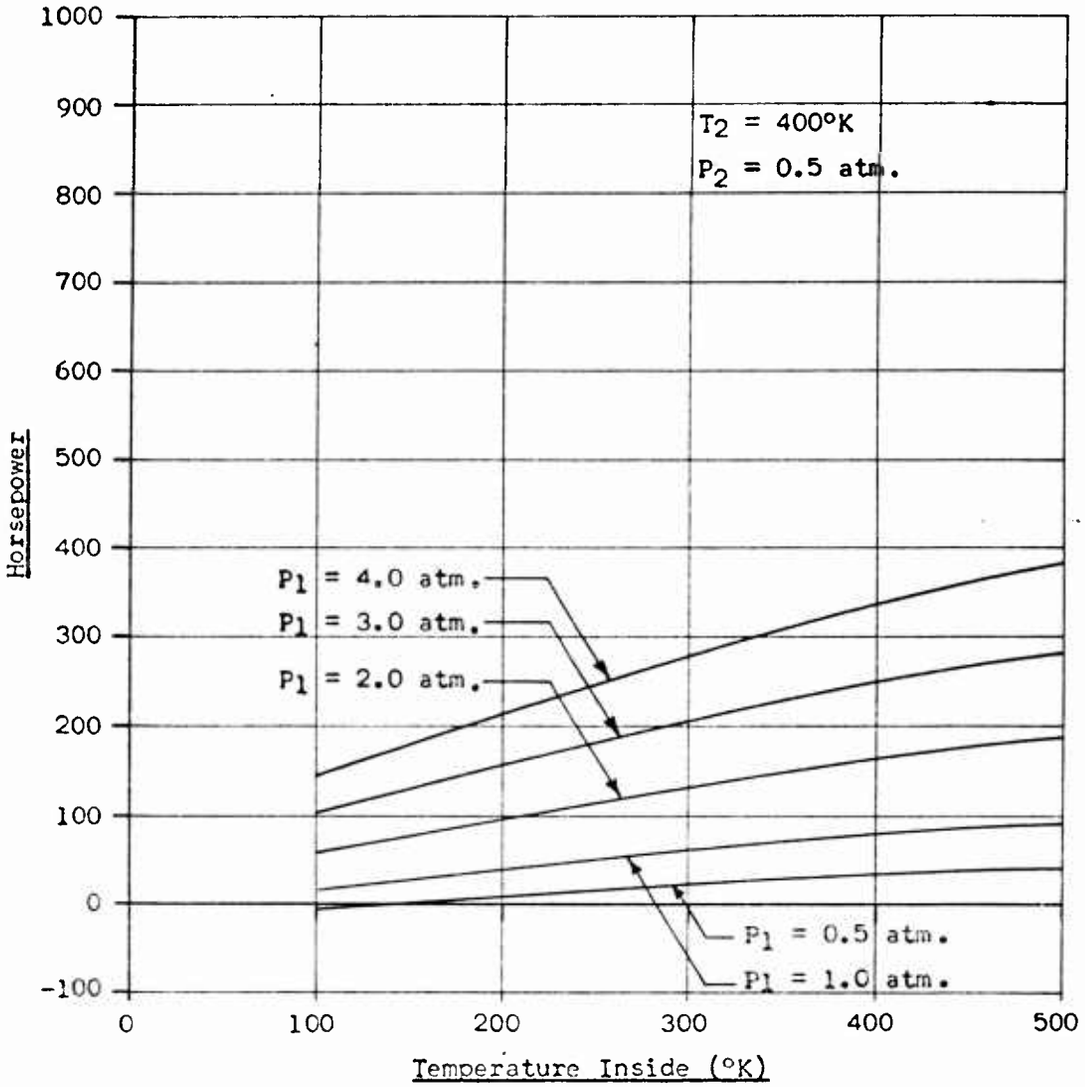

Figure 39. Horsepower as a Function of Effusion-Chamber Temperature for P_2 = 0.5 Atm., T_2 = 400°K.

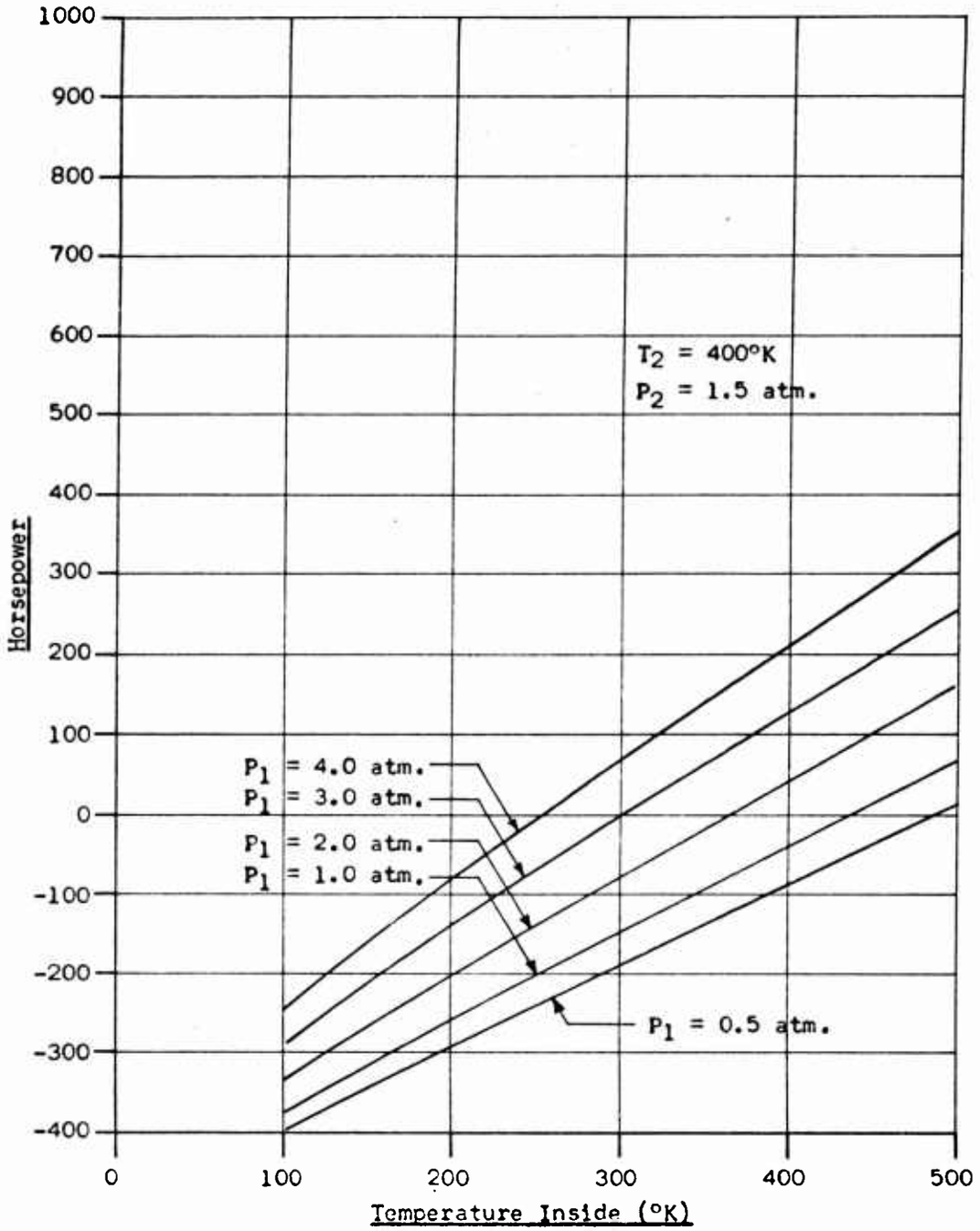

Figure 40. Horsepower as a Function of Effusion-Chamber Temperature for P_2 = 1.5 Atm., T_2 = 400°K.

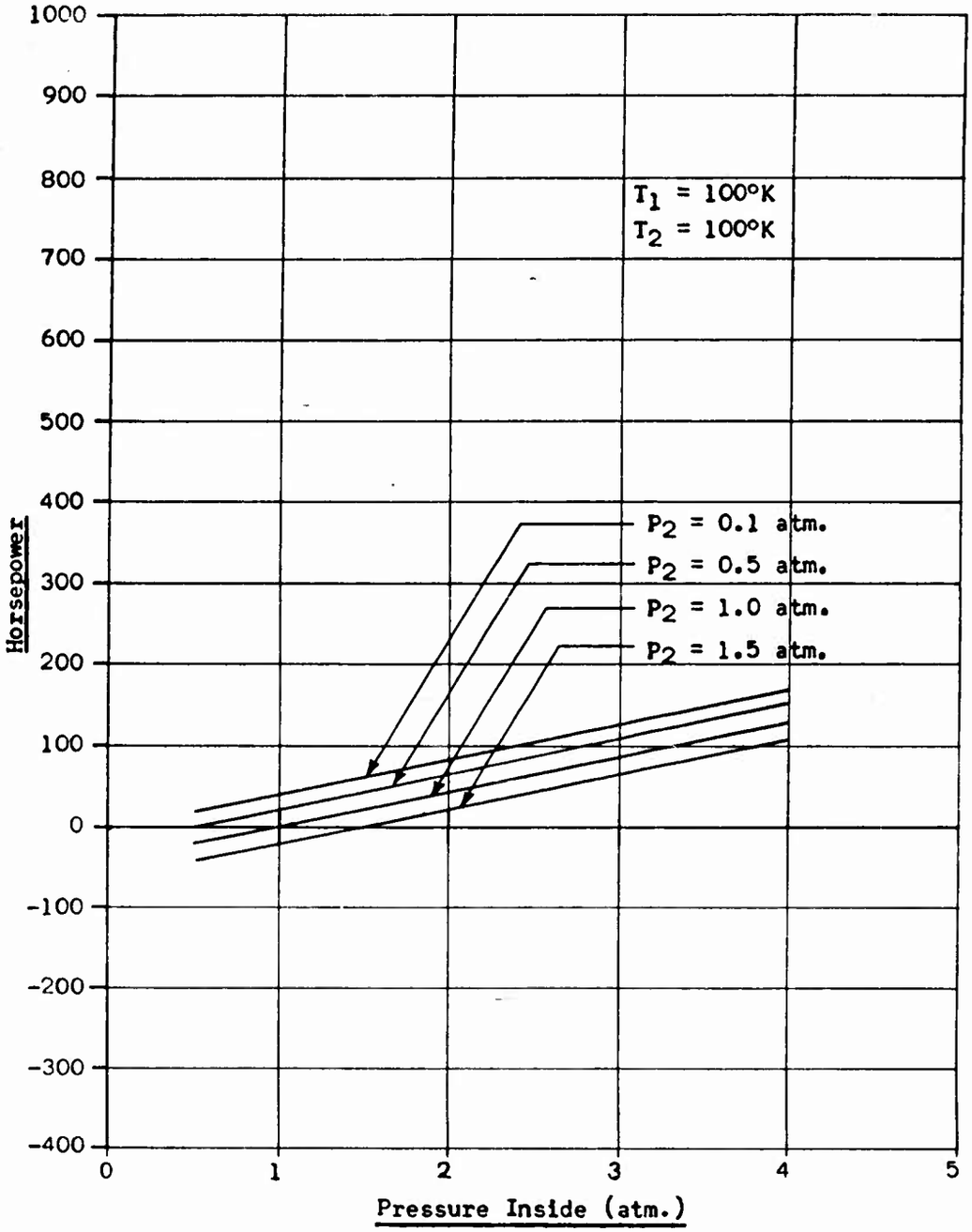

Figure 41. Horsepower as a Function of Effusion-Chamber Pressure for $T_1 = 100^{\circ}K$, $T_2 = 100^{\circ}K$.

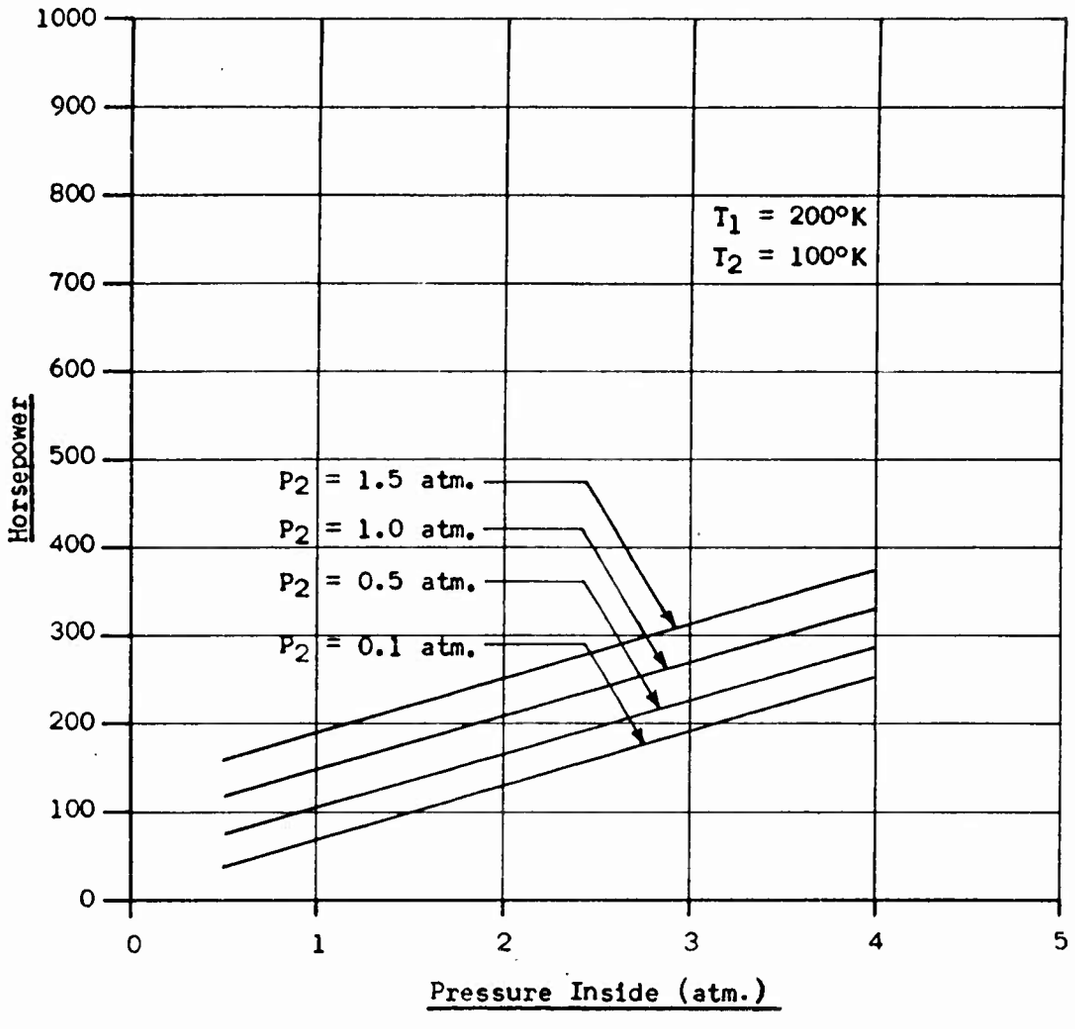

Figure 42. Horsepower as a Function of Effusion-Chamber Pressure for T_1 = 200°K & T_2 = 100°K.

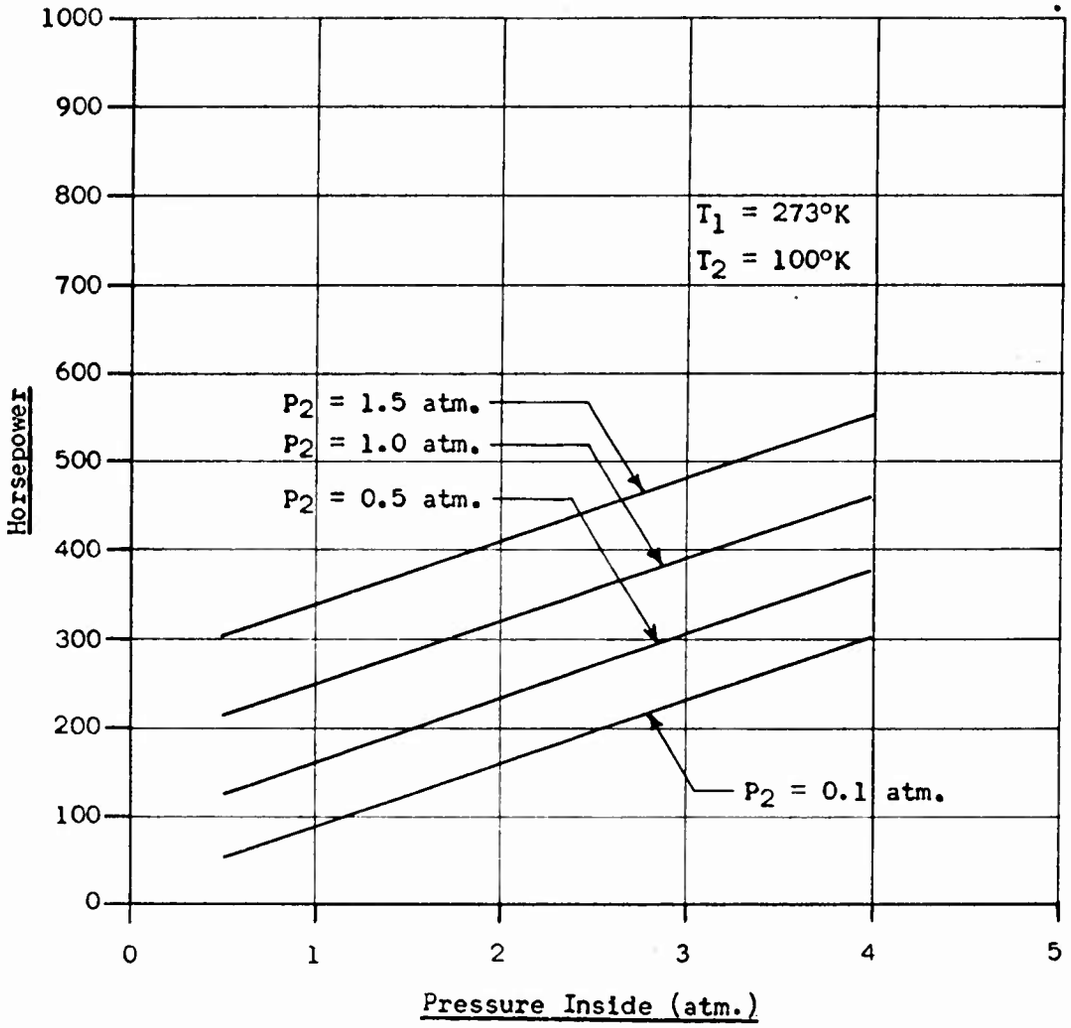

Figure 43. Horsepower as a Function of Effusion-Chamber Pressure for T_1 = 273°K & T_2 = 100°K.

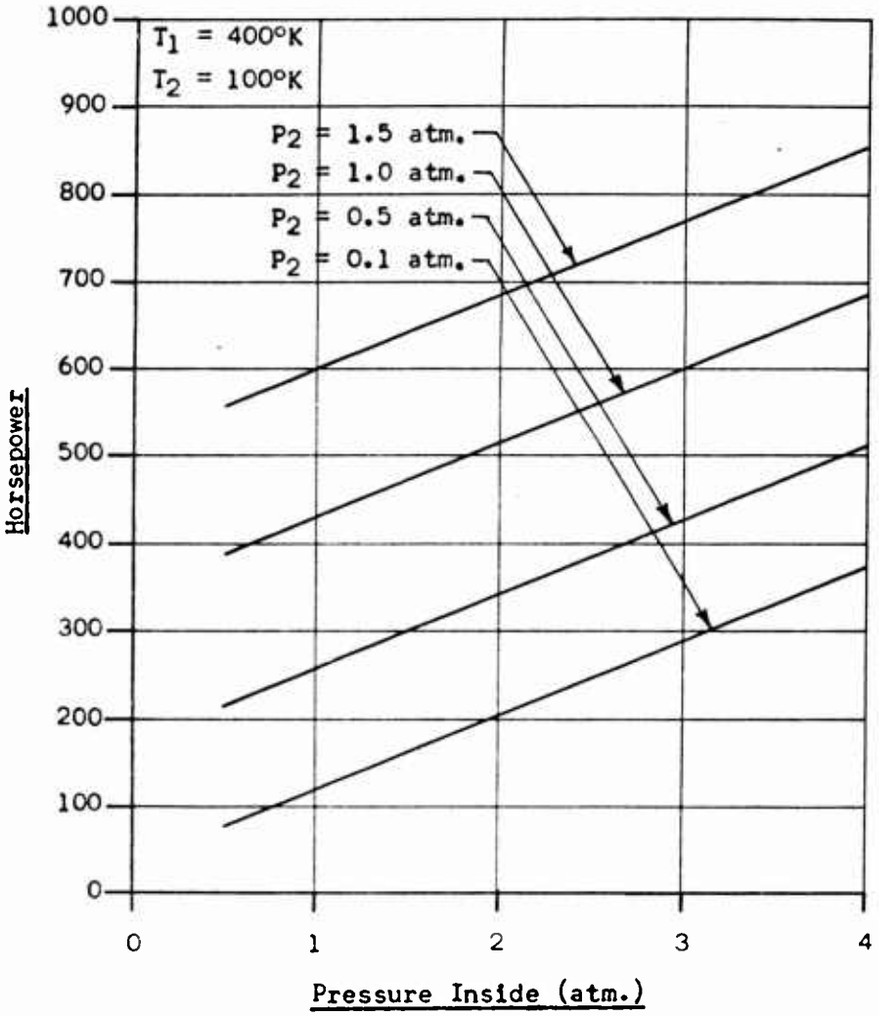

Figure 44. Horsepower as a Function of Effusion-Chamber Pressure for T_1 = 400°K & T_2 = 100°K.

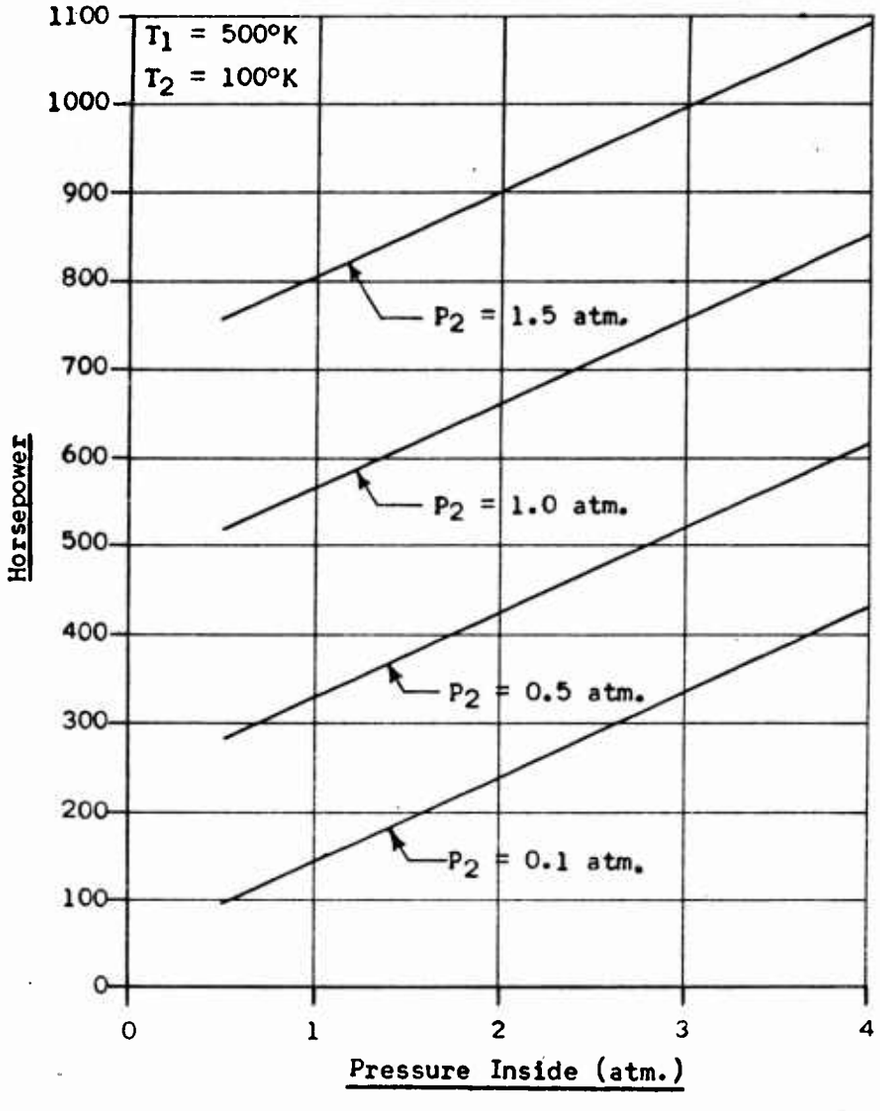

Figure 45. Horsepower as a Function of Effusion-Chamber Pressure for $T_1 = 500^{o}K$ & $T_2 = 100^{o}K$.

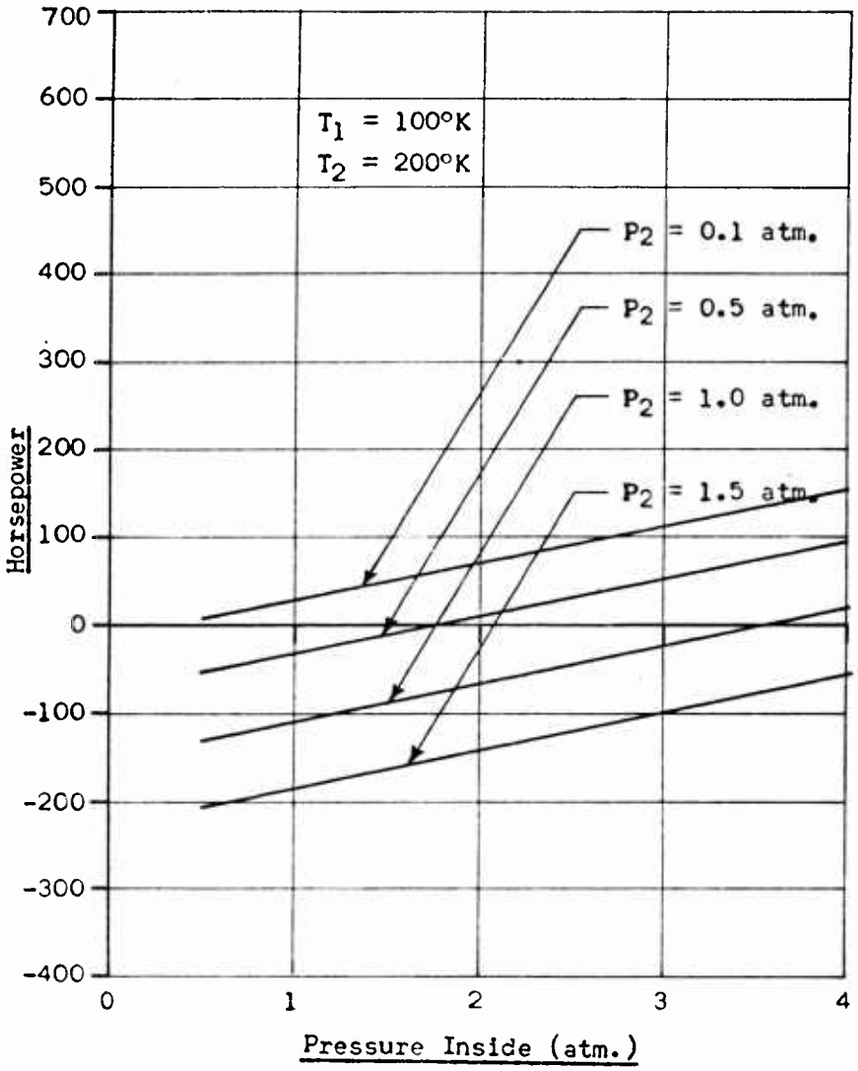

Figure 46. Horsepower as a Function of Effusion-Chamber Pressure for T_1 = 100°K & T_2 = 200°K.

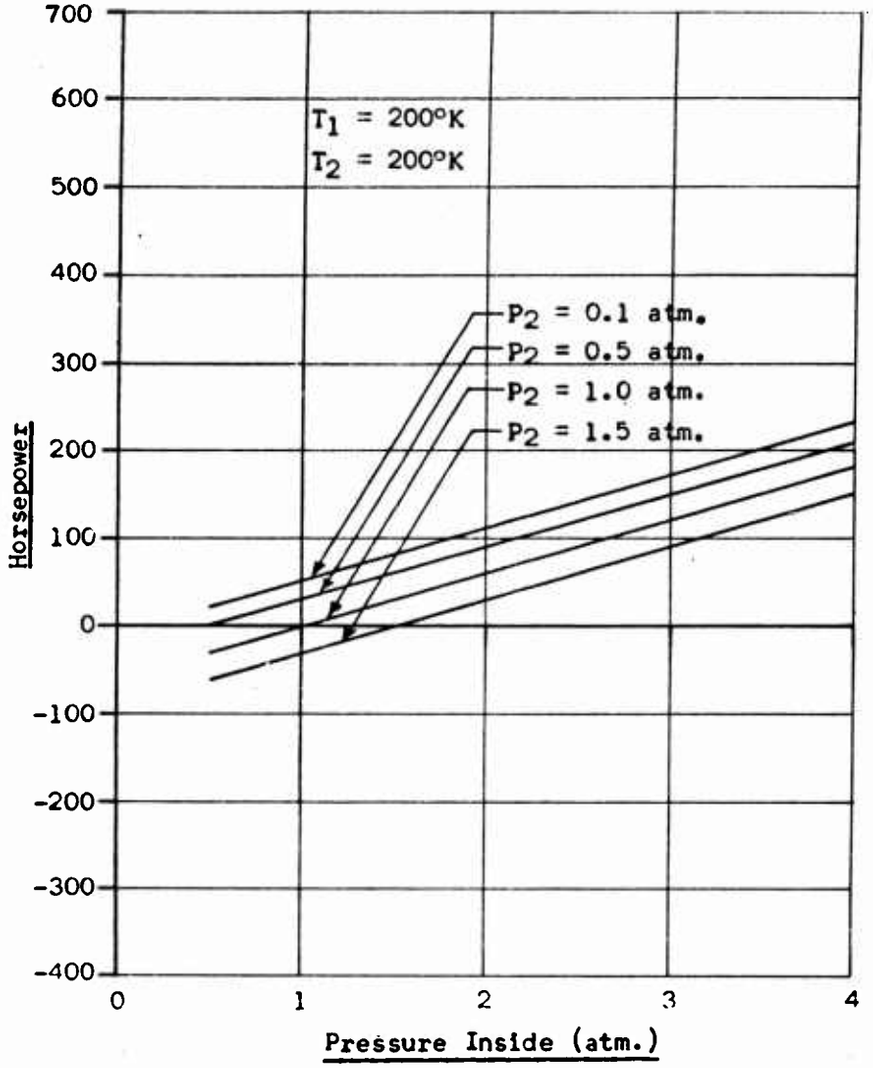

Figure 47. Horsepower as a Function of Effusion-Chamber Pressure for T_1 = 200°K & T_2 = 200°K.

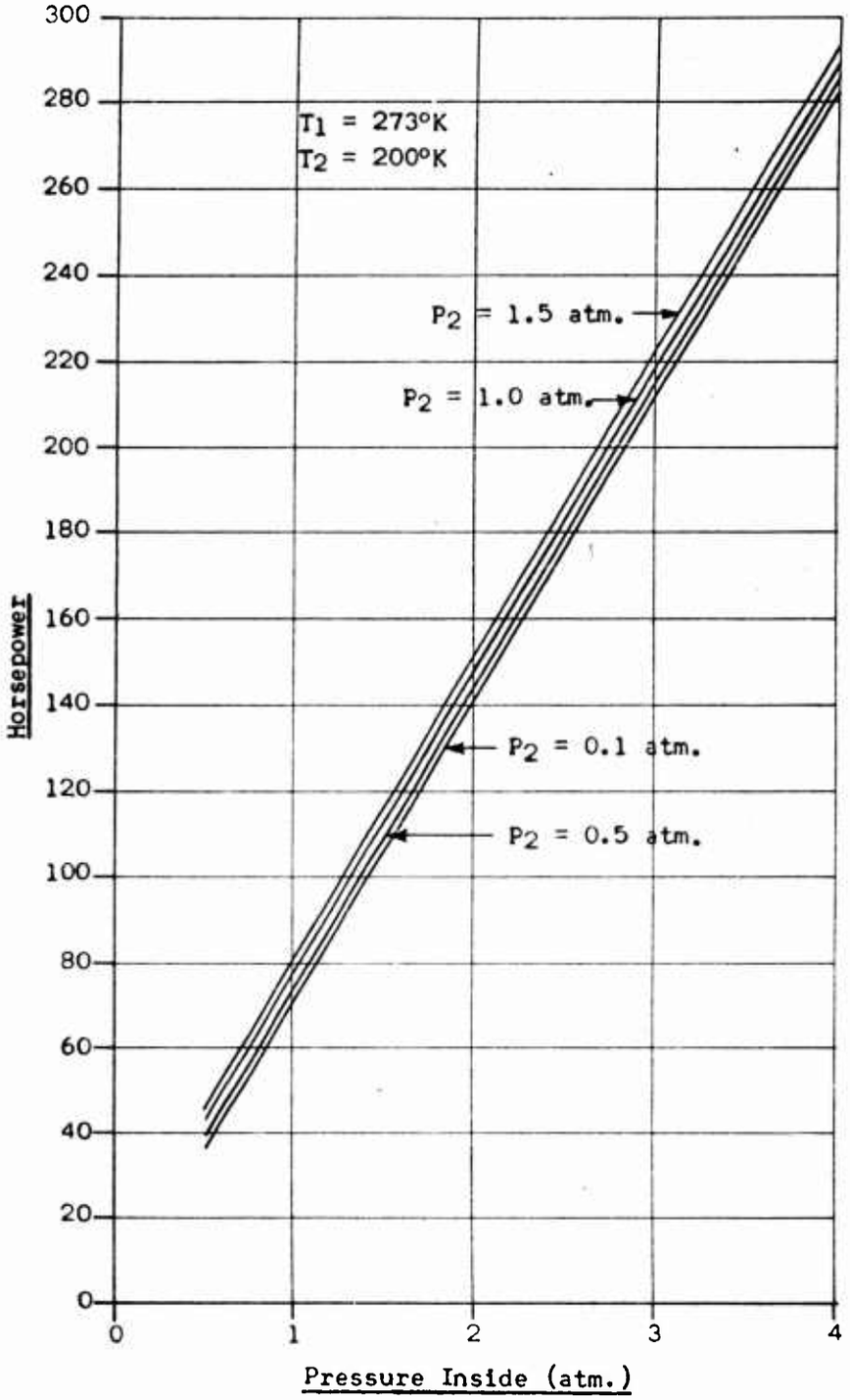

Figure 48. Horsepower as a Function of Effusion-Chamber Pressure for T_1 = 273°K & T_2 = 200°K.

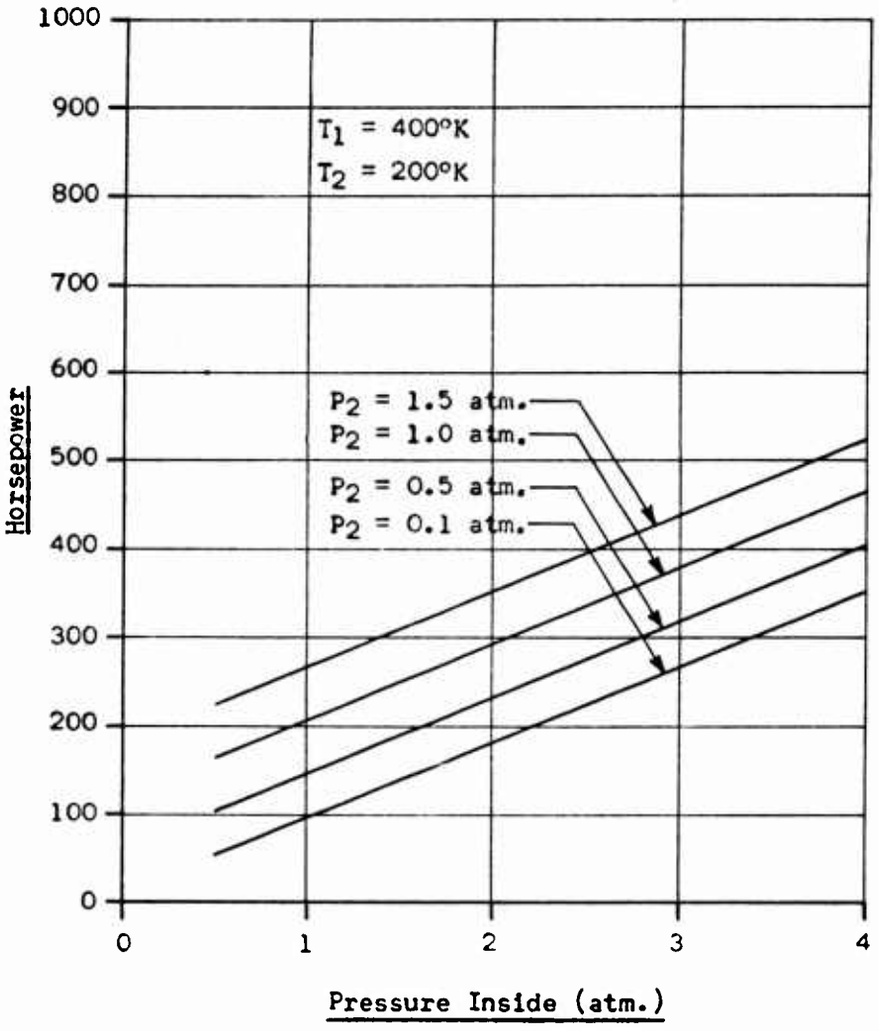

Figure 49. Horsepower as a Function of Effusion-Chamber Pressure for T_1 = 400°K & T_2 = 200°K.

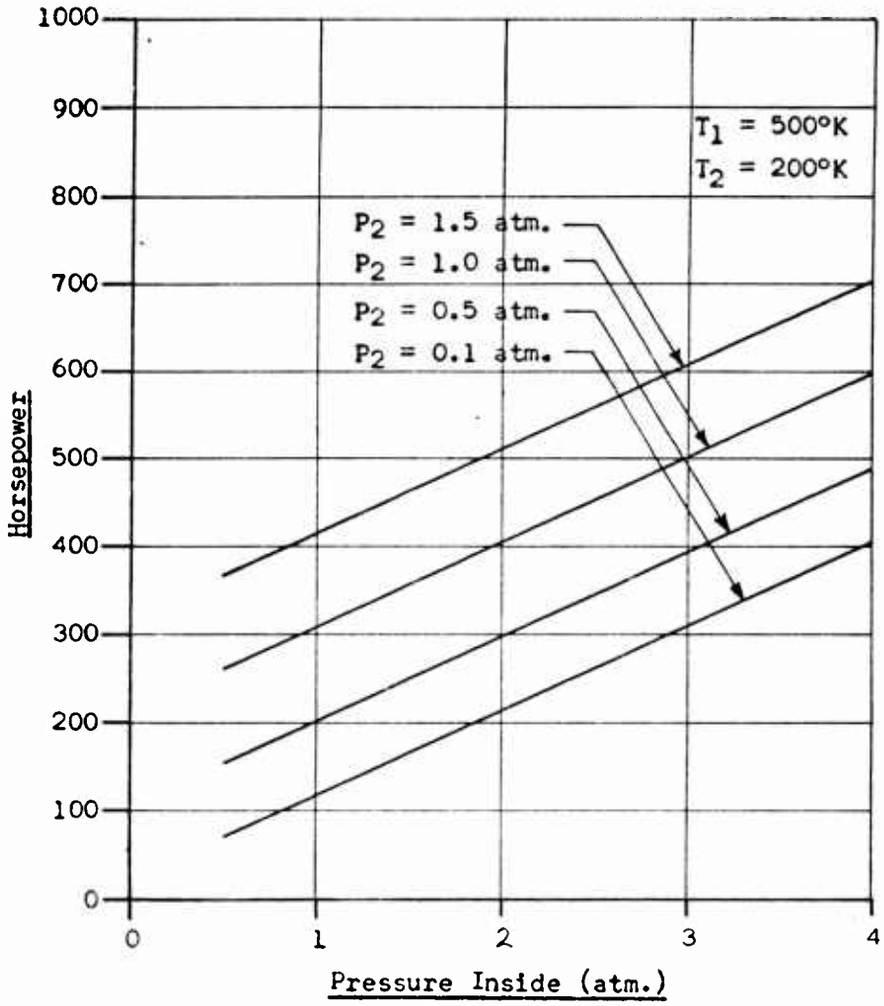

Figure 50. Horsepower as a Function of Effusion-Chamber Pressure for $T_1 = 500^{\circ}K$ & $T_2 = 200^{\circ}K$.

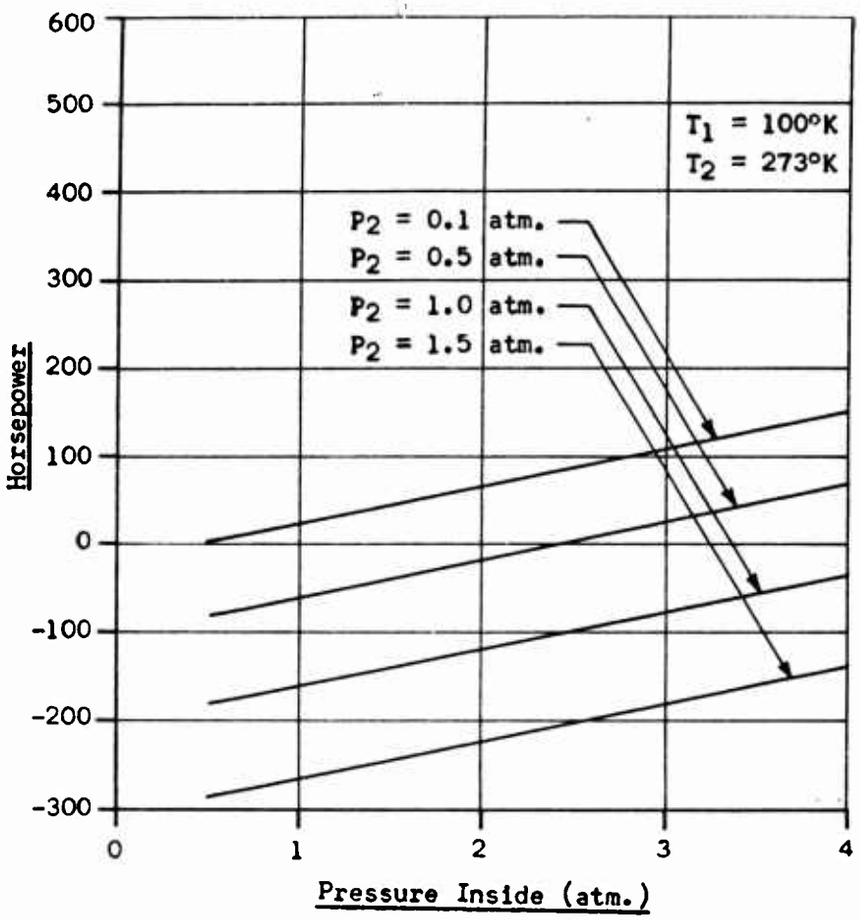

Figure 51. Horsepower as a Function of Effusion-Chamber Pressure for T_1 = 100°K & T_2 = 273°K.

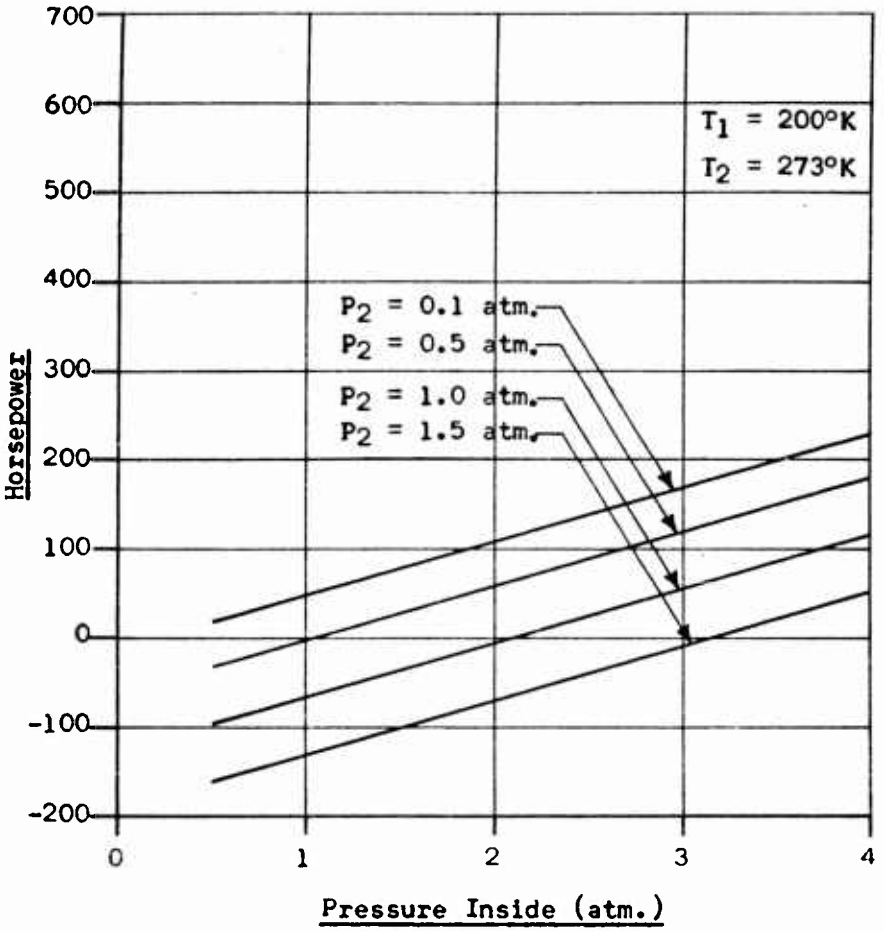

Figure 52. Horsepower as a Function of Effusion-Chamber Pressure for T_1 = 200°K & T_2 = 273°K.

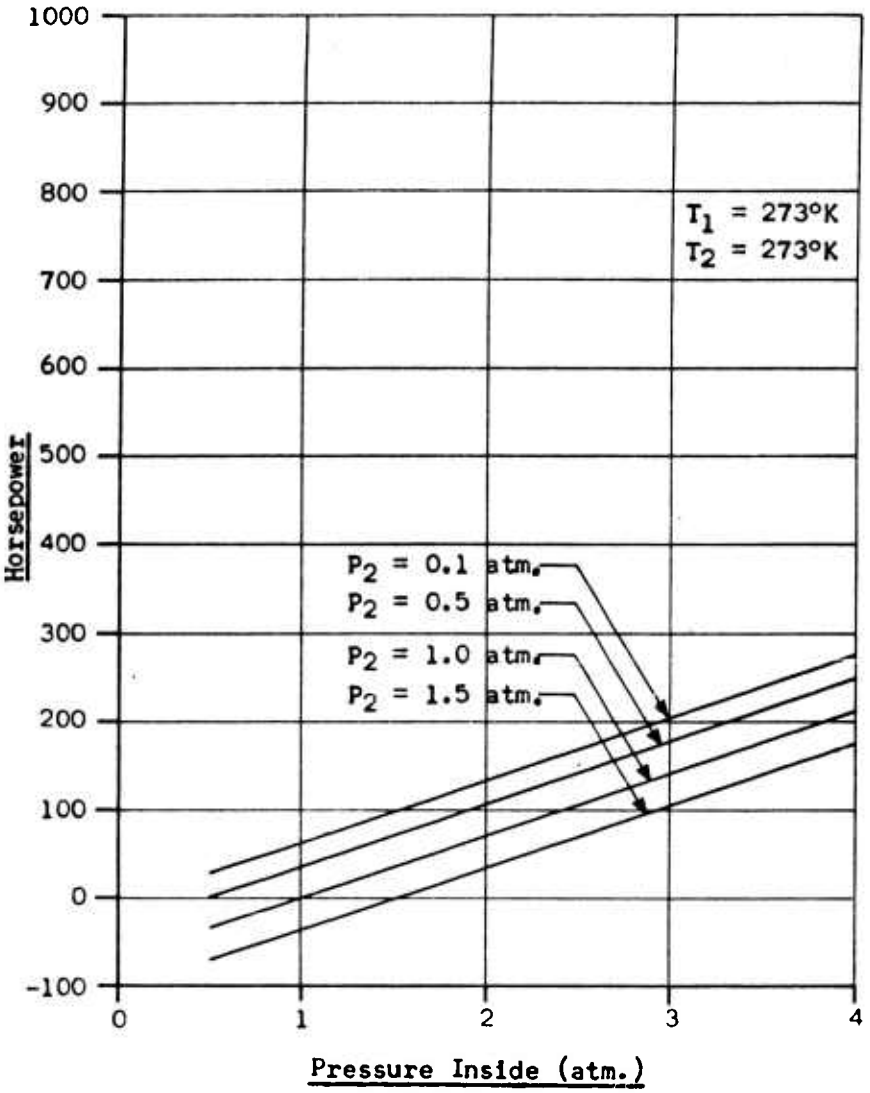

Figure 53. Horsepower as a Function of Effusion-Chamber Pressure for T_1 = 273°K & T_2 = 273°K.

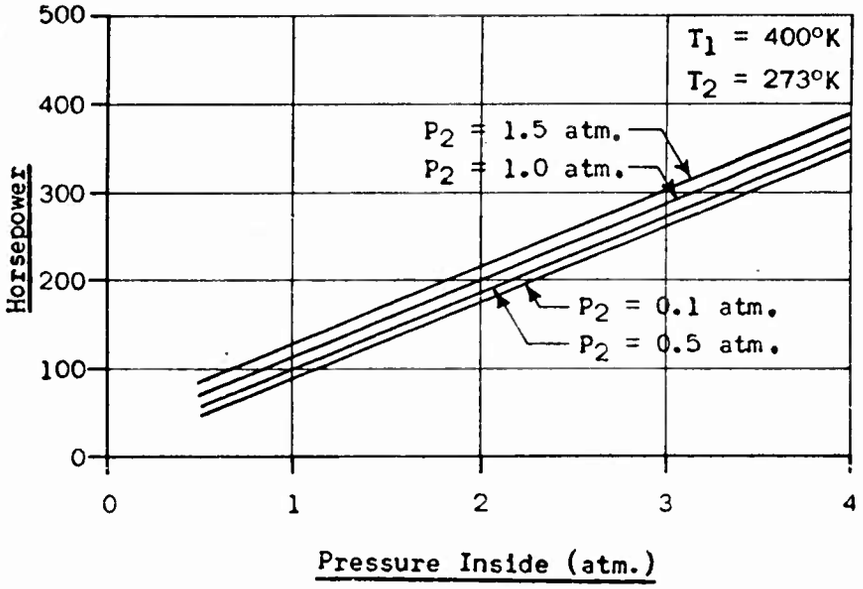

Figure 54. Horsepower as a Function of Effusion-Chamber Pressure for T_1 = 400°K & T_2 = 273°K.

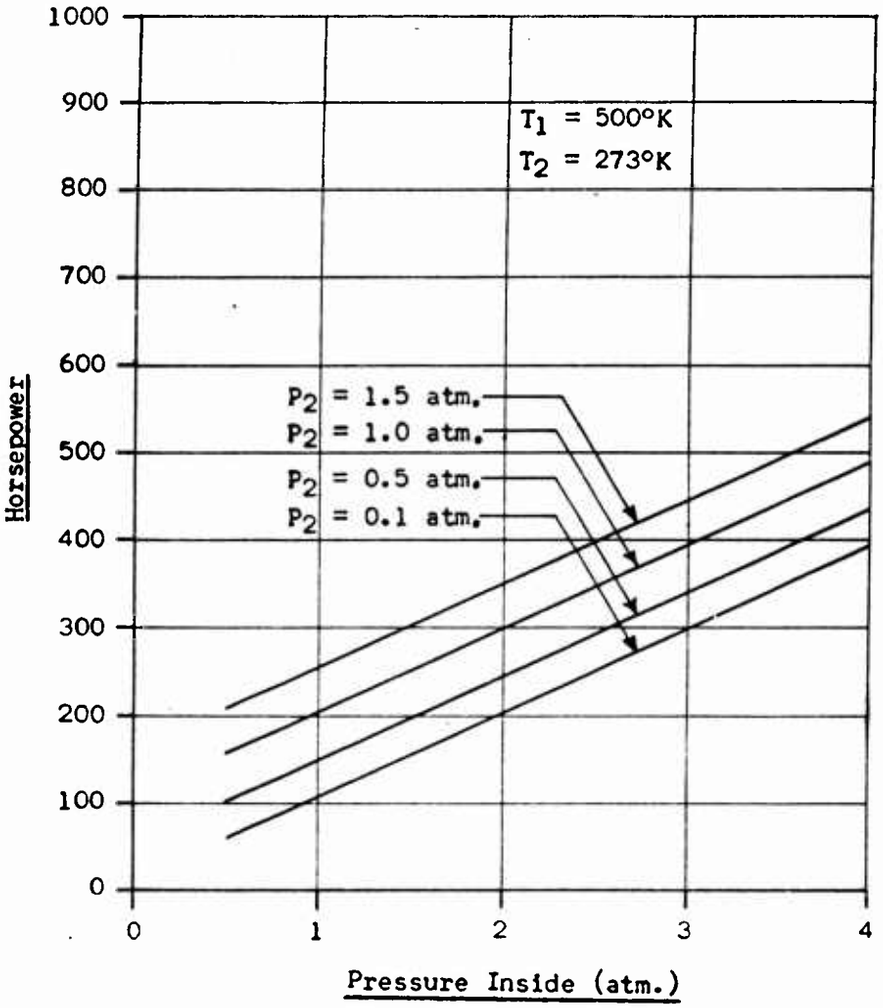

Figure 55. Horsepower as a Function of Effusion-Chamber Pressure for T_1 = 500°K & T_2 = 273°K.

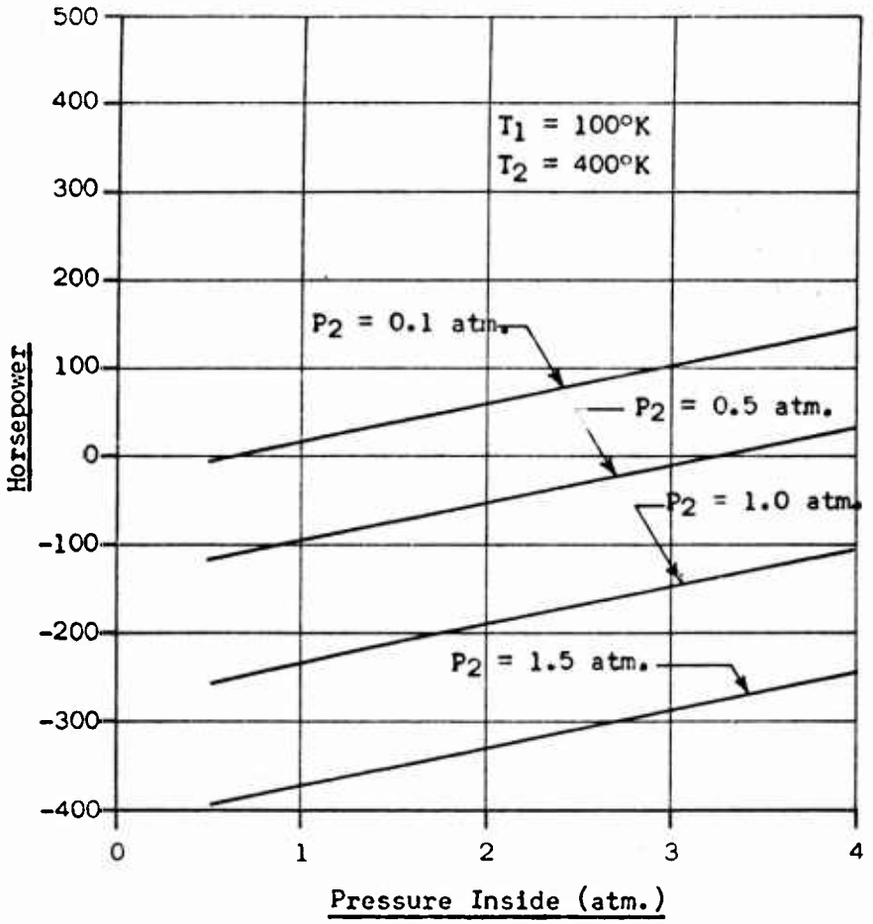

Figure 56. Horsepower as a Function of Effusion-Chamber Pressure for T_1 = 100°K & T_2 = 400°K.

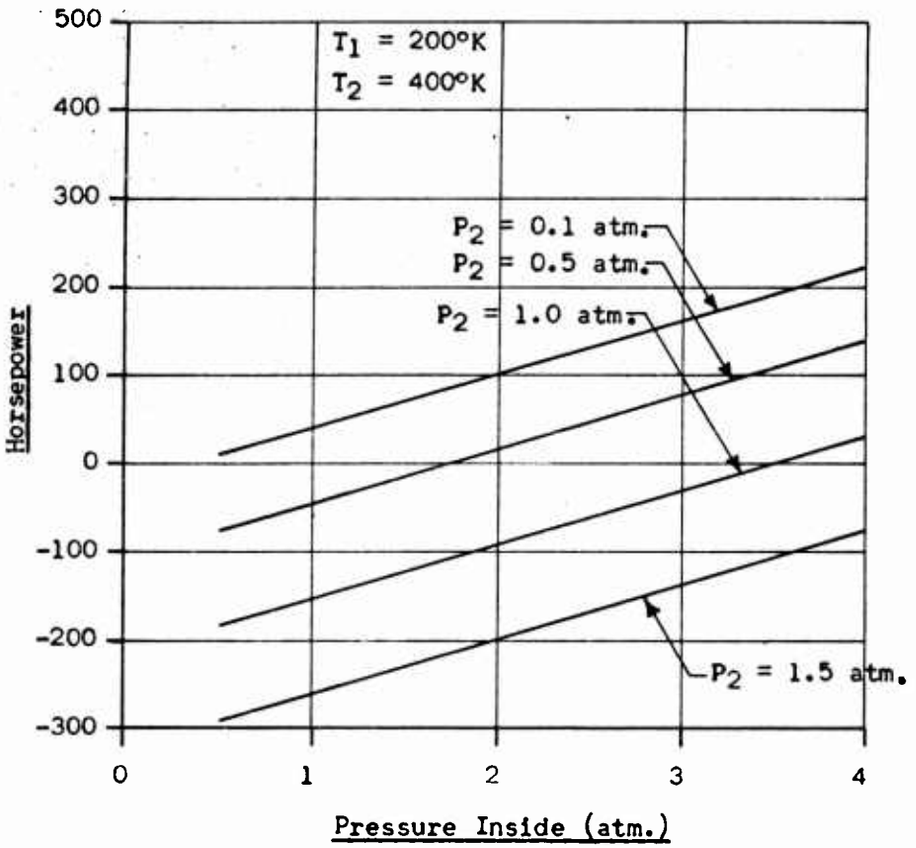

Figure 57. Horsepower as a Function of Effusion-Chamber Pressure for $T_1 = 200^{\circ}K$ & $T_2 = 400^{\circ}K$.

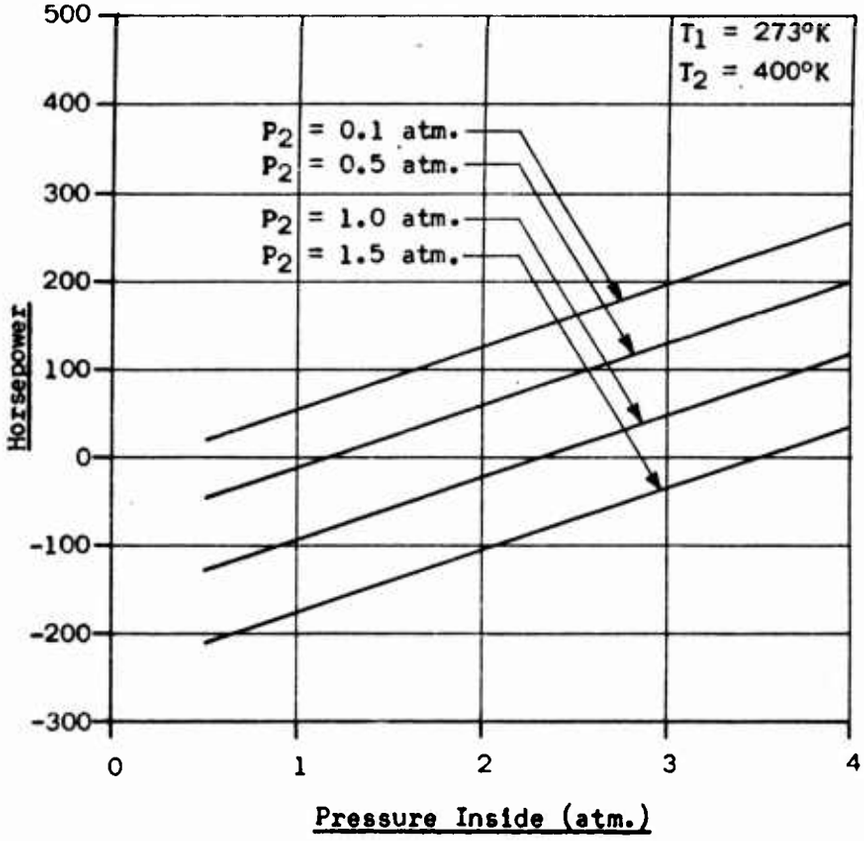

Figure 58. Horsepower as a Function of Effusion-Chamber Pressure for $T_1 = 273^{\circ}K$ & $T_2 = 400^{\circ}K$.

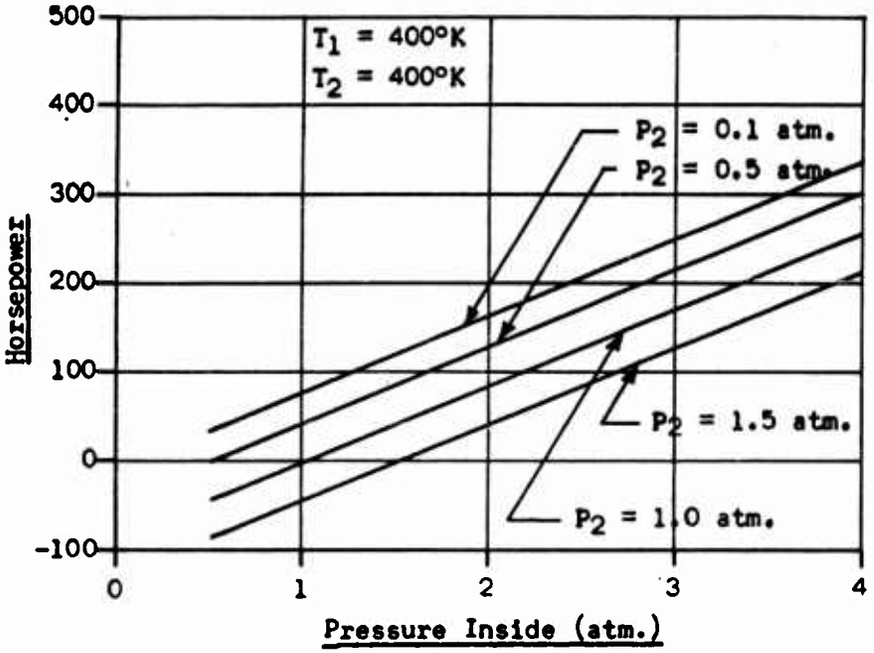

Figure 59. Horsepower as a Function of Effusion-Chamber Pressure for T_1 = 400°K & T_2 = 400°K.

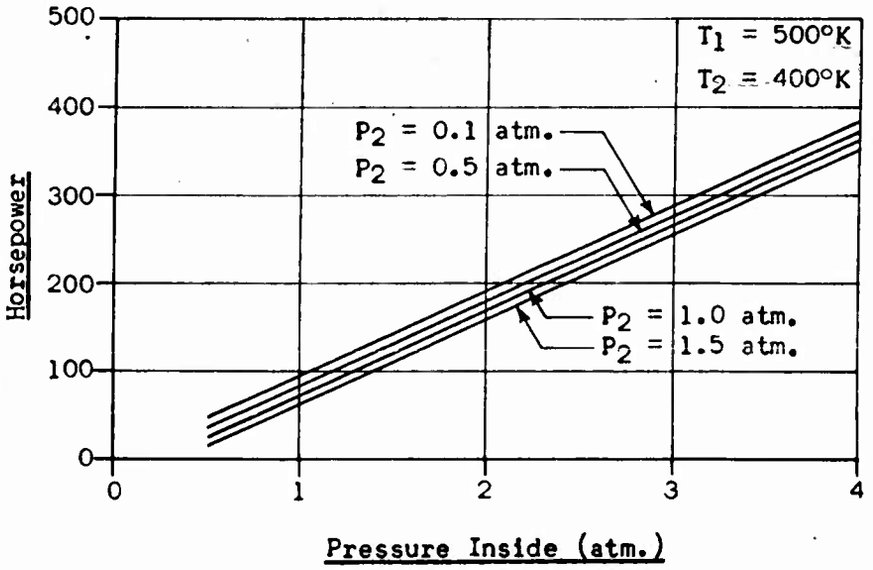

Figure 60. Horsepower as a Function of Effusion-Chamber Pressure for $T_1 = 500^{\circ}K$ & $T_2 = 400^{\circ}K$.

APPENDIX IV, VISCOSITY OF AIR AS A FUNCTION OF TEMPERATURE

The graphs contained in this appendix were plotted from data appearing in the 1960-1961 edition of Handbook of Chemistry and Physics. This information was used in the calculations appearing in Appendix V of this report.

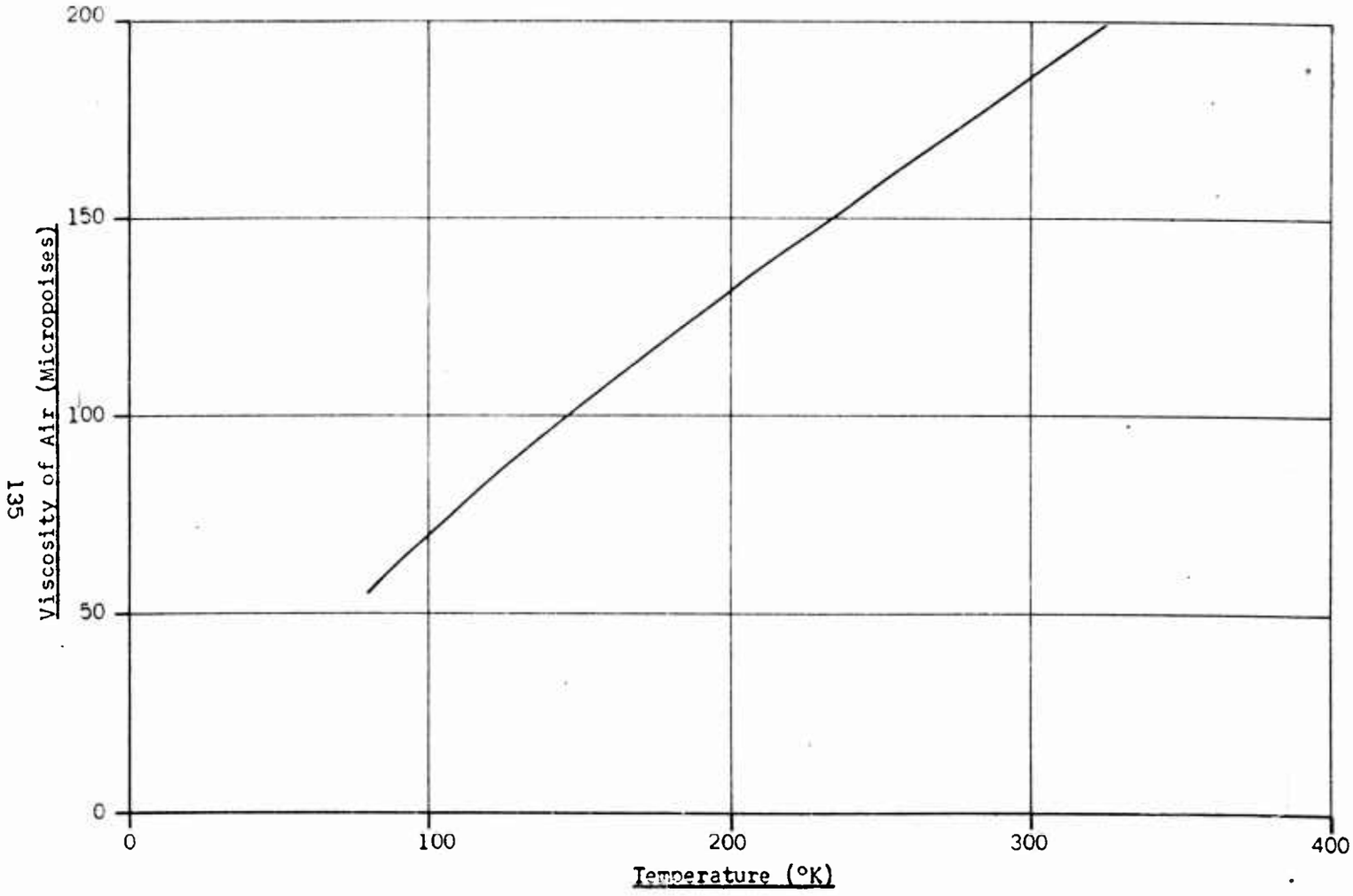

Figure 61. Viscosity of Air from 0°K to 400°K.

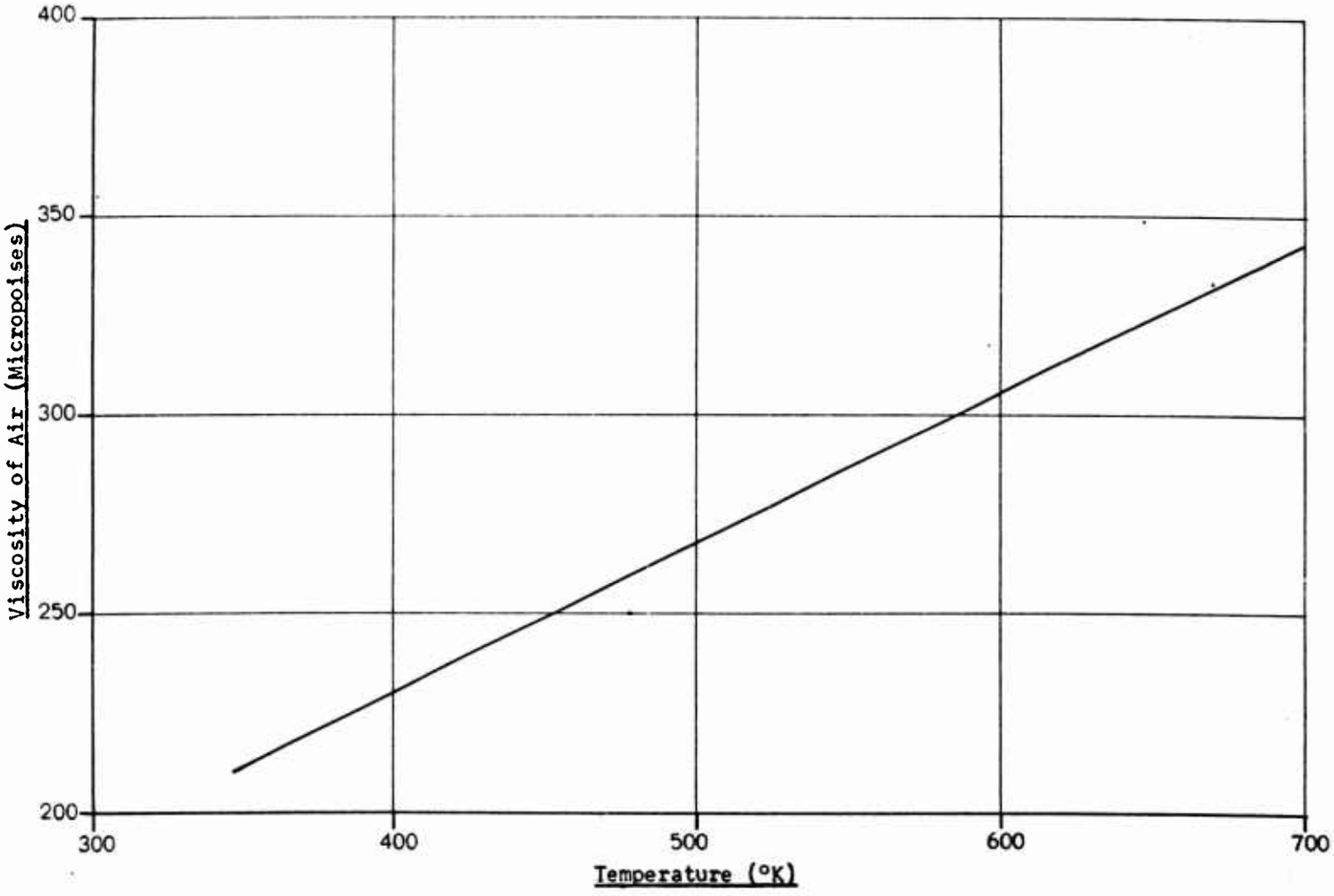

Figure 62. Viscosity of Air from 400°K to 700°K.

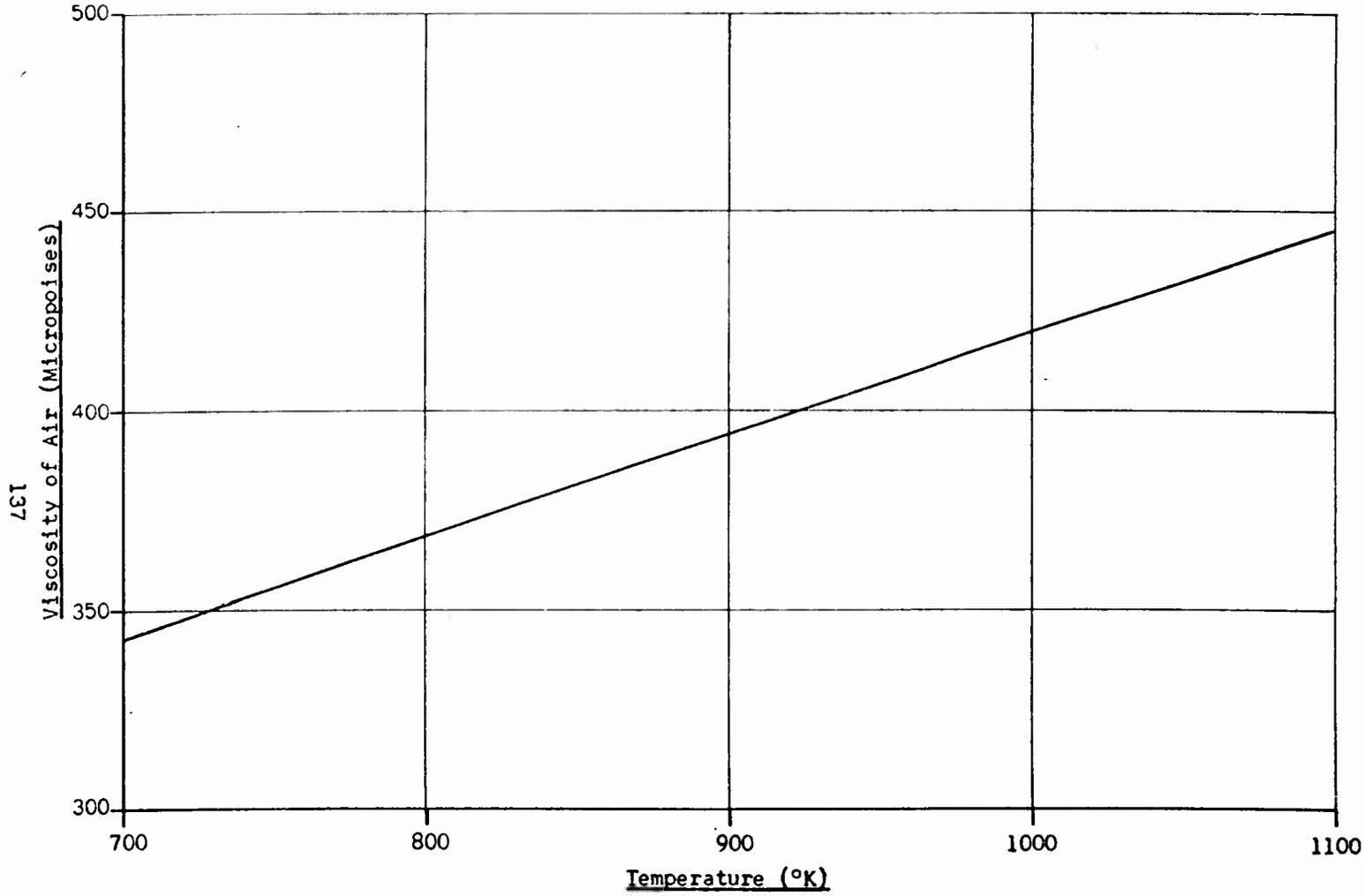

Figure 63. Viscosity of Air from 700° to 1100°K.

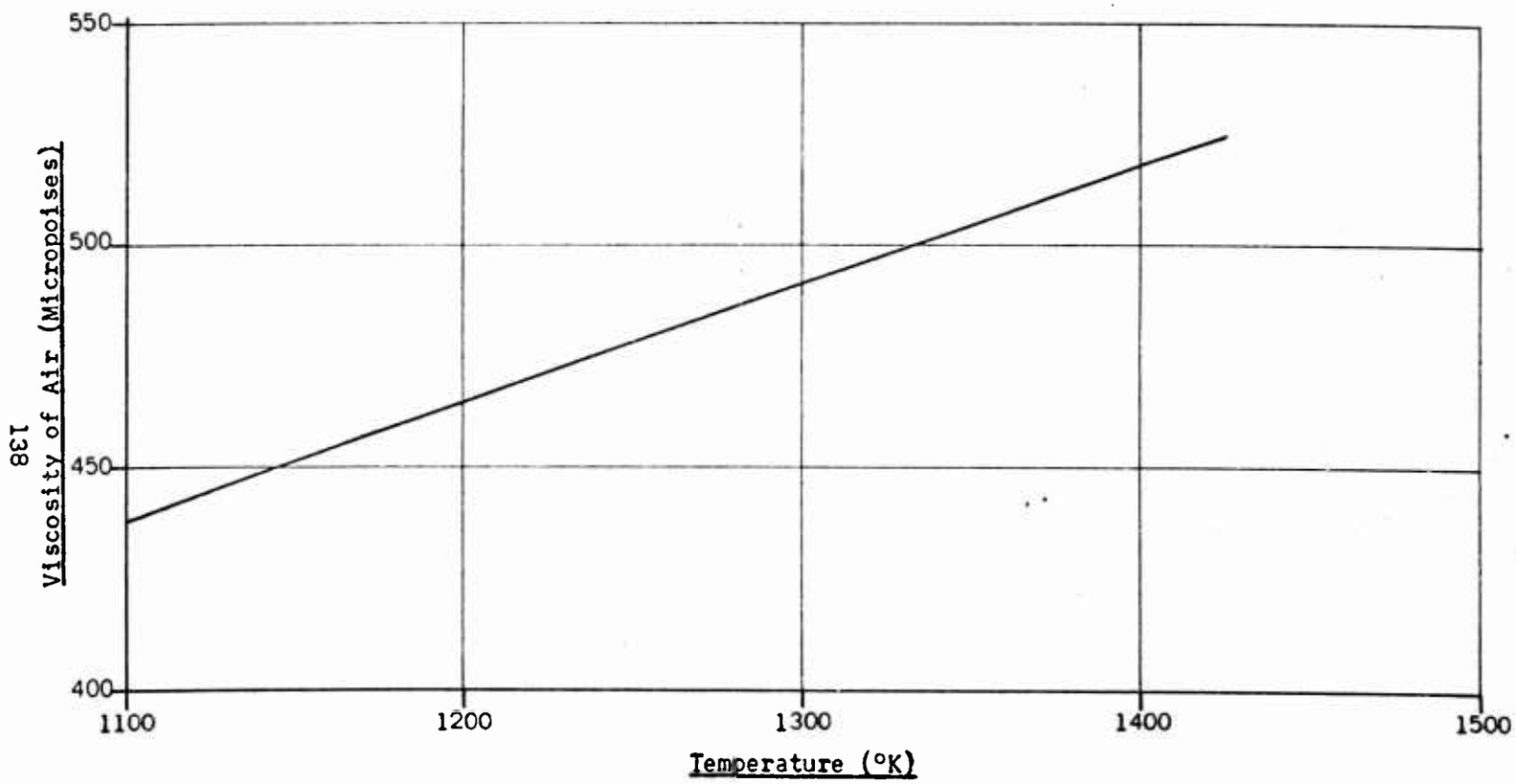

Figure 64. Viscosity of Air from 1100°K to 1425°K.

APPENDIX V, CALCULATION OF THE PRESSURE (P_o) AT THE EXTERNAL EFFUSION SURFACE

This appendix contains calculations of P_o based upon the Tube Model discussed in the theoretical section of the text. The modified form of the equation is given and the values of P_o are tabulated. The range of the calculations is indicated.

FINAL FORM OF TUBE MODEL EQUATION USED TO CALCULATE P_o

$$\frac{a^2 \bar{P} \triangle P}{8 \; k \; T \eta \; L} = \frac{1}{4} \; n_1 \bar{v}_1 \; A' - \frac{1}{4} \; n_o \; \bar{v}_o \; A' \qquad (57)$$

$$\bar{P} \triangle P = \left[\frac{8 \; k \; L \; T \eta}{a^2}\right]^{\frac{1}{4}} A' \left[n_1 \bar{v}_1 - n_o \; \bar{v}_o\right] \qquad (58)$$

$$P_o^2 - P_2^2 = 0.4 \left[\frac{k}{a^2}\right] \left[2\left(\frac{2k}{\pi m}\right)^{\frac{1}{2}}\right] \left[\frac{n_{STP} \; T_{STP}}{P_{STP}}\right] \left[L \; T \eta\right] \left[\frac{P_1}{T_1^{\frac{1}{2}}} - \frac{P_o}{T_o^{\frac{1}{2}}}\right] \qquad (59)$$

$$P_o^2 + 0.4 \left[\frac{k}{a^2}\right] \left[2 \left(\frac{2 \; k}{\pi m}\right)^{\frac{1}{2}}\right] \left[\frac{n_{STP} \; T_{STP}}{P_{STP}}\right] \left[\frac{L \; T \; \eta}{T_o^{\frac{1}{2}}}\right] P_o -$$

$$\left[0.4 \left[\frac{k}{a^2}\right] \left[2 \left(\frac{2k}{\pi m}\right)^{\frac{1}{2}}\right] \left[\frac{n_{STP} \; T_{STP}}{P_{STP}}\right] \left[L \; T \eta\right] \left[\frac{P_1}{T_1^{\frac{1}{2}}}\right] - P_2^2\right] = 0 \qquad (60)$$

The equation above was used to calculate P_o. The calculations were made with the aid of the IBM 650 Computer.

RANGE OF VARIABLES USED IN CALCULATION OF P_o

L (Cm.) = 50, 100

P_1 (Atm.) = 0.0001, 0.001, 0.1, 2.0, 4.0

P_2 (Atm.) = 0.000001, 0.00001, 0.0001, 0.001, 0.01, 1.0

T_1 (^oK) = 100, 273, 600

T_2 (^oK) = 100, 273, 300

TABLE 46

CALCULATIONS OF PRESSURE (P_o) AT THE EXTERNAL EFFUSION SURFACE

P_1 (dynes/cm^2)	T_1 (^oK)	P_2 (dynes/cm^2)	P_o (dynes/cm^2)
2.0264×10^6	100.0	1.0132×10^3	1.1540950×10^3
2.0264×10^6	100.0	1.0132×10^5	1.0132144×10^5
2.0264×10^6	100.0	1.0132×10^6	1.0132001×10^6
4.0528×10^6	100.0	1.0132×10^3	1.2796241×10^3
4.0528×10^6	100.0	1.0132×10^5	1.0132295×10^5
4.0528×10^6	100.0	1.0132×10^6	1.0132003×10^6
2.0264×10^6	273.0	1.0132×10^3	1.1006052×10^3
2.0264×10^6	273.0	1.0132×10^5	1.0132084×10^5
2.0264×10^6	273.0	1.0132×10^6	1.0132001×10^6
4.0528×10^6	273.0	1.0132×10^3	1.1816216×10^3
4.0528×10^6	273.0	1.0132×10^5	1.0132176×10^5
4.0528×10^6	273.0	1.0132×10^6	1.0132002×10^6
2.0264×10^6	600.0	1.0132×10^3	1.0729187×10^3
2.0264×10^6	600.0	1.0132×10^5	1.0132055×10^5
2.0264×10^6	600.0	1.0132×10^6	1.0132000×10^6
4.0528×10^6	600.0	1.0132×10^3	1.1295462×10^3
4.0528×10^6	600.0	1.0132×10^5	1.0132116×10^5
4.0528×10^6	600.0	1.0132×10^6	1.0132001×10^6
1.0132×10^5	100.0	1.0132×10^3	1.0206419×10^3
1.0132×10^5	100.0	1.0132×10^4	1.0132685×10^4

P_1 (dynes/cm^2)	T_1 (^oK)	P_2 (dynes/cm^2)	P_o (dynes/cm^2)
1.0132×10^5	273.0	1.0132×10^3	1.0176835×10^3
1.0132×10^5	273.0	1.0132×10^4	1.0132388×10^4
1.0132×10^5	600.0	1.0132×10^3	1.0162041×10^3
1.0132×10^5	600.0	1.0132×10^4	1.0132239×10^4
1.0132×10^3	100.0	1.0132×10^1	1.5913113×10^1
1.0132×10^3	100.0	1.0132×10^2	1.0200227×10^2
1.0132×10^3	273.0	1.0132×10^1	1.3899600×10^1
1.0132×10^3	273.0	1.0132×10^2	1.0170644×10^2
1.0132×10^3	600.0	1.0132×10^1	1.2777434×10^1
1.0132×10^3	600.0	1.0132×10^2	1.0155850×10^2
1.0132×10^2	100.0	1.0132×10^0	3.9694134×10^0
1.0132×10^2	100.0	1.0132×10^1	1.0791117×10^1
1.0132×10^2	273.0	1.0132×10^0	3.1369221×10^0
1.0132×10^2	273.0	1.0132×10^1	1.0509823×10^1
1.0132×10^2	600.0	1.0132×10^0	2.6270520×10^0
1.0132×10^2	600.0	1.0132×10^1	1.0366631×10^1

$T = 110^oK$

$T_o = 120^oK$

$\eta = 75 \times 10^6$ Poises

$T_2 = 100^oK$

$L = 50$ cm

TABLE 47

CALCULATIONS OF PRESSURE (P_o) AT THE EXTERNAL EFFUSION SURFACE

P_1 (dynes/cm^2)	P_2 (dynes/cm^2)	P_o (dynes/cm^2)
2.0264×10^6	1.0132×10^3	1.6590643×10^3
2.0264×10^6	1.0132×10^5	1.0132826×10^5
2.0264×10^6	1.0132×10^6	1.0132006×10^6
4.0528×10^6	1.0132×10^3	2.1163730×10^3
4.0528×10^6	1.0132×10^5	1.0133678×10^5
4.0528×10^6	1.0132×10^6	1.0132015×10^6
1.0132×10^5	1.0132×10^3	1.0546891×10^3
1.0132×10^5	1.0132×10^4	1.0136002×10^4
1.0132×10^3	1.0132×10^1	3.0824471×10^1
1.0132×10^3	1.0132×10^2	1.0523714×10^2
1.0132×10^2	1.0132×10^0	9.0926320×10^0
1.0132×10^2	1.0132×10^1	1.3492139×10^1

$T = 273^\circ K$

$T_o = 273^\circ K$

$T_1 = 100^\circ K$

$\eta = 170.8 \times 10^{-6}$ Poises

$T_2 = 273^\circ K$

$L = 50$ cm

TABLE 48

CALCULATIONS OF PRESSURE (P_o) AT THE EXTERNAL EFFUSION SURFACE

P_1 (dynes/cm^2)	T_1 (^oK)	P_2 (dynes/cm^2)	P_o (dynes/cm^2)
2.0264×10^6	100.0	1.0132×10^3	1.7647008×10^3
2.0264×10^6	100.0	1.0132×10^5	1.0133001×10^5
2.0264×10^6	100.0	1.0132×10^6	1.0132007×10^6
4.0528×10^6	100.0	1.0132×10^3	2.2809003×10^3
4.0528×10^6	100.0	1.0132×10^5	1.0134031×10^5
4.0528×10^6	100.0	1.0132×10^6	1.0132018×10^6
2.0264×10^6	273.0	1.0132×10^3	1.5132016×10^3
2.0264×10^6	273.0	1.0132×10^5	1.0132594×10^5
2.0264×10^6	273.0	1.0132×10^6	1.0132003×10^6
4.0528×10^6	273.0	1.0132×10^3	1.8851162×10^3
4.0528×10^6	273.0	1.0132×10^5	1.0133218×10^5
4.0528×10^6	273.0	1.0132×10^6	1.0132009×10^6
1.0132×10^5	100.0	1.0132×10^3	1.0631904×10^3
1.0132×10^5	100.0	1.0132×10^4	1.0136855×10^4
1.0132×10^5	273.0	1.0132×10^3	1.0436276×10^3
1.0132×10^5	273.0	1.0132×10^4	1.0134821×10^4
1.0132×10^3	100.0	1.0132×10^1	3.3570855×10^1
1.0132×10^3	100.0	1.0132×10^2	1.0605166×10^2
1.0132×10^3	273.0	1.0132×10^1	2.6809626×10^1
1.0132×10^3	273.0	1.0132×10^2	1.0409539×10^2

P_1 (dynes/cm^2)	T_1 (^oK)	P_2 (dynes/cm^2)	P_o (dynes/cm^2)
1.0132×10^2	100.0	1.0132×10^0	9.9760810×10^0
1.0132×10^2	100.0	1.0132×10^1	1.4096144×10^1
1.0132×10^2	273.0	1.0132×10^0	7.7224555×10^0
1.0132×10^2	273.0	1.0132×10^1	1.2584663×10^1

$T = 300^oK$

$T_o = 300^oK$

$\eta = 188 \times 10^{-6}$ Poises

$T_2 = 300^oK$

$L = 50$ cm

TABLE 49

CALCULATIONS OF PRESSURE (P_o) AT THE EXTERNAL EFFUSION SURFACE

(dynes/cm^2)	T_1 (^{o}K)	P_2 (dynes/cm^2)	P_o (dynes/cm^2)
2.0264×10^6	273.0	1.0132×10^3	1.5132141×10^3
2.0264×10^6	273.0	1.0132×10^5	1.0132595×10^5
2.0264×10^6	273.0	1.0132×10^6	1.0132003×10^6
4.0528×10^6	273.0	1.0132×10^3	1.8851287×10^3
4.0528×10^6	273.0	1.0132×10^5	1.0133219×10^5
4.0528×10^6	273.0	1.0132×10^6	1.0132009×10^6
2.0264×10^6	600.0	1.0132×10^3	1.3705761×10^3
2.0264×10^6	600.0	1.0132×10^5	1.0132392×10^5
2.0264×10^6	600.0	1.0132×10^6	1.0132001×10^6
4.0528×10^6	600.0	1.0132×10^3	1.6525748×10^3
4.0528×10^6	600.0	1.0132×10^5	1.0132813×10^5
4.0528×10^6	600.0	1.0132×10^6	1.0132005×10^6
1.0132×10^5	273.0	1.0132×10^3	1.0436401×10^3
1.0132×10^5	273.0	1.0132×10^4	1.0134834×10^4
1.0132×10^5	600.0	1.0132×10^3	1.0337404×10^3
1.0132×10^5	600.0	1.0132×10^4	1.0133819×10^4
1.0132×10^3	273.0	1.0132×10^1	2.6822040×10^1
1.0132×10^3	273.0	1.0132×10^2	1.0410790×10^2
1.0132×10^3	600.0	1.0132×10^1	2.2716777×10^1
1.0132×10^3	600.0	1.0132×10^2	1.0311794×10^2

P_1 (dynes/cm^2)	T_1 (^{o}K)	P_2 (dynes/cm^2)	P_o (dynes/cm^2)
1.0132×10^2	273.0	1.0132×10^o	7.7345485×10^o
1.0132×10^2	273.0	1.0132×10^1	1.2596928×10^1
1.0132×10^2	600.0	1.0132×10^o	6.3287855×10^o
1.0132×10^2	600.0	1.0132×10^1	1.1772076×10^1

$T = 300^oK$

$T_o = 273^oK$

$\eta = 188 \times 10^{-6}$ Poises

$T_2 = 273^oK$

$L = 50$ cm

TABLE 50

CALCULATIONS OF PRESSURE (P_o) AT THE EXTERNAL EFFUSION SURFACE

P_1 (dynes/cm^2)	P_2 (dynes/cm^2)	P_o (dynes/cm^2)
2.0264×10^6	1.0132×10^3	1.4224956×10^3
2.0264×10^6	1.0132×10^5	1.0132461×10^5
2.0264×10^6	1.0132×10^6	1.0132002×10^6
4.0528×10^6	1.0132×10^3	1.7381359×10^3
4.0528×10^6	1.0132×10^5	1.0132953×10^5
4.0528×10^6	1.0132×10^6	1.0132007×10^6
1.0132×10^5	1.0132×10^3	1.0372107×10^3
1.0132×10^5	1.0132×10^4	1.0134144×10^4
1.0132×10^3	1.0132×10^1	2.4211118×10^1
1.0132×10^3	1.0132×10^2	1.0343549×10^2
1.0132×10^2	1.0132×10^0	6.8248930×10^0
1.0132×10^2	1.0132×10^1	1.2037296×10^1

$T = 330^oK$

$T_o = 360^oK$

$T_1 = 600^oK$

$\eta = 200 \times 10^{-6}$ Poises

$T_2 = 300^oK$

$L = 50$ cm

TABLE 51

CALCULATIONS OF PRESSURE (P_o) AT THE EXTERNAL EFFUSION SURFACE

P_1 (dynes/cm^2)	T_1 (^oK)	P_2 (dynes/cm^2)	P_o (dynes/cm^2)
2.0264×10^6	100.0	1.0132×10^3	1.2795553×10^3
2.0264×10^6	100.0	1.0132×10^5	1.0132288×10^5
2.0264×10^6	100.0	1.0132×10^6	1.0132002×10^6
4.0528×10^6	100.0	1.0132×10^3	1.4994135×10^3
4.0528×10^6	100.0	1.0132×10^5	1.0132589×10^5
4.0528×10^6	100.0	1.0132×10^6	1.0132004×10^6
2.0264×10^6	273.0	1.0132×10^3	1.1815528×10^3
2.0264×10^6	273.0	1.0132×10^5	1.0132169×10^5
2.0264×10^5	273.0	1.0132×10^6	1.0132001×10^6
4.0528×10^6	273.0	1.0132×10^3	1.3288508×10^3
4.0528×10^6	273.0	1.0132×10^5	1.0132351×10^5
4.0528×10^6	273.0	1.0132×10^6	1.0132002×10^6
2.0264×10^6	600.0	1.0132×10^3	1.1294774×10^3
2.0264×10^6	600.0	1.0132×10^5	1.0132109×10^5
2.0264×10^6	600.0	1.0132×10^6	1.0132000×10^6
4.0528×10^6	600.0	1.0132×10^3	1.2349680×10^3
4.0528×10^6	600.0	1.0132×10^5	1.0132232×10^5
4.0528×10^6	600.0	1.0132×10^6	1.0132001×10^6
1.0132×10^5	100.0	1.0132×10^3	1.0280288×10^3

P_1 (dynes/cm^2)	T_1 (^oK)	P_2 (dynes/cm2)	P_o (dynes/cm^2)
1.0132×10^5	100.0	1.0132×10^4	1.0133370×10^4
1.0132×10^5	273.0	1.0132×10^3	1.0221466×10^3
1.0132×10^5	273.0	1.0132×10^4	1.0132775×10^4
1.0132×10^5	600.0	1.0132×10^3	1.0191989×10^3
1.0132×10^5	600.0	1.0132×10^4	1.0132478×10^4
1.0132×10^3	100.0	1.0132×10^1	2.0066233×10^1
1.0132×10^3	100.0	1.0132×10^2	1.0267910×10^2
1.0132×10^3	273.0	1.0132×10^1	1.6820709×10^1
1.0132×10^3	273.0	1.0132×10^2	1.0209089×10^2
1.0132×10^3	600.0	1.0132×10^1	1.4942298×10^1
1.0132×10^3	600.0	1.0132×10^2	1.0179612×10^2
1.0132×10^2	100.0	1.0132×10^o	5.4835320×10^o
1.0132×10^2	100.0	1.0132×10^1	1.1404825×10^1
1.0132×10^2	273.0	1.0132×10^o	4.2823687×10^o
1.0132×10^2	273.0	1.0132×10^1	1.0869967×10^1
1.0132×10^2	600.0	1.0132×10^o	3.5390924×10^o
1.0132×10^2	600.0	1.0132×10^1	1.0593125×10^1

$T = 110^oK$

$T_o = 120^oK$

$\eta = 75 \times 10^{-6}$ Poises

$T_2 = 100^oK$

$L = 100$ cm

TABLE 52

CALCULATIONS OF PRESSURE (P_o) AT THE EXTERNAL EFFUSION SURFACE

P_1 (dynes/cm^2)	P_2 (dynes/cm^2)	P_o (dynes/cm^2)
2.0264×10^6	1.0132×10^3	2.1161151×10^3
2.0264×10^6	1.0132×10^5	1.0133653×10^5
2.0264×10^6	1.0132×10^6	1.0132012×10^6
4.0528×10^6	1.0132×10^3	2.8161628×10^3
4.0528×10^6	1.0132×10^5	1.0135356×10^5
4.0528×10^6	1.0132×10^6	1.0132029×10^6
1.0132×10^5	1.0132×10^3	1.0945880×10^3
1.0132×10^5	1.0132×10^4	1.0140002×10^4
1.0132×10^3	1.0132×10^1	4.2259246×10^1
1.0132×10^3	1.0132×10^2	1.0899583×10^2
1.0132×10^2	1.0132×10^0	1.2674036×10^1
1.0132×10^2	1.0132×10^1	1.6085496×10^1

$T = 273^oK$

$T_o = 273^oK$

$T_1 = 100^oK$

$\eta = 170.8 \times 10^{-6}$ Poises

$T_2 = 273^oK$

$L = 100$ cm

TABLE 53

CALCULATIONS OF PRESSURE (P_o) AT THE EXTERNAL EFFUSION SURFACE

P_1 (dynes/cm^2)	T_1 (^oK)	P_2 (dynes/cm^2)	P_o (dynes/cm^2)
2.0264×10^6	100.0	1.0132×10^3	2.2806029×10^3
2.0264×10^6	100.0	1.0132×10^5	1.0134002×10^5
2.0264×10^6	100.0	1.0132×10^6	1.0132015×10^6
4.0528×10^6	100.0	1.0132×10^3	3.0622717×10^3
4.0528×10^6	100.0	1.0132×10^5	1.0136063×10^5
4.0528×10^6	100.0	1.0132×10^6	1.0132036×10^6
2.0264×10^6	273.0	1.0132×10^3	1.8848187×10^3
2.0264×10^6	273.0	1.0132×10^5	1.0133188×10^5
2.0264×10^6	273.0	1.0132×10^6	1.0132006×10^6
4.0528×10^6	273.0	1.0132×10^3	2.4657779×10^3
4.0528×10^6	273.0	1.0132×10^5	1.0134435×10^5
4.0528×10^6	273.0	1.0132×10^6	1.0132019×10^6
1.0132×10^5	100.0	1.0132×10^3	1.1109080×10^3
1.0132×10^5	100.0	1.0132×10^4	1.0141707×10^4
1.0132×10^5	273.0	1.0132×10^3	1.0731763×10^3
1.0132×10^5	273.0	1.0132×10^4	1.0137641×10^4
1.0132×10^3	100.0	1.0132×10^1	4.6220044×10^1
1.0132×10^3	100.0	1.0132×10^2	1.1055680×10^2
1.0132×10^3	273.0	1.0132×10^1	3.6379459×10^1
1.0132×10^3	273.0	1.0132×10^2	1.0678369×10^2

P_1 (dynes/cm^2)	T_1 (^oK)	P_2 (dynes/cm^2)	P_o (dynes/cm^2)
1.0132×10^2	100.0	1.0132×10^o	1.3904749×10^1
1.0132×10^2	100.0	1.0132×10^1	1.7064928×10^1
1.0132×10^2	273.0	1.0132×10^o	1.0709394×10^1
1.0132×10^2	273.0	1.0132×10^1	1.4551601×10^1

$T = 300^oK$

$T_o = 300^oK$

$\eta = 188 \times 10^{-6}$ Poises

$T_2 = 273^oK$

$L = 100$ cm

TABLE 54

CALCULATIONS OF PRESSURE (P_o) AT THE EXTERNAL EFFUSION SURFACE

P_1 (dynes/cm^2)	T_1 (^oK)	P_2 (dynes/cm^2)	P_o (dynes/cm^2)
2.0264×10^6	273.0	1.0132×10^3	1.8848438×10^3
2.0264×10^6	273.0	1.0132×10^5	1.0133191×10^5
2.0264×10^6	273.0	1.0132×10^6	1.0132007×10^6
4.0528×10^6	273.0	1.0132×10^3	2.4658030×10^3
4.0528×10^6	273.0	1.0132×10^5	1.0134438×10^5
4.0528×10^6	273.0	1.0132×10^6	1.0132020×10^6
2.0264×10^6	600.0	1.0132×10^3	1.6522899×10^3
2.0264×10^6	600.0	1.0132×10^5	1.0132784×10^5
2.0264×10^6	600.0	1.0132×10^6	1.0132003×10^6
4.0528×10^6	600.0	1.0132×10^3	2.0159241×10^3
4.0528×10^6	600.0	1.0132×10^5	1.0133626×10^5
4.0528×10^6	600.0	1.0132×10^6	1.0132011×10^6
1.0132×10^5	273.0	1.0132×10^3	1.0732014×10^3
1.0132×10^5	273.0	1.0132×10^4	1.0137666×10^4
1.0132×10^5	600.0	1.0132×10^3	1.0538697×10^3
1.0132×10^5	600.0	1.0132×10^4	1.0135637×10^4
1.0132×10^3	273.0	1.0132×10^1	3.6404160×10^1
1.0132×10^3	273.0	1.0132×10^2	1.0680865×10^2
1.0132×10^3	600.0	1.0132×10^1	3.0343892×10^1
1.0132×10^3	600.0	1.0132×10^2	1.0487551×10^2

P_1 (dynes/cm^2)	T_1 (^oK)	P_2 (dynes/cm^2)	P_o (dynes/cm^2)
1.0132×10^2	273.0	1.0132×10^o	1.0733197×10^1
1.0132×10^2	273.0	1.0132×10^1	1.4575732×10^1
1.0132×10^2	600.0	1.0132×10^o	8.7370000×10^o
1.0132×10^2	600.0	1.0132×10^1	1.3150467×10^1

$T = 300^oK$

$T_o = 327^oK$

$\eta = 188 \times 10^{-6}$ Poises

$T_2 = 273^oK$

$L = 100$ cm

TABLE 55

CALCULATIONS OF PRESSURE (P_o) AT THE EXTERNAL EFFUSION SURFACE

P_1 (dynes/cm^2)	P_2 (dynes/cm^2)	P_o (dynes/cm^2)
2.0264×10^6	1.0132×10^3	1.7378182×10^3
2.0264×10^6	1.0132×10^5	1.0132922×10^5
2.0264×10^6	1.0132×10^6	1.0132003×10^6
4.0528×10^6	1.0132×10^3	2.2394244×10^3
4.0528×10^6	1.0132×10^5	1.0133906×10^5
4.0528×10^6	1.0132×10^6	1.0132013×10^6
1.0132×10^5	1.0132×10^3	1.0606640×10^3
1.0132×10^5	1.0132×10^4	1.0136287×10^4
1.0132×10^3	1.0132×10^1	3.2543888×10^1
1.0132×10^3	1.0132×10^2	1.0549615×10^2
1.0132×10^2	1.0132×10^0	9.4247690×10^0
1.0132×10^2	1.0132×10^1	1.3606627×10^1

$T = 330^oK$

$T_o = 360^oK$

$T_1 = 600^oK$

$\eta = 200 \times 10^{-6}$ Poises

$T_2 = 300^oK$

$L = 100$ cm

DISTRIBUTION

Lt. Col. Oliver R. Dinsmore
Army Research Office
Box CM Duke Station
Durham, North Carolina (1)

Army Research Office
Office of the Chief of Research and Development
ATTN: Research Support Division
Department of the Army
Washington 25, D. C. (1)

Chief of Transportation
ATTN: TCDRD
Department of the Army
Washington 25, D. C. (1)

Commanding Officer
U. S. Army Transportation Combat Development Group
Fort Eustis, Virginia (1)

Commandant
U. S. Army Transportation School
ATTN: Adjutant
Fort Eustis, Virginia (4)

Commanding Officer
U. S. Army Transportation Research Command
ATTN: Long Range Technical Forecast Office (1)
ATTN: Aviation Directorate (1)
ATTN: Deputy Commander for Aviation (1)
ATTN: Executive for Programs (1)
ATTN: Research Reference Center (14)
ATTN: Research Directorate (10)
ATTN: Military Liaison & Advisory Office (4)
Fort Eustis, Virginia

U. S. Army Transportation Corps Liaison Officer
Airborne and Electronics Board
Fort Bragg, North Carolina (1)

U. S. Government Printing Office
Division of Public Documents
ATTN: Library
Washington 25, D. C. (1)

Exchange and Gift Division
Library of Congress
Washington 25, D. C. (1)

Major Thomas Benson
Office of Assistant Director (Army Reactors)
Division of Reactor Development, USAEC
Washington 25, D. C. (1)

John J. Glennon, Librarian
Institute of Aeronautical Sciences
2 E. 64th Street
New York 21, N. Y. (1)

Canadian Army Liaison Officer
Liaison Group, Room 208
U. S. Army Transportation School
Fort Eustis, Virginia (2)

Commander
Armed Services Technical Information Agency
ATTN: TIPCR
Arlington Hall Station
Arlington 12, Virginia (10)

AD_____Accession No._____ The Hayes Corporation, Birmingham, Ala., EFFUSION RESEARCH PROGRAM - C. M. Askey, U. M. Robinson, A. R. Phillips Report No. 595, April 1961, 156 pp. (Contract DA-44-177-TC-697)USATRECOM Proj 9R99-20-001, Unclassified Report An account of a theoretical study and an experimental evaluation of the phenomenon of gaseous effusion (over)	UNCLASSIFIED 1. Effusion Research Program 2. Contract DA-44-177-TC-697	AD_____Accession No._____ The Hayes Corporation, Birmingham, Ala., EFFUSION RESEARCH PROGRAM - C. M. Askey, U. M. Robinson, A. R. Phillips Report No. 595, April 1961, 156 pp. (Contract DA-44-177-TC-697)USATRECOM Proj 9R99-20-001, Unclassified Report An account of a theoretical study and an experimental evaluation of the phenomenon of gaseous effusion (over)	UNCLASSIFIED 1. Effusion Research Program 2. Contract DA-44-177-TC-697
AD_____Accession No._____ The Hayes Corporation, Birmingham, Ala., EFFUSION RESEARCH PROGRAM - C. M. Askey, U. M. Robinson, A. R. Phillips Report No. 595, April 1961, 156 pp. (Contract DA-44-177-TC-697)USATRECOM Proj 9R99-20-001, Unclassified Report An account of a theoretical study and an experimental evaluation the phenomenon of gaseous effusion (over)	UNCLASSIFIED 1. Effusion Research Program 2. Contract DA-44-177-TC-697	AD_____Accession No._____ The Hayes Corporation, Birmingham, Ala., EFFUSION RESEARCH PROGRAM - C. M. Askey, U. M. Robinson, A. R. Phillips Report No. 595, April 1961, 156 pp. (Contract DA-44-177-TC-697)USATRECOM Proj 9R99-20-001, Unclassified Report An account of a theoretical study and an experimental evaluation of the phenomenon of gaseous effusion (over)	UNCLASSIFIED 1. Effusion Research Program 2. Contract DA-44-177-TC-697

as applied to a lifting system is given. Included is a description of the apparatus employed to test four different microporous media selected to demonstrate any lift reaction exhibited as a result of the effusion process. The four microporous media selected were: (1) Code 7930, Vycor brand glass, (2) Sintered, granular nickel, (3) Sintered, granular stainless steel, (4) Cellulosic membrane. Based upon the theoretical analysis and the laboratory evaluation, it is concluded that no practical lift is obtainable from the effusion process.	as applied to a lifting system is given. Included is a description of the apparatus employed to test four different microporous media selected to demonstrate any lift reaction exhibited as a result of the effusion process. The four microporous media selected were: (1) Code 7930, Vycor brand glass, (2) Sintered, granular nickel, (3) Sintered, granular stainless steel, (4) Cellulosic membrane. Based upon the theoretical analysis and the laboratory evaluation, it is concluded that no practical lift is obtainable from the effusion process.
as applied to a lifting system is given. Included is a description of the apparatus employed to test four different microporous media selected to demonstrate any lift reaction exhibited as a result of the effusion process. The four microporous media selected were: (1) Code 7930, Vycor brand glass, (2) Sintered, granular nickel, (3) Sintered, granular stainless steel, (4) Cellulosic membrane. Based upon the theoretical analysis and the laboratory evaluation, it is concluded that no practical lift is obtainable from the effusion process.	as applied to a lifting system is given. Included is a description of the apparatus employed to test four different microporous media selected to demonstrate any lift reaction exhibited as a result of the effusion process. The four microporous media selected were: (1) Code 7930, Vycor brand glass, (2) Sintered, granular nickel, (3) Sintered, granular stainless steel, (4) Cellulosic membrane. Based upon the theoretical analysis and the laboratory evaluation, it is concluded that no practical lift is obtainable from the effusion process.

AD_____Accession No._____ The Hayes Corporation, Birmingham, Ala., EFFUSION RESEARCH PROGRAM - C. M. Askey, U. M. Robinson, A. R. Phillips Report No. 595, April 1961, 156 pp. (Contract DA-44-177-TC-697)USATRECOM Proj 9R99-20-001, Unclassified Report An account of a theoretical study and an experimental evaluation of the phenomenon of gaseous effusion (over)	UNCLASSIFIED 1. Effusion Research Program 2. Contract DA-44-177-TC-697	AD_____Accession No._____ The Hayes Corporation, Birmingham, Ala., EFFUSION RESEARCH PROGRAM - C. M. Askey, U. M. Robinson, A. R. Phillips Report No. 595, April 1961, 156 pp. (Contract DA-44-177-TC-697)USATRECOM Proj 9R99-20-001, Unclassified Report An account of a theoretical study and an experimental evaluation of the phenomenon of gaseous effusion (over)	UNCLASSIFIED 1. Effusion Research Program 2. Contract DA-44-177-TC-697
AD_____Accession No._____ The Hayes Corporation, Birmingham, Ala., EFFUSION RESEARCH PROGRAM - C. M. Askey, U. M. Robinson, A. R. Phillips Report No. 595, April 1961, 156 pp. (Contract DA-44-177-TC-697)USATRECOM Proj 9R99-20-001, Unclassified Report An account of a theoretical study and an experimental evaluation the phenomenon of gaseous effusion (over)	UNCLASSIFIED 1. Effusion Research Program 2. Contract DA-44-177-TC-697	AD_____Accession No._____ The Hayes Corporation, Birmingham, Ala., EFFUSION RESEARCH PROGRAM - C. M. Askey, U. M. Robinson, A. R. Phillips Report No. 595, April 1961, 156 pp. (Contract DA-44-177-TC-697)USATRECOM Proj 9R99-20-001, Unclassified Report An account of a theoretical study and an experimental evaluation of the phenomenon of gaseous effusion (over)	UNCLASSIFIED 1. Effusion Research Program 2. Contract DA-44-177-TC-697

as applied to a lifting system is given. Included is a description of the apparatus employed to test four different microporous media selected to demonstrate any lift reaction exhibited as a result of the effusion process. The four microporous media selected were:

(1) Code 7930, Vycor brand glass,
(2) Sintered, granular nickel,
(3) Sintered, granular stainless steel,
(4) Cellulosic membrane.

Based upon the theoretical analysis and the laboratory evaluation, it is concluded that no practical lift is obtainable from the effusion process.

as applied to a lifting system is given. Included is a description of the apparatus employed to test four different microporous media selected to demonstrate any lift reaction exhibited as a result of the effusion process. The four microporous media selected were:

(1) Code 7930, Vycor brand glass,
(2) Sintered, granular nickel,
(3) Sintered, granular stainless steel,
(4) Cellulosic membrane.

Based upon the theoretical analysis and the laboratory evaluation, it is concluded that no practical lift is obtainable from the effusion process.

as applied to a lifting system is given. Included is a description of the apparatus employed to test four different microporous media selected to demonstrate any lift reaction exhibited as a result of the effusion process. The four microporous media selected were:

(1) Code 7930, Vycor brand glass,
(2) Sintered, granular nickel,
(3) Sintered, granular stainless steel,
(4) Cellulosic membrane.

Based upon the theoretical analysis and the laboratory evaluation, it is concluded that no practical lift is obtainable from the effusion process.

as applied to a lifting system is given. Included is a description of the apparatus employed to test four different microporous media selected to demonstrate any lift reaction exhibited as a result of the effusion process. The four microporous media selected were:

(1) Code 7930, Vycor brand glass,
(2) Sintered, granular nickel,
(3) Sintered, granular stainless steel,
(4) Cellulosic membrane.

Based upon the theoretical analysis and the laboratory evaluation, it is concluded that no practical lift is obtainable from the effusion process.